Phytochrome studies *via* locked chromophores, DNA interference and temperature effects

Zur Erlangung des akademischen Grades eines

DOKTORS DER NATURWISSENSCHAFTEN

(Dr. rer. Nat.)

der Fakultät für Chemie und Biowissenschaften

des Karlsruher Instituts für Technologie (KIT)-Universitätsbereich

genehmigte

Dissertation

von

Rui Yang

Aus Shanxi, China

Dekan: Prof. Dr. Martin Bastmeyer

Referent: Prof. Dr. Tilman Lamparter

Korreferent: Prof. Dr. Holger Puchta

Tag der mündlichen Prüfung: 09.02.2012

die vorliegende Dissertation wurde am Botanischen Institut des Karlsruhe Instituts für Technologie (KIT), Lehrstuhl 1 für Molekulare Zellbiologie, im Zeitraum von Sep 2008 bis Feb 2012 angefertigt.

Hiermit erkläre ich, dass ich die vorliegende Dissertation, abgesehen von der Benutzung der angegebenen Hilfsmittel, selbständig verfasst habe.

Alle Stellen, die gemäß Wortlaut oder Inhalt aus anderen Arbeiten entnommen sind, wurden durch Angabe der Quelle als Entlehnungen kenntlich gemacht.

Diese Dissertation liegt in gleicher oder ähnlicher Form keiner anderen Prüfungsbehörde vor.

Karlsruhe, den 1. Dec 2011

Rui Yang

Contents

Zusammenfassung

Phytochrome sind Photorezeptoren, die in einer Vielzahl von Organismen, darunter in Pflanzen, Pilzen und Bakterien gefunden wurden. Phytochrome treten in zwei Formen auf. Während die Pr-Form rotes Licht absorbiert, hat die Pfr-Form ein Absorptionsmaximum im dunkelroten Spektralbereich. Physiologische Reaktionen werden durch die Pfr-Form vermittelt, weswegen dieser Zustand als der aktive angesehen wird. Beide Zustände der Phytochrome können in den jeweils anderen durch Bestrahlung mit rotem beziehungsweise dunkelrotem Licht überführt werden. Phytochrome sind chromophorbindende Proteine, deren Apoproteinanteil aus einem N-terminalen Chromophormodul, bestehend aus PAS-, GAF- und PHY-Domänen und einem C-terminalen Histidinkinase- oder histidinkinaseähnlichen Modul aufgebaut ist. Der Chromophor ist stets ein linearer Tetrapyrrol, wobei Phytochrome entweder Biliverdin (BV), Phycocyanobilin (PCB) oder Phytochromobilin (PÖB) binden. In bakteriellen und pilzlichen Phytochromen ist Biliverdin in der PAS-Domäne an die Seitenkette eines konservierten Cysteins an das Protein gebunden. Im Gegensatz dazu ist das Phycocyanobilin cyanobakterieller und das Phytochromobilin pflanzlicher Phytochrome eine Cysteinseitenkette der GAF-Domäne gebunden. Aus diesem Grund kann Phycocyanobilin als funktioneller Surrogat in pflanzlichen Phytochromen verwendet werden. Um die Inkorporationseffizienz und die Fähigkeit, biologische Antworten im Dunkeln zu induzieren zu testen, wurden die Phycocyanobilinderivate 15*Za*PCB und 15*Ea*PCB verwendet. Bei diesen Chromophoren ist die Isomerisierung am C15 durch Cyclisierung mittels eines Kohlenwasserstoffrestes zwischen den Ringen C und D blockiert. *In vitro* Studien ergaben, dass rekombinante bakterielle und pflanzliche Phytochrome die blockierten Phycocyanobilinderivate nichtkovalent beziehungsweise kovalent inkorporieren und dass diese Addukte nicht mehr konvertierbar sind. Die Absorptionsspektren der 15*Za*PCB- und 15*E*aPCB-Addukte sind vergleichbar mit denen der Pr- beziehungsweise Pfr-Form des Phycocyanobilin. Die

Zugabe von 15*Ea*PCB, nicht jedoch 15*Za*PCB, zu *Ceratodon purpureus* Protonemazellen bewirkte eine erhöhte Chlorophyllakkumulation und vermittelte eine gravitrope Antwort sowie die Induktion von Seitenverzweigungen in Dunkelheit. Auch in *Arabidopsis thaliana* induzierte 15*Ea*PCB sowohl im Wildtyp als auch in den chromophordefizienten Mutanten *hy1* und *hy2* phytochromvermittelte Antworten im Dunkeln. Allerdings war die Induktion von Phytochromantworten in der *hy1* Mutante durch 15*Ea*PCB weniger effizient als die Induktion durch Biliverdin und anschließender Bestrahlung mit rotem Licht. Diese Ergebnisse weisen darauf hin, dass in *Arabidopsis thaliana* die zyklische Konversion von Pr und Pfr für das Erreichen einer effizienten Phytochromaktivität notwendig ist.

In *Ceratodon purpureus* konnten vier Phytochromgene identifiziert werden. Die Lokalisierung und biologische Funktion dieser Phytochrome konnte bisher nicht für jedes dieser Proteine geklärt werden. Im Zuge dieser Arbeit wurden verschiedene verkürzte Versionen sowie die vollständige Sequenz des Hämoxygenase-Gens für DNA-Interferenz-Experimente verwendet (N-terminal, C-terminal und Full-length). Die Ergebnisse zeigen, dass etwa 20 % der neu regenerierten Filamente einen negativen Phototropismus aufweisen. Darüber hinaus wurden spezifisch Phytochrome mittels dieser Technik herunter reguliert. Die Ergebnisse zeigen, dass CerpuPhy2 möglicherweise für die Bildung von Verzweigungen verantwortlich ist und dass CerpuPhy3 die Rolle des Phototropismus übernehmen könnte. PEB-Färbungen zeigten, dass CerpuPhy3 an der Membran lokalisiert ist.

Die Phosphorylierungsaktivität des Phytochroms Agp1 aus Agrobacterium tumefaciens sinkt mit steigender Temperatur. Bei 25 °C weist die Histidinkinase die höchste Aktivität auf, bei einer Temperatur von 40 °C die geringste. Absorptionsspektren von Agp1 zeigen, dass bei 40 °C und lange Bestrahlung die Prx-Form gebildet wird, was jedoch nicht bei der N-terminalen Version dieses Proteins beobachtbar ist. In dieser Thesis wurden auch Cph1 und dessen N-terminale Version getestet. Bei 40 °C zeigten die Spektren von Cph1-PCB geringere Absorptionsmaxima

für sowohl Pr als auch Pfr. Bei der N-terminalen Version konnte keine Änderung beobachtet werden. Es wurden am Beispiel pflanzlicher Phytochrome einige phytochromregulierte physiologische Funktionen bei verschiedenen Temperaturen getestet. Chromophormutanten von *Ceratodon purpureus* gestörten Gravitropismus bei 29 °C, BV Behandlung in der Dunkelheit gerettet. während *phyA* und *phyB* Mutanten von *Arabidopsis thaliana* eine geringere Hypokotyl elongation im Dunkeln bei 32 °C aufwiesen.

Summary

Phytochromes are photoreceptors, which have been found in a wide range of organisms from plants, fungi to bacteria. There are two forms of phytochrome, red light absorbing form (Pr) and far red light absorbing form (Pfr). Physiological responses are initiated as Pfr, which is, therefore, considered to be active form. Those two forms can convert to each other by red/far red light irradiation. Phytochrome is composed of two components - a protein and a chromophore. The protein comprises of an N-terminal chromophore module which consists of PAS, GAF and PHY domain, and a C-terminal His-Kinase or His-Kinase-related module. Three linear tetrapyrrole chromophores are found in phytochromes: biliverdin (BV), phycocyanobilin (PCB) and phytochromobilin (PΦB). In bacterial and fungal phytochrome, BV binds to a conserved Cys residue in the PAS domain, whereas the PCB of cyanobacterial and PΦB of plant phytochromes bind to Cys residue in the GAF domain. Plant phytochrome also can use PCB as a functional chromophore. PCB derivatives termed 15*Za*PCB and 15*Ea*PCB, in which the double bond between ring C and D are fixed, were used to study the incorporate ability and their ability of triggering biological responses in darkness. *In vitro* studies showed that recombinant agrobacterial and plant phytochrome incorporate locked PCB chromophores non-covalently and covalently, respectively and adducts were photo-inconvertible. The absorption spectra of 15*Za*PCB and 15*Ea*PCB adduct was comparable with Pr and Pfr form, respectively. Feeding of 15*Ea*PCB, not 15*Za*PCB to *Ceratodon purpureus* protonemal resulted in an increased chlorophyll accumulation, mediated gravitropic response and induction of side branches in darkness. Phytochrome mediated responses in *Arabidopsis thaliana* were also induced by 15*Ea*PCB in both wild type and chromophore deficient *hy1*, *hy2* mutants in darkness. However, the phytochrome responses in the *hy1* mutant induced by 15*Ea*PCB were less efficient than by BV

followed by red light irradiation. The results indicated that in *Arabidopsis thaliana*, cycling of Pr and Pfr is necessary to achieve efficient phytochrome activity.

Four phytochromes genes have been found in moss *Ceratodon purpureus*. The localization and biological functions of those phytochromes have not been clearly assigned to each individual. In this experiment, heme oxygenase genes, were used for DNA interference (N-terminal, C-Terminal and Full-length) and the results showed that the approximately 20% of new regenerated filaments shows aphototropism. Single/multiple gene/genes was/were also used to silence specific phytochromes. Results showed that CerpuPhy2 was probably responsible for branch formation and CerpuPhy3 might undertake the role of phototropism. Combination with PEB staining indicated CerpuPhy3 was likely to membrane attached.

Phosphorylation activities of *Agrobacterium tumefaciens* phytochrome Agp1 is down regulated by temperature. At 25 °C His-Kinase has the highest phosphorylation activity, and at 40 °C lowest. Absorbance spectra of Agp1 show that at high temperature (40 °C) and long irradiation induced a new species, Prx, but not its N-terminal version. Cph1 and its N-terminal truncated version were tested. Results showed there was an effect of temperature (40 °C) and light for Cph1, this was reversible if low intensity light was chosen and irreversible if high light intensity was chosen. No temperature effect was detected for N-terminal truncated version. Using plant phytochrome for example, some phytochrome controlled physiological functions at different temperatures were tested. Chromophore mutant of *Ceratodon purpureus* showed disturbed gravitropism at 29 °C; this can be rescued by BV treatment in darkness; *phyA* and *phyB* mutants of *Arabidopsis thaliana* showed shorter hypocotyl at 32 °C in darkness.

0 A List of Abbreviations

Agp1, *Agrobacterium tumefaciens* phytochrome 1

Agp1-M15, truncated version of Agp1, containing PAS-GAF-PHY domains

Agp1-M15CV, site-mutant of Agp1-M15, Cys 20 to Ala, Val 249 to Cys

Ax nm, absorbance at X nm

BSA, bovine serum albumin

BV, biliverdin

CerpuPhy1-4, *Ceratodon purpureus* phytochrome 1-4

Cph1, Cyanobacterial phytochrome 1

DMSO, dimethyl sulfoxide

E_m, emission

E_x, excitation

FR, far red light

GAF, cGMP phosphodiesterase/Adenyl-cyclase/FhlA

M, molar (mole /liter)

MS, Murashige and Skoog medium

NMR, nuclear magnetic resonance

PAGE, polyacrylamid-Gel electrophoreses

PAS, Per/Arnt/Sim

PBS, phosphate buffered saline

PCB, Phycocyanobilin

15ZaPCB, locked PCB chromophore, the double bond between C15 and C16 is fixed at Z configuration and a conformation

15EaPCB, locked PCB chromophore, the double bond between C15 and C16 is fixed at E configuration and a conformation

PΦB, phytochromobilin

PEB, phycoerythrobilin

PEG, Polyethylene glycol

Pfr, far red light absorbing form

phyA-E, *Arabidopsis* phytochrome A to E

PhyB-N651, *Arabidopsis* phytochrome B, N-terminal part

PHY, phytochrome

Pr, red light absorbing form

R, red light

SE, standard error

TCEP, tris (2-carboxyethyl) phosphine

Tris, tris (hydroxymethl)-aminomethane

b

1 Introduction

Light is a dominant environmental factor for almost all cellular organisms, which serves not only as the energy source, but also provides information. As the cornerstone of photomorphogenesis, organisms have evolved a delicate perception system which covers the whole range of the sunlight spectrum to sense the light surrounding them (Figure 1.1). Photoreceptors are composed of polypeptides with specific co-factors (chromophores), which are able to assess quality, quantity, and duration of light, and thus trigger corresponding responses. Depending on the chromophores they are carrying, seven classes of photoreceptors have been categorized: light oxygen-voltage (LOV), xanthopsins, phytochromes, and blue-light sensors using flavin adenine dinucleotide (BLUF), cryptochromes, rhodopsin and UV-B. (Moglich, A. et al 2010) Chromophores are listed in Figure 1.2.
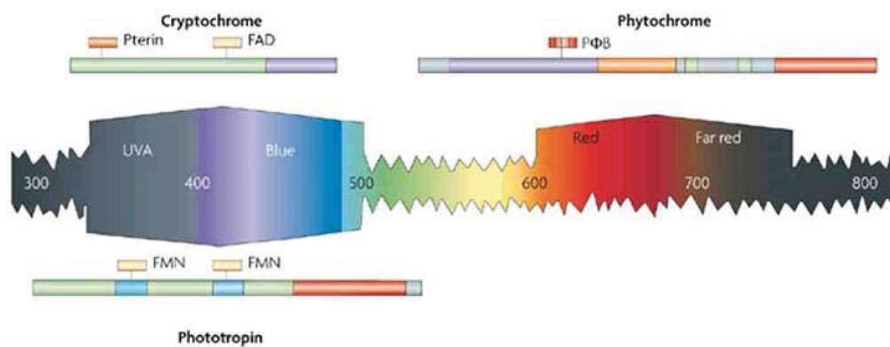
Figure 1.1 Schematic representation of the visible light spectrum and the main families of plant photoreceptors (protein domain arrangements and used chromophores. Phytochromes, cryptochromes, and phototropins are shown (Jiao, Y. et al. 2007)
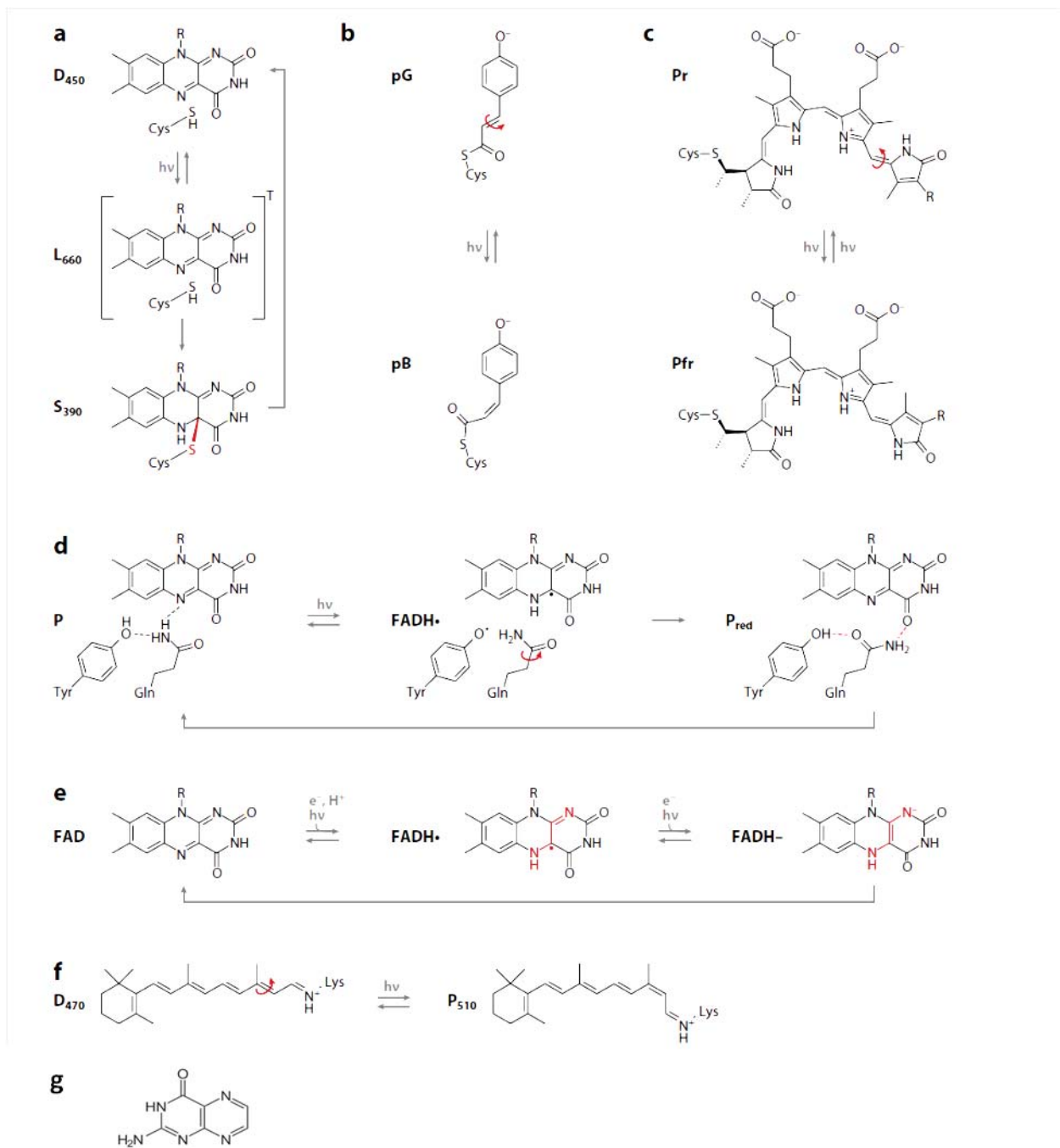
Figure 1.2 Chromophores and simplified photochemistry of the seven photoreceptor classes. (a) Light-Oxygen-voltage (LOV). (b) Xanthopsin. (c) Phytochrome. (d) Blue light sensors using FAD. (e) Cryptochrome. (f) Rhodopsin. (Moglich,A. et al. 2010) (g) Pterin. Pterin is highly candidate chromophore for (Moon, Y. J. et al. 2010) UVR8 a new defined UVB receptor in *Arabidopsis thaliana.*

Phytochrome was discovered as first plant photoreceptor in 1950s. It plays critical roles in monitoring light quantity, quality, and periodicity in plants and relays this photo-sensory information to a large number of signaling pathways that regulate plant growth and development. It is wide spread and can be found in plants, bacteria and fungi. They are most sensitive in the red and far red spectral region (Schaefer, E. and Nagy, F. 2006). Like all other photoreceptors phytochrome is composed of an apoprotein and a chromophore. The apoprotein is encoded by a small multigene family. Three types of natural phytochrome chromophores have been found. Biliverdin (BV), the typical chromophore for bacterial and fungal, becomes covalently attaches to a conserved Cys residue at the N-terminal of the protein. Phycocyanobilin (PCB) or phytochromobilin (PÖB) is the natural chromophore for cyanobacterial and plant phytochromes, respectively. They covalently attach to a Cysteine residue, which lies within the so-called cGMP phosphodiesterase/Adenyl-cyclase/FhlA (GAF) domain. The phytochrome bilins are the tetrapyrrole rings, which using its ring A to bind to protein, and undergo photoconversion through ring C and D (Figure 1.3). In these bilins the vinyl side chain of the ring A is converted to an ethylidene side chain of PCB and PÖB (Lamparter, T. 2004). Since the only chemical structure differences between PCB and PÖB is the ring D side chain, these chromophores can replace each other *in vitro* or *in vivo*, whereas BV is usually not accepted as a functional chromophore by PCB and PÖB binding phytochromes. Figure 1.3 below show the chromophore structures of BV, PCB and PÖB used in Agrobacterium, Cyanobacteria and plants, respectively.
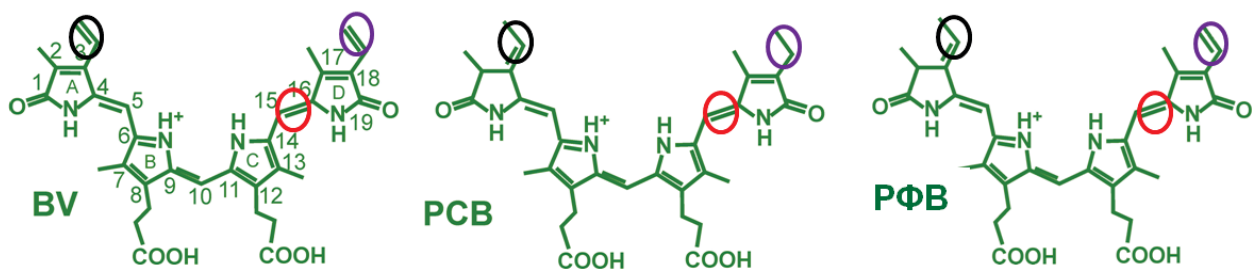
Figure 1.3 Chromophore structures of Agrobacterium, Cyanobacteria and plants

Plant Phytochrome protein is synthesized in the cytosol, whereas the PÖB is synthesized in the plasmid and leak out of the plasmid into the cytosol by a passive process. Assembly of the phytochrome apoprotein with its chromophore is autocatalytic. It can occur spontaneously *in vitro* when purified phytochrome protein is mixed with purified chromophore in the test tube, without additional proteins or cofactors. The resulting holoprotein has spectral properties similar to those observed phytochrome purified from plants, and it exhibits red/far red reversibility (Li, L. M. and Lagarias, J. C. 1992). Light triggers the photoconversion between the inactive red-absorbing form, Pr, and the active far red -absorbing form, Pfr.

According to the described above, phytochrome have their natural chromophores, which lead to special absorbance spectra, and photoconversion. When photoconversion is inhibited through low temperature, specific chromophore replacement or apoprotein mutation, fluorescence spectra is detected. Details about the absorbance spectra and fluorescence spectra are described below.

1.1 Biochemical characteristics of phytochrome

1.1.1 Absorbance spectra

As mentioned above phytochrome is composed of an apoprotein and a chromophore. The apoprotein (Figure 1.4) has usually two domains: The N-terminal chromophore binding domain and the C-terminal outputting Kinase domain. Once the chromophore is assembled to the apoprotein, a specific absorbance spectrum can be measured and photoconversion can be induced.

1.1.2 Photoconversion

NMR studies with plant phytochrome shows that the first step of chromophore photoisomerization when irradiate with red light takes place around the double bond connecting the rings C and D during photoconversion from Pr to Pfr (Rüdiger, W. et al 1983). The configuration of this double bond is *Z* in the Pr and *E* in the Pfr form (Inomata, K. et al. 2006a).

4
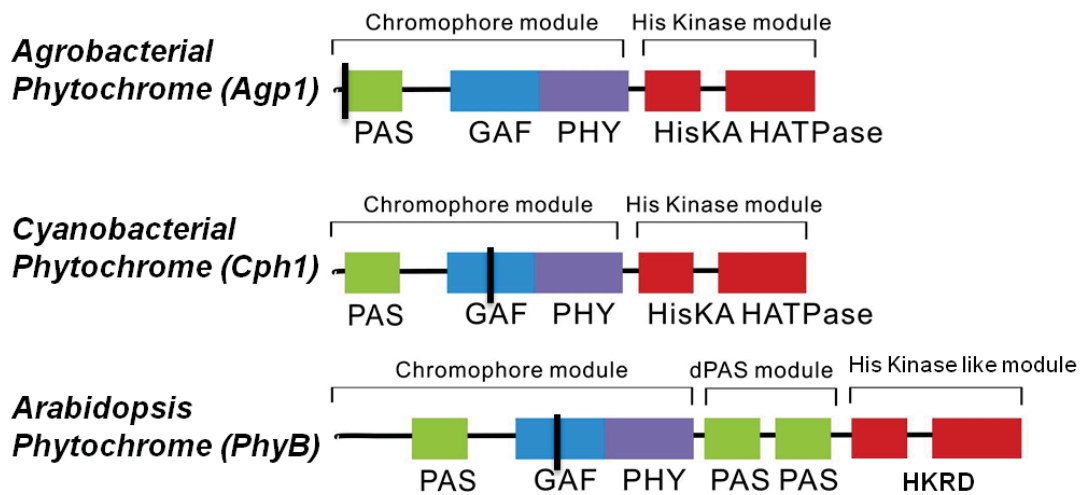
Figure 1.4 Apoprotein structures of bacterial and plant phytochromes. Black lines mark the chromophore binding site.

Figure 1.5 below shows the Pr and Pfr absorbance spectra of agrobacterial, cyanobacterial and plant phytochrome with their natural chromophores.
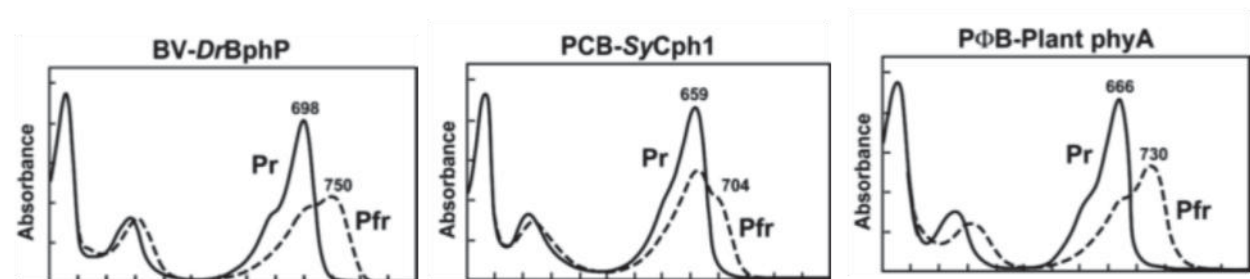
Figure 1.5 Absorption spectra of agrobacterial, cyanobacterial and plant phytochrome (Schaefer, E. and Nagy, F. 2006)

Time-resolved spectroscopy techniques show that this *Z-E* isomerization, leads to the first photoisomerization product lumi-R, which takes place within a picosecond (Heyne, K. et al. 2002, Rentsch, S. et al. 1997). Meta-Ra, meta-Rb, and meta-Rc come later, as well as the photoproduct Pfr which is formed in the microsecond and millisecond time range (Borucki, B. et al. 2005, Inomata, K. et al. 2006a, Rüdiger, W. et al 1983, van Thor, J. J. et al. 2001). Chromophore conformational changes from Pr to Pfr, further induced conformational changes of the apoprotein in its chromophore pocket; at last the holoprotein moiety undergoes changes (Rohmer, T. et al. 2008). For the reverse photoreaction from Pfr to Pr, which is formed by a

rapid C15=C16 *E* to *Z* isomerization, lumi-F is formed first (Rüdiger, W. et al 1983), then isomerization proceeds *via* intermediates back to Pr. The whole structure of the phytochrome protein then also convert back to the Pr state (Figure 1.6).
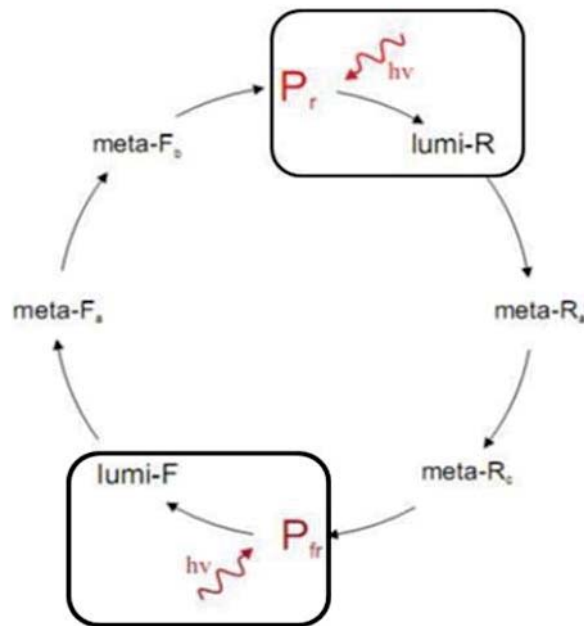
Figure 1.6 Photoconversion model. Note only at the first step need light to induce conversion need. (Borucki, B. et al. 2005, Inomata, K. et al. 2006a, Rüdiger, W. et al 1983, van Thor, J. J. et al. 2001)

1.1.3 Fluorescence

Early studies on plant phytochromes have shown that the fluorescence quantum yield of Pr is quite low at ambient temperature, but significantly increased under certain conditions where photoconversion is blocked (Sineshchekov, V. A. 1995). Using Phycoerythrobilin (PEB), a bilin chromophore of the phycoerythrin antenna of cyanobacteria and red algae, which lacks the C15=C16 double bond between pyrrole rings C and D, high fluorescence can be detected at ambient temperature. A quantum yield of 0.82 has been reported for the Cph1-PEB adduct (Figure 1.7) (Boese, G. et al. 2004a). An adduct of *Pseudomonas aeruginosa* phytochrome PaBphP with 15,16-dihydrobiliverdin, which also lacks the ring C-D connecting double bond, is also fluorescent (Tasler, R. et al. 2005). The inhibition of photoconversion by low temperature

or chromophore replacement correlates with an increase of Pr fluorescence, indicating that photoisomerization provides a major role.
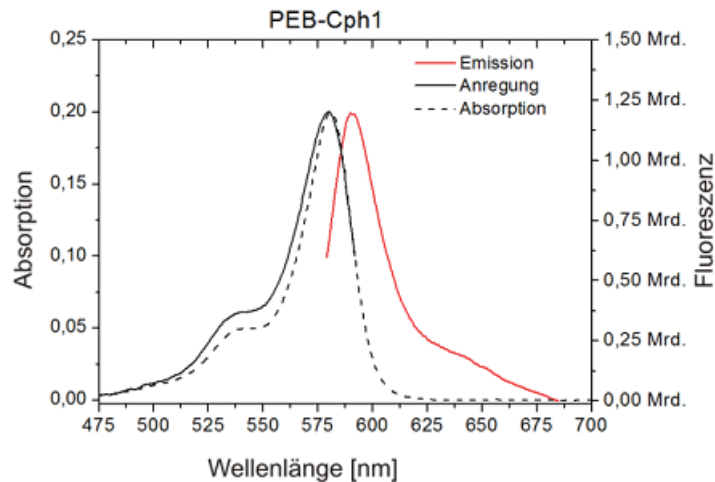
Figure 1.7 Absorbance and fluorescence spectra of Cph1-PEB adduct (Zienicke, B. et al. 2011b).

1.2 Physiological functions of phytochrome

Many studies have been performed since the discovery of phytochrome. In *Arabidopsis* phytochrome control many activities, such as seed germination, flowering and shade avoidance. Less function is known about bacterial phytochrome. Studies in our group shown Agrobacterium phytochrome Agp1 and Agp2 might be responsible for tumor induce. Agp1 might works as a thermo sensor, and Agp2 might be worked as pH indicator. Cph1 was first discovered real *Cyabobacterial* phytochrome in 1997, but the function of this phytochrome is still not known. In *Adiantum venustum* and *Ceratodon purpureus*, phytochrome control phototropism, mediates chlorophyll accumulation and chloroplasts movement. Mutant generation and functional complementation experiments have been used to study the functions of each single phytochrome. The most important findings regarding to the function of phytochrome in *Ceratodon purpureus*, *Adiantum venustum,* and *Arabidopsis thaliana* will be summarized in the following section.

1.2.1 *Ceratodon purpureus*

ptr mutants, which deficient phototropism response, had been isolated from *Ceratodon purpureus* after UV light mutagenesis. They are a good tool to study the functions of phytochrome. Two sets of mutants are identified that have different phenotypes in continuous red light. Class I mutants grow upwards and, produce only very low levels of chlorophyll compared to the wild type have been indicated as defective in the heme oxygenase (Lamparter, T. et al. 1996a). Whereas Class II mutants grow in random directions and, produce normal wild type levels of chlorophyll the molecular basis of Class II mutant is not clear yet. Using the Class I mutants, Phytochrome functions have been studied. The phototropic response and other phytochrome controlled responses of Class I mutants can be rescued by BV feeding. This indicates a deficiency in the chromophore synthesis. In plants, PΦB is synthesized from BV, which itself is formed from heme by the enzyme heme oxygenase.

In total there are now four fully sequenced phytochrome genes in *Ceratodon purpureus*, named CerpuPhy1-4. CerpuPhy1 is the first discovered moss phytochrome gene, homologous to known plant phytochromes in its N-terminus moiety, but divergent in its remaining C-terminus. It has a molar weight 145 kDa, which is significantly larger than common plant phytochromes (Thummler, F. et al. 1992). A function of this phytochrome was described by Mittmann. Using the knock out mutant he could show that it is maybe responsible for control chlorophyll accumulation at low fluorescence red light (Mittmann, F. et al. 2009). Using a 5´-end of CerpuPhy1 as a probe, CerpuPhy2 was identified. This performs like a conventional phytochrome (Lamparter, T. et al. 1995). Phytochrome in *Ceratodon purpureus* control phototropism, polarotropism, branches formation, chlorophyll synthesis, and gravitropism response; some of the phytochromes have overlapping functions like plant phytochromes. Using knockout mutants' researchers found out that CerpuPhy2 and CerpuPhy3 seem to contribute to polarotropism with overlapping functions. CerpuPhy4 may responsible for phototropism and polarotropism, at moderate fluence rates of red light (Mittmann, F. et al. 2009). Table 1.1 below shows the phytochrome effects on the moss life cycle.

Light effect	Species	Photoreceptor	Reference
Induction of spore germination	*Funaria hygrometrica, Ceratodon purpureus, Dicranium scoparium, Physcomitrella patens*	phytochrome	Bauer and Mohr 1959; Valanne, 1966; Schild, 1981; Cove et al.,1978
Formation of protonemal side branches	*Physcomitrella patens, Funaria hygrometrica*	phytochrome and blue light receptor	Kagawa et al., 1997; Imaizumi et al., 2002
Phototropism and polarotropism of protonemal tip cell	*Physcomitrium turbinatum, Funaria hygrometrica, Ceratodon purpureus, Physcomitrella patens, Pottia intermedia*	phytochrome	Bünning and Etzold, 1958; Nebel, 1968; Jenkins and Cove, 1983b; Hartmann et al., 1983; Demkiv et al., 1998; Esch et al.,1999
Chloroplast orientation	*Funaria hygrometrica, Ceratodon purpureus, Physcomitrella patens*	blue light receptor and / or phytochrome, depending on species	Voerkel, 1933; Kagawa et al., 1997; Kadota et al., 2000
Inhibition of gravitropism of protonemal tip cell	*Ceratodon purpureus, Pottia intermedia*	phytochrome and blue light receptor	Cove et al., 1978; Jenkins et al., 1986; Young and Sack,1992; Lamparter et al.,1996; Demkiv et al.,1997a; Lamparter et al., 1998b; Kern and Sack, 1999
Induction of chlorophyll synthesis in protonemal tip cell	*Ceratodon purpureus*	phytochrome and blue light receptor	Lamparter et al., 1997

Light effect	Species	Photoreceptor	Reference
Increase of protoplast regeneration, direction of outgrowth	*Ceratodon purpureus*	phytochrome and blue light receptor	Cove et al., 1996
Modulation of auxin sensitivity	*Physcomitrella patens*	Cryptochrome	Imaizumi et al., 2002

Table 1.1 light effect on moss (Lamparter, T. 2006)

Phytochrome controlled phototropism needs a gradient of Pfr state. Sensing the direction of light is different from other ways of light sensing, because of the vectorial information. Signal transport have to keep the gradual imformation. The response can not be controlled by gene expression, because when the signal go into the nucleus the gradual infromation will be lost. A vectorial signal could be passed on basis of two principles; (1) light attenuation and refraction, which can cause the different light intensity, then induce gradient signal (2) dichromatic action of the photoreceptors. In the case of phytochrome, the transition dipole moment of the Pr and Pfr form are thought to be parallel and vertical to the cell surface, respectively (Figure 1.8). Polar red light with a oscillation plane parallel to the chromophore is resulting in the highest transition from Pr to Pfr, which coures the outgrowth of the filament because of gradient level of Pfr (Figure 1.8 a). Under unilateral red light, the highest transition happen at the side which the transition dipole is perpendicaular to the light direction (Figure 1.8 b). Figure 1.8 b,c shows the two Pfr maxima at the cross section of the cell, light towards side and light avoids side, light attenuation and light refraction now helps to produce the Pfr gradient. Light towards side gets more Pfr because of light attenuation by the plastid, and light refrection by the difference optical between air and moss filament.
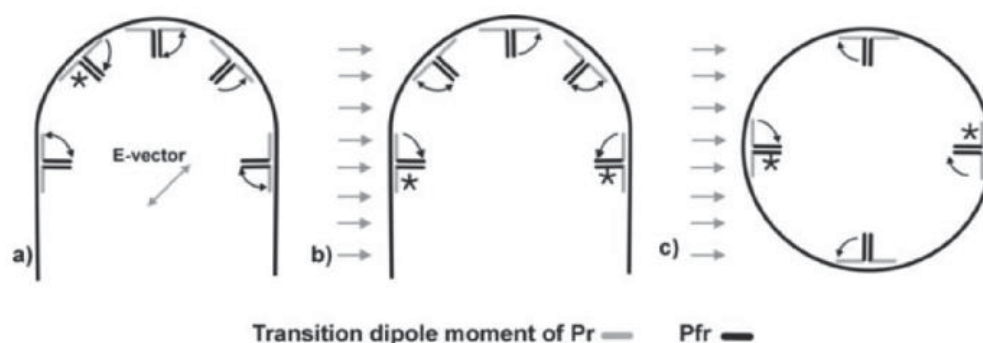
Figure 1.8 Model of phytochrome arrangement attach to the cell membrane (Lamparter, T. 2006).

1.2.2 *Adiantum* venustum

Fern phytochrome is encoded by a small gene family as in seed plants. In 1993 Wada and his group first reports the isolation of a phytochrome cDNA (FP1) from *Adiantum*. Using this phytochrome sequence as a probe, they screened the *Adiantum venustum* genomic library and obtain four different genome segments, named *Adiantum* phytochrome 1-4 (AcPHY1-4). AcPHY2 was shown to be the photoreceptor for the chloroplasts avoidance response; AcPHY3 is responsible for red light induced phototropism and chloroplasts accumulation.

Also spore germination is controlled by phytochrome. Furuya (Furuya, M. et al. 1997) observed that the first cell division is promoted by red light, but inhibited by blue light. These light effects were mediated by phytochrome and a blue light receptor, both of which regulate the entry into the S phase during the first cell cycle in fern spores (Uchida, K. and Furuya, M. 1997). Given that blue light advances the timing of cell division and red light inhibits the division in protonema cells (Wada, M. and Furuya, M. 1978), the light effects on the first cell division within the spores are just the opposite from those on cell division in the protonema cells.

Phytochrome-dependent chloroplast movement in *Adiantum* was first described by Yatsuhashi (Yatsuhashi, H. et al. 1985). Chloroplast movement is induced by polarized red light (Yatsuhashi, H. et al. 1985) and shows a typical dichromatic effect, i.e. polarized red light vibrating parallel to cell axis is more effective in inducing chloroplast movement than red light vibrating perpendicular to cell axis. Table 1.2 below shows the light effect on fern.

Light effect	Photoreceptor	Reference
Spore germination	Phytochrome And Blue light receptor	Furuga *et al.*, 1997; Uchida and Furuga, 1997
Protonemal cell division	Phytochrome And Blue light receptor	Wada and Furuga, 1978
Chloroplast movement	Phytochrome And Blue light receptor	Yatsuhashi, 1985; Kagava and Wada, 1994; Kagawa *et al.*,2004
Protonemal phototropism	Phytochrome	Kodota *et al.*,1982; Wada and Sugai, 1995
Fern leave phototropism	Phytochrome	Wada and Sei, 1994

Table 1.2 light effects on fern

1.2.3 *Arabidopsis thaliana*

In higher plants, phytochrome is encoded by a small multigene family. Five genes PHYA–PHYE, (Clack, T. et al. 1994, Sharrock, R. A. and Quail, P. H. 1989) have been identified in *Arabidopsis*. Three distinct response modes of phytochrome action have been characterized in *Arabidopsis thaliana*, which differ in fluence requirements and red/far red reversibility. According to different fluence rates, those responses are called: high irradiation responses (HIR), low fluence responses (LFR), and the very low fluence responses (VLFR). phyB is responsible for the LFR together with, but to a lesser extent, the other light stable phytochromes, phyC, phyD and phyE. phyA is responsible for the HIR response and VLFR response (Nagy, F. and Schaefer, E. 2002). In *Arabidopsis* Phytochrome performs a diverse array of regulatory functions throughout its development, from seed germination to flowering. The different phytochromes have their own special functions, but most times they have overlapping functions to regulate the growth. Table 1.3 below shows the functions of different phytochromes.

Function	Phytochrome	References
Promotion seed germination	phyA, phyB, phyE	Botto et al., 1996; Shinomura et al., 1996; Hennig et al., 2002; Heschel et al., 2007
Regulate seedling	phyA, phyB, phyC, phyD, phyE	Koorneef et al., 1980; Nagatani et al., 1991; Somers et al., 1991; Dehesh et al., 1993; Nagatani et al., 1993; Parks and Quail, 1993; Whitelam et al., 1993; Neff and Vanvolkenburgh,1994; Reed et al., 1994; Aukerman et al., 1997; Casal and Mazella, 1998; Neff and Chory, 1998; McCormac and Terry, 2002; Franklin et al. 2003a, b; Monte et al., 2003; Franklin et al.,2007
Regulation of hypocotyl randomization	phyA, phyB	Liscum and Hangarter, 1993; Poppe et al., 1996; Robson et al., 1996
Regulation of root gravitropism curvature	phyB	Correll and Kiss, 2005
Suppression of root hair growth	phyB	Reed et al.,1993
Regulation of leaf architecture	phyA, phyB, phyC, phyD, phyE	Nagatani et al., 1991; Reed et al., 1994; Devlin et al.,1998, 1999; Franklin et al.,2003a, b; Monte et al., 2003
Suppression of internode elongation	phyA, phyB, phyE	Devlin et al., 1998
Function	Phytochrome	References
Suppression of shade avoidance	phyB, phyD, phyE	Nagatani et al., 1991; Somers et al., 1991; Whitelam and Smith, 1991; Aukerman et al., 1997; Devlin et al.,1998, 1999; Franklin et al.,2003b
Antagonism of shade avoidance	phyA	Johnson et al. 1994; Yanovsky et al., 1995; Smith et al., 1997; Salter et al., 2003
Function	Phytochrome	References
Regulation of stomatal index	phyB	Boccalandro et al., 2009; Casson et al., 2009
Entrainment of the circadian clock	phyA, phyB, phyD, phyE	Somers et al., 1998; Devlin and Kay, 2000.

Function	Phytochrome	References
Photoperiodic perception	phyA, phyC	Johnson et al., 1994; Reed et al., 1994; Neff and Chory,1998; Monte et al.,2003
Repression of flowering	phyB, phyC, phyD, phyE	Goto et al., 1991; Whitelam and Smith, 1991; Reed et al.,1993; Halliday et al., 1994, 2003; Monte et al.,2003
Suppression of the CBF regulon	phyB, phyD	Franklin and Whitelam, 2007

Table 1.3 Function conclusion of recent work on *Arabidopsis* phytochrome (Franklin, K. A. and Quail, P. H. 2010).

1.3 Intracellular localization of Phytochrome

In higher plants the active form, Pfr, is transfer to the nucleus to regulate gene expression. In some case the Pfr form also works in the cytosol to regulate rapid activities (Nagy, F. and Schaefer, E. 2000). In lower plants, like the moss *Ceratodon purpureus* there is no evidence supporting that Pfr is functioning in the nucleus, however, much evidence indicates that phytochrome acts in the cytosol and shows action dichroism characteristic. The following describes detail for the localization of phytochromes in lower and higher plants.

1.3.1 *Ceratodon purpureus*

Biochemical and immune-cytological studies provided some evidence for the cytosol and membrane localization of phytochromes. Especially immune-cytochemical localization assays demonstrated that the majority of phytochromes, both the Pr and Pfr forms, are localized in the cytosol in light- and/or dark-grown plants (Pratt, L. H 1994). In early study of the moss *Ceratodon purpureus* using fluorescence correlation microscope (Boese, G. et al. 2004b) it was shown that phytochromes are both membrane attached and cytosol contained, according to the mobility of single molecular phytochrome (Figure 1.9).
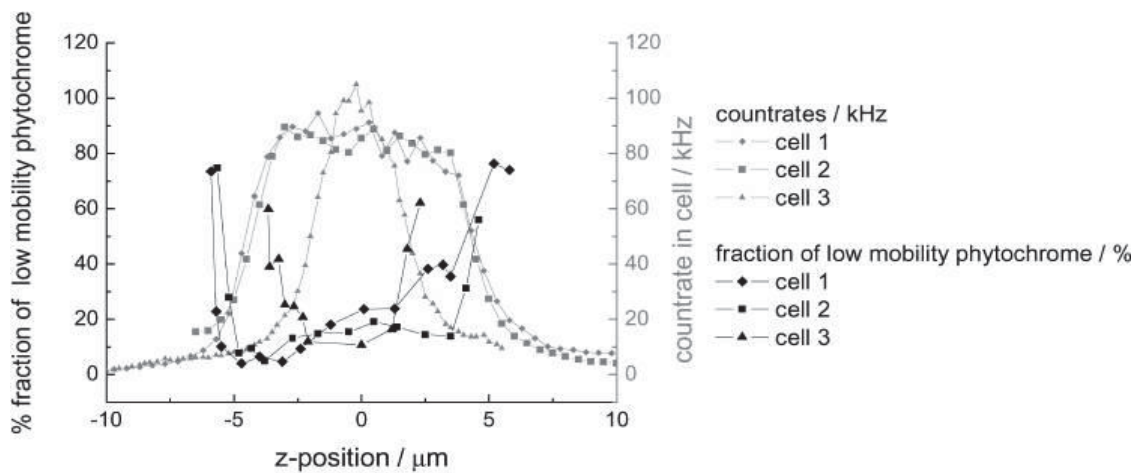
Figure 1.9 Fluorescence intensity and fraction of phytochrome with low mobility of three different cells plotted against the relative *z*-position. The fluorescence intensity is measured in the same focus used for FCS analysis; the profile gives the cell dimension in *z*-direction. The low-mobility fraction was determined by autocorrelation analysis and nonlinear least-square fit. Fixed diffusion times were used in a fit function with two components (see text). The relative contribution of the high- and low-mobility component was obtained from these fits. For cell 1 and cell 2, the measuring position was ~6 μm behind the tip, where the cell diameter in *z*-direction is ~10 μm. The measuring position of cell 3 was closer to the tip region; therefore, the diameter was only ~5 μm (Lamparter, T. 2006).

PEB used as a chromophore by red algae can also assemble with moss phytochrome but cannot undergo photoconversion. The high fluorescence signal of PEB, help researchers to use it as a marker to check the localization of phytochrome. In principle PEB is able to assemble with any kind of phytochrome apoprotein in the cell. Given externally to protonemal moss cultures, PEB enters the tip cells and leads to a specific fluorescence. The Class I mutant ptr116 shows a stronger fluorescence signal than the wild type. This is because the PEB can be principally assembled to all phytochrome, while in the wild type competition with the natural chromophore occurs. The staining can give an impression of the distribution of phytochrome molecules in the cell. Figure 1.10 shows that bulk of phytochrome is located in the cytosol, whereas no phytochrome signal can be detected in the nuclei: This is in accordance with the results of fluorescence correlation microscopy (Figure 1.9). The disadvantage of both methods is that there is no way to check the localization of Pfr.
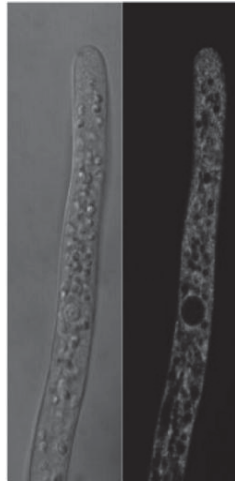
Figure 1.10 Intracellular phytochrome distributions in a tip cell of the class 1 mutant ptr116 monitored by PEB labeling. Left: transmission image, right: fluorescence of the PEB-phytochrome adducts. Before the fluorescence assay, cells were kept for 24 h on agar-medium containing 6 μM PEB at 20 °C (Lamparter, T. 2006).

1.3.2 *Adiantum venustum*

Etzold (Etzold, H. 1965) and Haupt (Haupt, W. 1970) observed an action dichroism for photo- and polarotropism of the chloronemata of fern and chloroplast orientation in the green alga *Mougeotia*. These findings suggested that Pr is parallel and that of Pfr is perpendicular to the cell surface. Since the reverse of subsequent far red light can only work when the far red light give at the same pot, it was concluded movement of phytochrome is limited. Evidence shows AcPHY3 has a C-terminal phototropin like domain structure, which in plants attach to the cell membrane. So AcPHY3 maybe also attaches to the cell membrane through its C-terminal domain. Some other studies use the cell fractionation method to test the whether the phytochromes are associate with membranes or not. In summary, those studies show phytochrome could be associated with various organelles and also the plasma membrane. However, the biological significance of these finding has not been demonstrated and there is a considerable doubt whether those observations indeed reflect the localization of phytochrome molecules *in vivo*.

1.3.3 *Arabidopsis thaliana*

Quail reports a red/far red reversible pellet ability of phytochrome (Quail, P. H. et al. 1973), which shows phytochrome might be light dependent membrane located. Later *in vivo* stains of phytochrome also showed localization in the cell periphery. Because of the water solubility of extracted phytochrome, most people think the bulk amount of phytochrome should be located in the cytosol. MacKenzie et al. (Mackenzie, J. M. et al. 1975) originally described nuclear localization of oat phyA using immune-cytochemical methods. Sakamoto and Nagatani (1996) show a light-dependent translocation of *Arabidopsis* phyB and phyB–GUS fusion proteins from cytosol to nuclear. Later, the same laboratory used the phyB–GFP fusion protein to complement an *Arabidopsis* phyB-deficient mutant *in vivo* and thereby demonstrated that the phyB–GFP fusion protein is a functional photoreceptor and that nuclear translocation of the fusion protein is indeed inducible by red light (Yamaguchi, R. et al. 1999). These findings were extended further by results reported by Kircher and Kleiner (Kircher, S. et al. 1999, Kircher, S. et al. 2002, Kleiner, O. et al. 1999). These authors studied partitioning of the phyB–GFP fusion protein in transgenic plants by overexpression this fusion protein in a wild-type background or by complementing the phenotype of the phyB-deficient mutant.

Furthermore, it was shown that the light-induced nuclear localization of the phyA photoreceptor is preceded by rapid cytosolic spot formation that is reminiscent of the previously described light-induced formation of sequestered areas of phytochrome in oat seedlings (Speth, V. et al. 1987). Using *Arabidopsis* phyA–GFP, nuclear localization in transgenic *Arabidopsis* seedlings could also be induced by continuous far red light, classifying this reaction as an example of the extensively studied far red light-related high irradiation response (HIR), shown to be mediated by phyA in dicotyledonous seedlings. phyC, phyD and phyE also can translocated to nuclei, according to different fluence, wavelength of light (Kircher, S. et al. 2002).
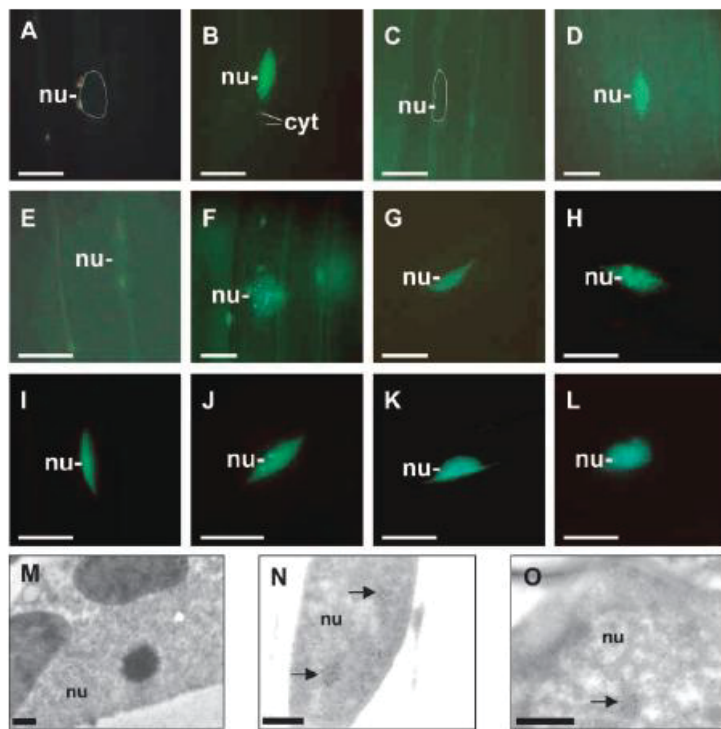
Figure 1.11 Nucleocytoplasmic Distribution and Formation of phyA to phyE:GFP-Containing Speckles in 7-Day-Old Dark-Adapted Seedlings Whose Germination Was Induced by 18 h of WL.

(A) to (L) Epifluorescence images of hypocotyl cells of transgenic *Arabidopsis* seedlings expressing the phyA:GFP ([A] to [D]), phyB:GFP ([E]and [F]), phyC:GFP ([G] and [H]), phyD:GFP ([I] and [J]), and phyE:GFP ([K] and [L]) fusion proteins. Epifluorescence images of nuclei of darkadapted seedlings ([A], [C], [E], [G], [I], and [K]) and of seedlings transferred to WL for 10 min (B) or 6 h ([F], [H], [J], and [L]) or to FR for 6 h (D) are shown. Positions of selected nuclei (nu) are outlined ([A] and [C]), and speckled areas of cytosol (cyt) are indicated.(M) to (O) Electron microscopic images of the cellular distribution and formation of intranuclear structures containing phyB. Seeds from transgenic *Arabidopsis* (line AB0 13) overexpressing phyB were germinated and grown in darkness. Electron microscopic images of nuclei of cotyledon cells from dark-adapted seedlings (M) and from seedlings transferred to R for 4 h ([N] and [O]) are shown. Arrows indicate the positions of nuclear areas highly enriched for phyB. Bars represent 10 µm in (A) to (L) and 0.5 µm in (M) to (O) (Kircher, S. et al. 2002).

1.4 Aims

1.4.1 Phytochrome chromophore structure

In the present work PCB derivatives, which have fixed C-D ring were used. The chromophores is either in *Z anti* stereochemistry or *E anti* stereochemistry between the C15=C16 double bond.

18

In order to find out whether those locked PCB chromophores can assemble with recombinant proteins *in vitro*? And what are the absorption spectral characters of those locked chromophore adducts? To clarify whether those locked chromophores can assemble with plant phytochrome *in vivo*? What kind of phytochrome function can be induced using those locked chromophores in darkness? In order to answer those questions recombinant phytochromes Agp1 of *Agrobacterium tumefaciens*, Cph1 from *Synechocystis PCC6803,* and plant phytochrome phyB were used to study the incorporation of these chromophores *in vitro*. *Ceratodon purpureus*, *Adiantum capillus-veneris*, *and Arabidopsis thaliana* are chose as our *in vivo* material. In *Ceratodon purpureus* and *Arabidopsis* both wild type and chromophore deficient mutants were tested, to find out whether those chromophores also compete with natural chromophore and induce phytochrome activity in darkness.

Locked phytochromes, which are fixed by the carbon ring at the C15 and C16 double bond, cannot undergo photoconversion. Fluorescence spectra was monitored, want to find out whether those phytochrome chromophores adducts also have highly fluorescence signal as PEB? Can those locked chromophores be use as markers to studying phytochrome localization, degradation and so on? In order to answer those questions, *in vitro* fluorescence spectra studies were carried on, to identify the quantum yields of locked chromophore adducts, followed by *in vivo* locked chromophore treatment want to find the phytochrome localization in moss *Ceratodon purpureus*.

1.4.2 Phytochrome intracellular localization and function

Four phytochromes have been found in *Ceratodon purpureus*. Studies showed that the large part of *Ceratodon purpureus* phytochrome lies in cytosol and at the same time a small fraction is attached to the plasma membrane, but not clear which one or ones (Boese, G. et al. 2004a). The main arm of this part of work is to gain further insight into the intracellular distribution of phytochrome in protonemal tip cells of *Ceratodon purpureus*. And find out the function of each single phytochrome. By DNA interference, it is possible to silence genes specifically (Bruecker, G. et al. 2005), which also used in Fern and other organisms (Akamatsu, T. and Taguchi, H. 2001, Bonnassie, S. et al. 1990, Bruecker, G. et al. 2005, Cove, D. J. et al. 2009b, Forsburg, S. L. 2003,

Kawai-Toyooka, H. et al. 2004). Through specifically silence each single phytochrome gene, the function of each single phytochrome might be found out. Combine multigene silence, and PEB staining the localization of each phytochrome might be found out. In this work DNA fragment of heme oxygenase gene, which is responsible for chromophore synthesis; phytochrome genes from Phy1 to Phy4 were used to interfere with specific genes' expression in wild type. For multigene silence experiments two of phytochrome genes with heme oxygenase were combined.

1.4.3 Phytochrome and temperature sensing

Lots of studies show that His-Kinase activities are changed according to the temperature (Albanesi, D. et al. 2009, Braun, Y. et al. 2008, Klinkert, B. and Narberhaus, F. 2009, Mikami, K. et al. 2002, Smirnova, A. V. et al. 2008). Recent studies by our group find out Agrobacterial phytochrome Agp1, might also works as a thermo sensor. The His-Kinase activities of Agp1 is down regulated by increased temperature, and at 40 °C and light irradiations, Prx only formed with the full-length Agp1, not the N-terminal part, Agp1-M15 (Njimona, I. and Lamparter, T. 2011). How about the other phytochromes? Do they have the similar working pattern as Agp1? Do they also can work as thermo sensor? What about plant phytochromes, do the physiological activates also regulated at different temperature through phytochrome? In order to answer these questions the spectral character of Cph1 and its N-terminal truncated version (PSA, GAF, and PHY domains) at different temperatures were tested. The physiological responses using chromophore mutant of *Ceratodon purpureus* and phytochrome mutants of *Arabidopsis thaliana* at different temperatures were also tested.

2 Materials and Methods

2.1 Materials

2.1.1 Plant materials and cultivation

Ceratodon purpureus

Ceratodon purpureus wild type wt4 (Hartmann, E. et al. 1983) and the aphototropic mutant *ptr116* (Lamparter, T. et al. 1997a) derived from the same strain were used in this study. A new *Ceratodon purpureus* wild type strain, kindly provided by Hölzer termed K1 ("Karlsruhe 1") was lab sterilized and cultivated from gametophyte. *ptr201* and *ptr202* new aphototropic mutants derived from K1, were also used. Protonemal filaments were grown under 16h / 8h light / dark cycles at 23°C on medium 1b (Lamparter, T. et al. 1996b). White light came from 9 fluorescent tubes above (Philips TLD 15W/25, made in Indonesia).

Adiantum capillus-veneris

The spores of *Adiantum capillus-veneris* were used, *Adiantum capillus-veneris* were grown in the botanical garden in Karlsruhe. Spores were harvested by lightly shake the envelope, which containing leaves of *Adiantum*, during the shaking process, the spores stick at the back of leave fall down to the envelope. Spores were then collect and stored at room temperature in 1.5 ml Eppendorf tubes.

Arabidopsis thaliana

Wild type *hy1*, *hy2* mutants and *phyA*, *phyB* mutants were used. (Koornneef, M. et al. 1980, Parks, B. M. and Quail, P. H. 1991, Reed, J. W. et al. 1993, Reed, J. W. et al. 1994). Wild type seeds were kindly provided by the botanical garden in Karlsruhe; *hy1* and *hy2* mutants delivered by NASC European *Arabidopsis* Stock Centre, *phyA*, *phyB* mutant were kindly provided by Haodong Chen and propagated in the botanical garden. All the seeds were stored at 4 °C in 1.5 ml Eppendorf tubes.

2.1.2 Chromophores

BV was purchased from Frontier Scientific, PCB and PEB were provided by Norbert Michael. Before doing the chromophore treat experiments both BV and PCB were purified through a C18 column. The locked PCB chromophores 15*Za*PCB and 15*Ea*PCB were synthesized by the group of Prof. Inomata (Nishiyama, K. et al. 2010). Chromophore stock solutions were prepared in DMSO at concentrations of 10–30 mM and stored at - 80 °C. The final chromophores concentration used for assembly with recombinant proteins were between 1 µM and 10 µM, the concentration in media for *in vivo* experiment were usually 10 µM; otherwise it was explicitly mentioned. Control medium was prepared with the same volume of DMSO.
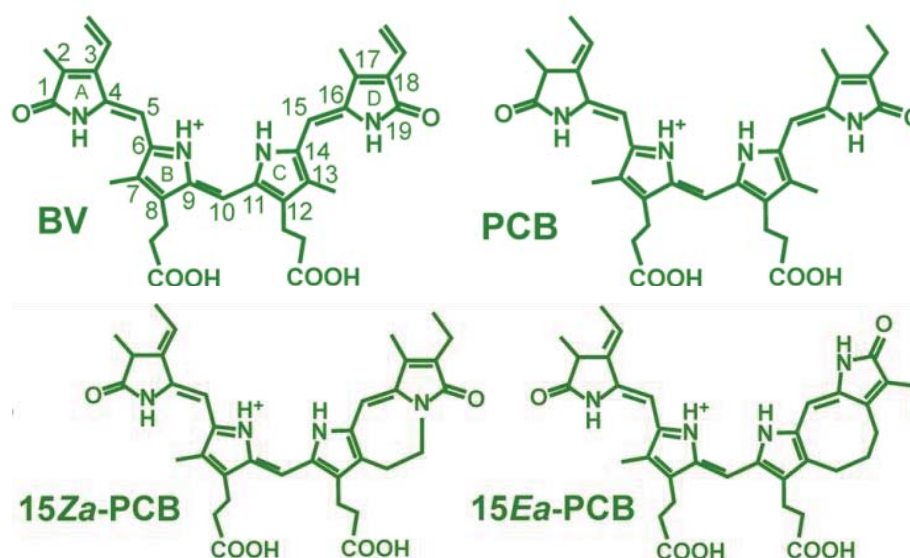
Figure 2.1 Chromophores used in this study.

2.1.3 Recombinant proteins

All recombinant proteins were expressed in *E. coli*. Protein expression vector for Agp1-M15 the truncated version of Agp1, its mutation Agp1-M15CV and Cph1 were directly taken from our stock (Lamparter, T. et al. 1997b). pET21b was used for expression of PhyB-N651. Cloning of the vector and the expression of PhyB-N651 protein is described in section 2.2.2.
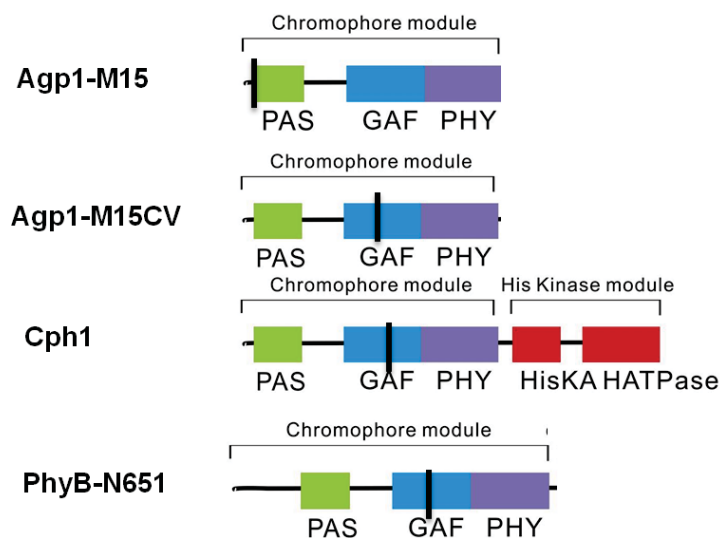
Figure 2.2 Domain arrangements of phytochrome proteins. Note: black indicated the chromophore binding site.

2.1.4 DNA fragments

DNA fragments used in this study are summarized in Table 2.1. Cloning procedure for CerpuPhy4 is described later (section 2.2.1). Vector pJL8 contains Exon I of CerpuPhy1, p781.A16 for full-length CerpuPhy2, pF115.14 included 800bp CerpuPhy3 were made by Bruecker.

DNA Fragments	Vector	Primer Sequence 5'- 3' forward	Primer Sequence 5'- 3' reverse
Heme oxygenase	pGEM T easy	CGAGTAGGCTTCACGTGAAC	TTGGACTGCACACCCCATACC
N-Terminal Heme oxygenase	pGEM T easy	CGAGTAGGCTTCACGTGAAC	GGCGCCGCCTCCTTCTCCCCCTCCTTCG
C-Terminal Heme oxygenase	pGEM T easy	GATTCGCCTGATGGAATCACATACG	TTGGACTGCACACCCCATACC
N-CerpuPhy4	pGEM T easy	ATGACGTCCACGAAGCTGTCCTACT	AGCAATCGGCGATCATACGAA

Table 2.1 DNA fragments used in this study

2.2 Methods

2.2.1 Cloning

PhyB-N651

Genomic DNA of *Arabidopsis thaliana* was extract using DNeasy Plant Mini Kit (QIAGEN); 100 mg of *Arabidopsis* seedling were used for gDNA extract. The coding sequence was amplified by PCR using Phusion polymerase (Finnzymes, Espo, Finland). PCR conditions were: 35 cycles, denature at 98 °C for 10 s, annealing at 62.4 °C for 30 s, extension at 72 °C for 70 s, and final extension for 7 min, 20 µl volume reaction system, given by the manufacturer (Finnzymes). The Primers were: forward, ATATGCTAGCATGGTTTCCGGAGTCGGGGGTAG, reverse GGAATTCGCACCTAACTCATCAATCCCCTGTTC. The PCR product was digested with NheI and EcoRI cloned into NheI-EcoRI digested expression vector PET 21b. The resulting ORF begins with the original start codon and ends with six additional Histidin codons (His-tag). The insert was sequenced and proved by alignment with NM_127435.3 using GENtle program.

Heme oxygenase

The coding sequence was amplified by PCR from cDNA of *Ceratodon purpureus* using Phusion polymerase according to the manufacturers protocol (Finnzymes). PCR Condition were: 30 cycles, denature at 98 °C for 10 s, annealing at 57 °C for 30 s, extension at 72 °C for 50 s, final extension at 72 °C for 7 min. Reactions were carried out in 20 µl samples. The PCR product was added an Adenosine tail at both 3´ ends and cloned into pGEM T easy vector according to the manufacturer's protocol. The insert was sequenced and proved by alignment with AJ489940.1 on NCBI.

N-terminal heme oxygenase

The coding sequence was amplified by PCR from cDNA of *Ceratodon purpureus* using Phusion polymerase according to the manufacturers protocol (Finnzymes). PCR Condition were: 30 cycles, denature at 98 °C for 10 s, annealing 55 °C for 30 s, extension 72 °C for 25 s. Reactions were carried out in 20 µl samples. The PCR product was added an Adenosine tail at both 3´ ends

and cloned into pGEM T easy vector according to the manufacturer's protocol. The insert was sequenced and proved by alignment with AJ489940.1 on NCBI.

C-terminal heme oxygenase

The coding sequence was amplified by PCR from cDNA of *Ceratodon purpureus* using Phusion polymerase according to the manufacturer's protocol (Finnzymes). PCR Condition were: 30 cycles, denature at 98 °C for 10 s, annealing 55 °C for 30 s, extension 72 °C for 25 s Reactions were carried out in 20 µl samples. The PCR product was added an Adenosine tail at both 3´ ends and cloned into pGEM T easy vector according to the manufacturer's protocol. The insert was sequenced and proved by alignment with AJ489940.1 on NCBI.

N-CerpuPhy4

The coding sequence was amplified by PCR from cDNA of *Ceratodon purpureus* using Phusion polymerase according to the manufacturers protocol (Finnzymes). PCR Condition were: 30 cycles, denature at 98 °C for 10 s, annealing 58 °C 30 s, extension 72 °C for 20 s. Reactions were carried out in 20 µl samples. The PCR product was added an Adenosine tail at both 3´ ends and cloned into pGEM T easy vector according to the manufacturer's protocol. The insert was sequenced and proved by alignment with EU122393.1 on NCBI.

2.2.2 Expression and purification of PhyB-N651

For recombinant PhyB-N651, the *E.coli* expression clones were initially grown over night in liquid 4 × 5 ml LB medium at 37 °C. The entire volume was added to 4 × 1 l LB medium, and cultures were propagated at 37 °C until $OD_{600\ nm}$ reached 0.5 (after approximately 3 h). Expression of phytochrome was induced by the addition of 25 µM isopropyl 1-thio-ß-D-galactopyranoside (IPTG). Thereafter, cultures were grown for ca. 22 h at 14 °C until $OD_{600\ nm}$ reached 2.0. Cells were then harvested by centrifugation (9000 x g for 10 min). The cell pellet was washed twice with 200 ml extraction buffer (20 mM Tris/Cl, 500 mM NaCl, 5 mM EDTA, pH 7.8). Cells were suspended in 40 ml extraction buffer and disrupted with a French pressure cell (American Instrument Company) at 1000 psi. The supernatant of a centrifugation (20000 x g for

30 min) was precipitated by adding same volume of saturated ammonium sulfate. After another centrifugation (20000 x g for 30 min), the pellet was suspended in 20 ml wash buffer (25 mM Imidazole, 500 mM NaCl, 20 mM Tris/Cl, pH 7.8) and centrifuged again. The supernatant was loaded to a Ni^+-NTA (Qiagen) affinity column size of 2 × 1.5 cm. The column was then washed with 4 l wash buffer and finally the protein was eluted with elusion buffer (100 mM imidazole, 500 mM NaCl, 20 mM Tris / HCl, pH 7.8). For each fraction 8 ml were collect, fractions with $A_{280 \, nm}$ > 0.3 were collected together and precipitated again with same volume of saturated ammonium sulfate. The protein pellet was dissolved in 2 ml extraction buffer (20 mM Tris/Cl, 500 mM NaCl, 5 mM EDTA, pH 7.8) with 2 mM TCEP, and stored at 80 °C.

2.2.3 UV/Visible spectroscopy measurement

For assembly and photoconversion assays, the samples were kept at 18 °C. Absorption spectra were measured in a JASCO V-550 photometer with a custom-built computer-controlled irradiation device. The scan speed was set to 1000 nm min^{-1}; scans were measured between 900 nm and 250 nm. To monitor chromophore assembly, 1-10 µM recombinant protein solution was prepared and DTT was added to a final concentration of 2 mM. Chromophore from DMSO stock solution was added to a final concentration equivalent to the recombinant protein. The sample was mixed rapidly within 30 s, absorption spectra were recorded immediately, and at different time points until no more absorption changes were apparent. Spectra of free chromophore in buffer solution were recorded in parallel. The protein-chromophore solution was passed over a NAP-10 column (GE healthcare), which containing Sephadex G-25 Medium of DNA Grade, to separate phytochrome from free chromophore. 1 ml of the protein-chromophore adduct were loaded to the column and eluted with 1.5 ml buffer, free chromophore cannot be eluted and kept in the column. See also Inomata et al. 2006 and Lamparter et al. 2002 (Inomata, K. et al. 2006b, Lamparter, T. et al. 2002) for details on chromophore assembly and NAP column separation.

For PhyB-N651 a slightly different protocol was used for assembly. The $OD_{280 \, nm}$ of purified protein was 0.6, according to the formula A = εcd, ε is 6 × 10^4 M^{-1} cm^{-1} for PhyB-N651 (calculated by GENtle according to the amino acids), a concentration of 10 µM of protein was

26

used. The chromophore was first added to a concentration of 5 µM. After 2 h assembly, chromophore was again added to a final concentration of 10 µM, till assembly finished no more spectral change was detected, the sample was then passed through a NAP 10 column.

For photoconversion 730 nm far red and 655 nm red light emitting diodes were used. Far Red light (500 µmol $m^{-2} s^{-1}$) was given for 120 s. Red light (250 µmol $m^{-2} s^{-1}$) was given for 60 s.

2.2.4 SDS-PAGE and Zn^{2+} fluorescence assay

SDS-PAGE-Zn^{2+} fluorescence is used to test the covalent chromophore bond. (Berkelman, T. R. and Lagarias, J. C. 1986). For this assay, assembly was performed for 5 h and the NAP column separation was omitted. SDS PAGE was performed under standard conditions. (Laemmli, U. K. 1970) using 3 % stacking gels and 10 % resolving gels. Prior to electrophoresis, Zn^{2+} acetate was added to the running buffer to form a 1 mM concentration. After electrophoresis the gel with fluorescent biliprotein bands were photographed using a UV trans-illuminator and then stained with coomassie (Sambrook, J. and Russell, D. W. 2001).

2.2.5 Fluorescence spectroscopy measurement

Fluorescence spectra were recorded using a Yobin-Yvon FluoroMax2 spectrofluorimeter at 20 °C in Campus North KIT with the help of Reichert. To avoid cross-talk and scattering artifacts, the emission monochromator was shielded with an appropriate cut-off filter (RG570, thickness 3 mm, Schott, Mainz, Germany). Slit widths of excitation and emission were set at 2 nm. Corrected excitation and emission spectra were obtained considering the spectral characteristics of the lamp, the filter, and the detector. The fluorescence quantum yield Ö of each sample was calculated by integrating its emission spectrum and referring it to fluorescein as a standard Φ of 0.95 (Lakowicz, J. R. 1999).

2.2.6 Mutant selection

Moss filaments grew for 5 d in darkness on 1 cm x 1 cm cellophane pieces which were positioned on 1b plates, vertically oriented. After 5 d pre-culture, plates containing the moss

filaments were transformed to UV-B light (40 W / 12 RS, PHILIPS, made in Holland), for 30 min. The plates were put under UV-B light horizontally, with the lid open. After the UV-B light treatment the plates were directly transfer to continue unilateral red light for 2 weeks. The plates were oriented vertically in the same direction as before. Filaments which did not grow to the direction of the incident light were chosen and picked to new plates. Those filaments were defined as aphototropic mutant. In total two mutants were identified, called *ptr201* and *ptr202*. Physiological studies were followed. *ptr201* which have low chlorophyll level and aphototropic response was classed to Class I mutant, and *ptr202* which have the normal chlorophyll level and random grown under unilateral red light was clarified to Class II mutant. Chromophore feeding experiments rescued the phytochrome response of *ptr201*, showed that it is a chromophore deficient mutant.

2.2.7 Chlorophyll autofluorescence assay

For chlorophyll synthesis level assays, moss filaments were grown for 3 d (K1) or 7 d (wt4, *ptr116*) in darkness on 1 cm x 1 cm cellophane pieces which were positioned on 1b plates. In most cases, the plates were vertically oriented. For chromophores treatments, moss filaments were transferred to new 1b plates with 10 µM bilin and kept for another 24 h either in darkness or in red light. The red light was from an array of 660 nm light emitting diodes, the light intensity was 4 µmol m^{-2} s^{-1}. Relative chlorophyll contents of tip cells were estimated on basis of induced fluorescence by a confocal laser scanning microscope (TCS SP1; Leica, Bensheim, Germany). The fixed stage configuration of the microscope with an Argon Krypton laser and a four-frame averaging protocol was used. The exciting light was set to a wavelength of 633 nm and the emission was recorded through a 670 nm band pass filter. The intensity of chlorophyll fluorescence in the tip cell area was measured by using the Image J 1.42 and the mean value was used for a rough estimation of chlorophyll content. The intensity of fluorescence of tip cell was reached by mean value subtract the background.

In order to make sure that the effect of the microscope light during the measurement did affect the chlorophyll level, experiment was set to test this effect. Results showed that chlorophyll levels did not change within 30 min, during the whole observation time.

28

2.2.8 Branch formation and gravitropism assay

For tests on branch formation and gravitropism the moss *Ceratodon purpureus* K1 was used. Moss filaments were first grown for 3 d in darkness on cellophane in 1b medium, vertical petri dish and then transferred to new plates with 10 µM locked chromophores. For branch formation test, the plates were stay in red light or darkness for one more day, with the original direction. For gravitropism tests the plates were rotated afterwards 90 ° compared to the original orientation and cultivated for another 48 h either in darkness or in red light. The light conditions were the same as before. Images were taken after treatment using Leica DFC500 camera, connected to a Leica M420 microscope and computer. Images were used to measure the angles of filament growth and by Image J 1.42. For branch formation test the numbers of site branch were counted and the percentage was calculated.

2.2.9 Spore germination assay

For each germination experiment, spores were scraped off the wall of the storage Eppendorf tube using a pipette tip. The spores were mixed with 2 ml 1/10 diluted MS medium containing 0.08% agar and poured into petri dishes (2 cm diameter). Thereafter the spores were kept for a total of 7 d at 25 °C and finally scored under a microscope. For testing the effect of red light on spore germination, the spores were irradiated during the first 3 d with a 660 nm LED array from above; the light intensity was 66 µmol m^{-2} s^{-1}. To test for an effect of external 15EaPCB chromophore on spore germination, the chromophore was directly added to the medium to reach a final concentration of 20 µM. In order to compensate for possible degradation, fresh chromophore was both added on day 1 and day 2 to the medium (each time 20 µM final concentration).

2.2.10 Seed germination assay

In seed germination test the wild type and the *hy1* and *hy2* mutants (Koornneef, M. et al. 1980, Parks, B. M. and Quail, P. H. 1991) were used. Seeds were surface sterilized for 1 min in 70 % EtOH, 7 min in 1:1 (v/v) sodium hypochlorite, rinsed 4 times with sterile H$_2$0, and planted on

cellophane in polystyrene Petri dishes containing growth medium (1/2 Murashige and Skoog salts (Murashige, T. and Skoog, F. 1962), 0.05 % MES, 0.8 % (w/v) agar without sucrose). Plates were incubated for 2 d at 4 °C in darkness. Thereafter, the seeds were transferred with cellophane to fresh plates either with 10 µM bilin or without. The seeds were then either irradiated with red light (660 nm, 66 µmol $m^{-2} s^{-1}$) for 5 min and transferred back to darkness, or continuously kept in darkness. Germination was checked after additional 2 d. All manipulation steps were performed under green dim safelight.

2.2.11 Hypocotyl length and cotyledon unfolding measurement

Arabidopsis seeds wild type and the *hy1* and *hy2* mutants were sterilized as before. Seeds were incubated for 4 d at 4 °C in darkness, and then put the plates contain seeds under 4 cool day light tubes (OSRAM L 360W/765 made in Germany) for 4 h to induce uniform germination. The light treated seeds were incubated in darkness at 25 °C for additional 48 h. Thereafter the seedlings were brought with cellophane to new growth medium plates with or without 10 µM bilin, respectively, and then moved to red or dark conditions for 2 more days. The intensity of red light is 66 µmol $m^{-2} s^{-1}$. The growth medium plates were always vertically oriented, in order to make sure the seedlings kept attached to the surface of the medium. In this way, bilin uptake is optimized. After treatment, the seedlings were photographed and growth parameters quantified using Image J 1.42.

2.2.12 Gravitropism response assay

Seeds wild type and the *hy1* were surface sterilized as above, kept at 4 °C for 2 d in darkness, then illuminated for 2 h with cool day light tubes, same as above to induce germination and incubated in darkness for 22 h. Thereafter, the seedlings were transferred to new plates with or without bilin-chromophore and kept for additional 2 days at 25 °C either in darkness or far red light flash; the plates were vertically oriented. The VLFR response was induced by far red (730 nm light emitting diodes, 10 µmol $m^{-2} s^{-1}$) given for 5 min per hour from above during the entire 2 d growth period. After treatment, images were taken using the same equipment described above, and the hypocotyl angles with respect to the vertical were measured using Image J 1.42.

30

An upward growth direction is defined as 0 °. For data presentation, five groups were distinguished: 0 °- 20 °, 20 °- 40 °, 40 °- 60 °, 60 °- 80 °, and 80 °- 90 °.

2.2.13 Gene expression test

Wild type *Arabidopsis* were used in this assay. The growth conditions were same as given above. After uniform seed germination 72 h old dark grown seedlings were transferred to plates with or without 15*Ea*PCB chromophore, in darkness or red light conditions for another 24 h. Then seedlings were frozen immediately using liquid nitrogen. mRNA was extracted using innuPREP Plant RNA kit. cDNA was synthesized using DyNAmo™ cDNA Synthesis Kit for qRT-PCR. Primers for amplifying target genes are shown below.

Genes	Primer Sequence 5'- 3' forward	Primer Sequence 5'- 3' reverse
ELIP2	TCTACGTACCGAGTCCCGCTAG	TCCAAACTTCGTACTCACCTTAGG
LHB1B2	GCT GTC AGA AGG AGT ACC AGTG	GGC TTC CTC AAC CAT GGC
PIL1	AAA TTG CTC TCA GCC ATT CGT GG	TTC TAA GTT TGA GGC GGA CGC AG
PP2A	TATCGGATGACGATTCTTCGTGCAG	GCTTGGTCGACTATCGGAATGAGAG

Table 2.2 Primers used for testing gene expression

2.2.14 DNA interference

Moss filaments were inoculated in 50 ml liquid 1b medium (see section 2.3.4) with 920 mg/l di-amonium tartrate and grown for 5 d at 25 °C in continuous cool day light. Older tissue may leave clumps of undigested tissue, which can act like glue and stick protoplasts together.

Plasmid DNA for transformation was prepared by QIAamp MinElute Media Kit (QIAGEN, Germany) and dissolved in sterile double distilled H_2O. The concentration of the DNA stocks was accurately determined by $A_{260\ nm}$ measurement. And plasmid DNA was delivered in a quantity of 20 µg in a volume of less than 30 µl.

Except where stated different, all procedures were carried out at room temperature between 20 °C and 25 °C. Otherwise a water bath was used.

Protoplast Isolation and transformation were done accordingly to the method used by Cove group (Cove, D. J. et al. 2009a). Slight modification has been done.

Protoplast Isolation

1. Collect the moss tissue through a filter; add tissue at the rate of about 100 mg (fresh wt.) per ml of sterile 0.5 % driselase solution (see section 2.3.1).
2. Incubate for 30 min at 25 °C with occasional gentle shaking every 10 min in darkness.
3. To isolate protoplasts from undigested tissue, filter sterilely through mesh with a pore size of approx.70 µm × 70 µm. Wet the nylon filter with 8 % mannitol before.
4. Sediment protoplasts by centrifugation at 400 x g, for 5 min. Remove supernatant.
5. Suspend protoplast pellet in 10 ml sterile 8 % (w/v) D-mannitol (see section 2.3.1). Centrifuge at 400 x g, for 5 min.
6. Repeat step 5, this time use 10 ml CaPW (see section 2.3.1) to dissolve the protoplast pellet. Count the protoplast at this step.
7. According to the number of protoplast the number of transformation were decided.

This normally yields about 0.5×10^7 to 10^8 viable protoplasts per g fresh weight of tissue.

Transformation (Schaefer, D. G. and Zryd, J. P. 1997)

8. Dissolve pellet in 300 µl of MMM solution (see section 2.3.1) for each transformation. For each transformation, 0.5×10^6 and 1.6×10^6 protoplasts were used and pipette into tubes. These tubes needed to be able to contain at least 12.5 ml of liquid.
9. Dispense 10 to 30 µg of DNA (volume less than 30 µl, otherwise transformation rate is affected) into the protoplast suspension.
10. Follow the time schedule (times in minutes). Add 300 µl PEGT solutions (see section 2.3.1) mix gently, stay room temperature for 5 min, then heat for 7 min at 42 °C, and return to room temperature stay for 10 min. After that each 5 min add CaPW and mix gently. The amount of CaPW adding each time are 600 µl, 1 ml, 2 ml, 3 ml and 4 ml.
11. Sediment protoplasts by centrifugation at 400 x g, for 20 min.

12. Suspend protoplast pellet in 0.5 ml of sterile 8 % (w/v) D-mannitol. This step protoplast can stay for overnight.

13. Dispense onto 90 mm plates of PRMB (see section 2.3.1) overlay with cellophane.

14. Add 2.5 ml of molten PRMT medium (see section 2.3.1), to step 12, and then mix well and transform them to PRMB medium.

After transformation, protoplasts were kept for 1 d in darkness. Thereafter, they were transferred to continue white light chamber for 2 d. After that, the regenerated protoplasts were transferred with cellophane to 1b medium and stay in continuous unilateral red light for another 3 d on vertical Petri dishes. Physiological studies were analyzed after that. PEB staining also followed
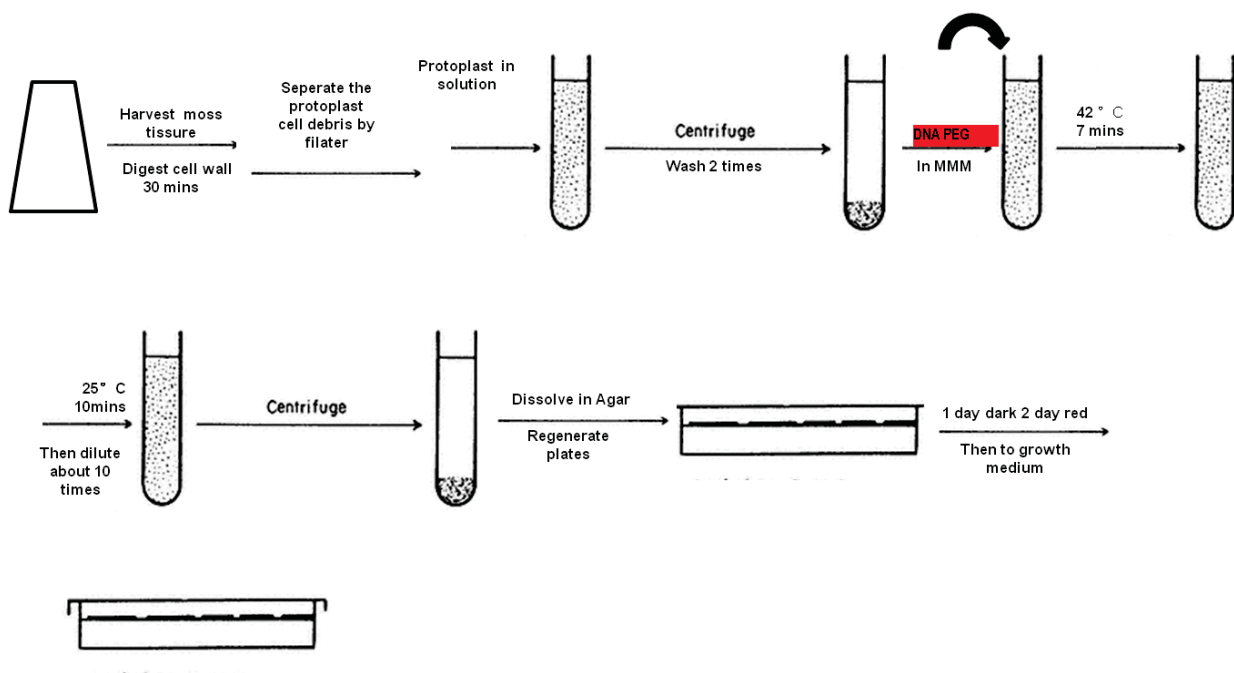

Figure 2.3 Schedule of protoplast isolation and transformation

2.2.15 PEB staining

After application of DNA for interference, according to the phenotype, new regenerated filaments were pick out to 1b plates, and kept growth. Moss filaments were first incubating in darkness for 3 d. Then moss filament were transferred with cellophane to fresh 1b medium

containing 7 µM PEB and incubated for 1 more day in darkness. Fluorescence of PEB was checked under the fluorescence microscope. The wavelength of exciting light was set to 570 nm and the emission was recorded through a 595 nm band pass filter. The fluorescence of tip cell was measured. Fluorescence intensity and localization was assayed.
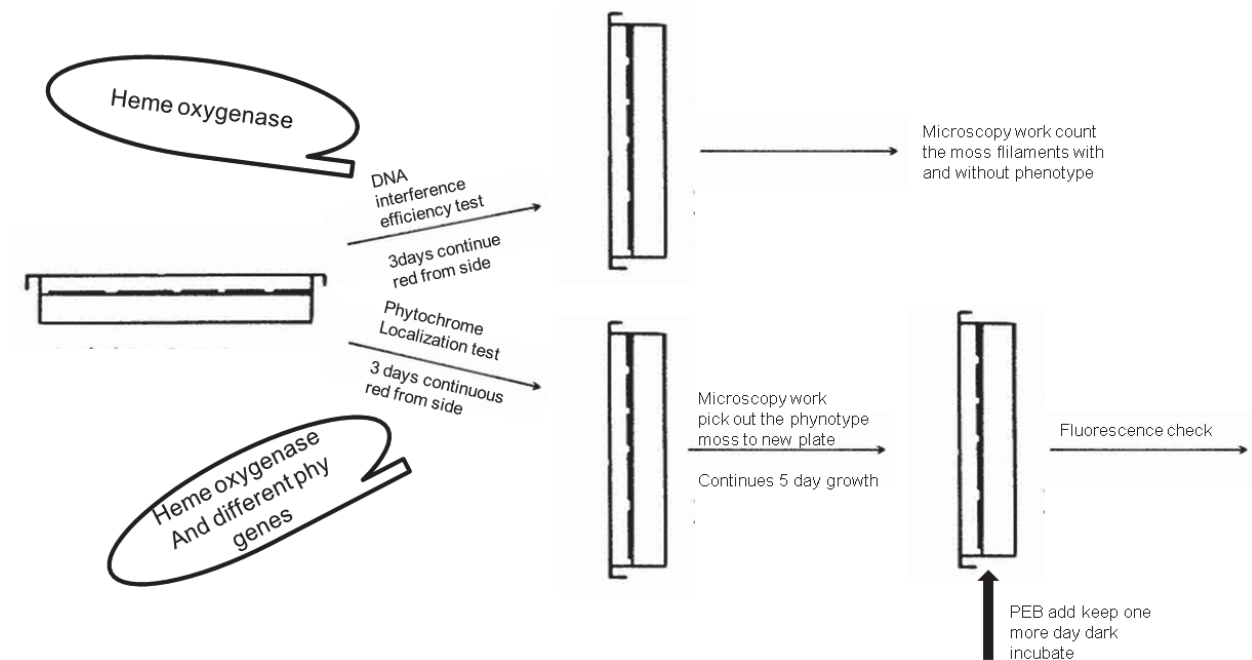
Figure 2.4 Schedule of biological studies after protoplast regeneration

2.2.16 Spectroscopy studies at different temperatures

Cph1 and NCph1 which contains PAS, GAF and PHY domains were kindly purified by Norbert. Cph1 and NCph1 were assembled with PCB as described before for 2 h. After assembly protein-chromophore adducts were passed through a NAP10 (Qigen) column to get rid of the free chromophore. The time schedule of temperature effect studies is given below. Four different temperatures were used, 3, 20, 30, and 40 °C. Each temperature treatment follows the same schedule. Here using 3 °C for example.

1. At 3 °C samples were first irradiated with far red light, then measure the full-length spectra (I) from 900 nm to 250 nm, followed by red light irradiation, measure the full-length spectra (II). Far red irradiation again.

34

2. Change the program of measurement to time drive, monitor the absorption change at 710 nm, at 3 °C, start the measurement, switch on the red light after 180 s, the red light irradiation is continuous during the 7000 s time drive measurement, spectra (III).

3. After the time drive, change program back to full-length measurement, immediately measure (IV), followed by far red light irradiation, measure (V), at 3 °C.

4. In some case for the reversible test, which only for 40 °C samples. After spectra V, red light were given again, and then temperature were slowly reduce from 40 to 20 °C within 90 min, during this time the red light continuous on. When the temperature reached 20 °C, measure the full-length spectra (VI), far red light again, and spectra (VII) were recorded.

Two light sources were used for photoconversion: high intensity far red light, 500 μ mol m^{-2}s^{-1} and red light, 250 μ mol m^{-2}s^{-1}. Low intensity far red/red light both 10 μmol m^{-2}s^{-1}

2.2.17 Physiological studies at different temperatures

Ceratodon purpureus and *Arabidopsis thaliana were* used for *in vivo* studies of phytochrome dependent temperature effects. Four different temperatures were tested: 18 °C, 23 °C, 29 °C and 32 °C.

Moss filaments were kept in darkness for 4 d at 23 °C in vertical plates, to get a uniform growth. At the 5th d the filaments were transported to new growth medium with or without BV at different temperature. Plates were rotated by 90 ° after transfer, in order to test the gravitropism response, after different temperature treatments. After application of the different temperatures for two days, in the whole process no light was given. After, photos were taken and the angles were measured using Image J 1.42.

Arabidopsis thaliana seeds were surface sterilized as before described, and kept in darkness for 2 d. Then germination was induced by applying 2 h white light at 23 °C. Afterwards seeds were taken back to darkness for 22 h at 23 °C. Then germinate seeds were transported to incubator set to different temperatures for another 48 h, each step, expect germination inducing, were

done under totally darkness. After that images were taken and hypocotyl length was measured using Image J 1.42.

2.3 Recipes used

2.3.1 Moss protoplasts isolation and transformation buffer

2 % Driselase

It is convenient to store Driselase as a 2 % (w/v) solution at − 20 °C, and dilute on the day you wish to obtain protoplasts.

Dissolve driselase in 8 % D-mannitol solution. Gently mix (do not shake vigorously). Staying at room temperature for 15 min. Centrifuge at 2500 × g for 5 min. Filter sterilizes supernatant. Dispense into convenient aliquots and freeze.

8% manitol

1 M MgCl$_2$ solution

1 % MES pH 5.6 solution

1 % Ca(NO$_3$)$_2$ solution

1 M Tris buffer pH 8.0

Calcium protoplasts wash (CaPW)

D-mannitol 80 g, CaCl$_2$ 2H$_2$0 7.35 g in 1 l distilled H$_2$0, sterilized by autoclaving

PEGT

PEG 6000 2 g, Autoclave in a glass Universal bottle or equivalent vessel. On day of transformation, melt PEG (this can be done in a water bath at 37 °C or above, or in a microwave) Add 5 ml D-mannitol/Ca (NO$_3$)$_2$ solution and mix well. Leave at room temperature for at least 2 h before use.

D-mannitol/MgCl$_2$/MES (MMM) solution

Make up fresh, on day of use

D-mannitol 910 mg, 1 M MgCl$_2$ solution 150 µl, 1 % MES pH 5.6 solution 1 ml, distilled water 8.85 ml, filter sterilize.

D-mannitol/Ca (NO₃)₂ solution

Make up fresh, on day of use

8 % (w/v) D-mannitol solution 9 ml, 1 M Ca(NO$_3$)$_2$ solution 1 ml, 1 M Tris buffer, pH 8.0 100 µl, filter sterilize.

PRMB (protoplast regeneration medium – bottom layer)

1 b medium without sugar, D-mannitol 60 g, di-ammonium (+) tartrate 920 mg (= 5 mM), agar 10 g, distilled H$_2$0 to 1 l. Sterilize by autoclaving.

PRMT (protoplast regeneration medium – top layer)

1 b medium without sugar, D-mannitol 80 g, di-ammonium (+) tartrate 920 mg (=5mM), agar 6 g, distilled H$_2$0 to 1 l. Sterilize by autoclaving.

PGML (protoplast grown medium – liquid)

1 b medium without sugar, di-ammonium (+) tartrate 920 mg (= 5 mM), distilled H$_2$0 to 1 l. Sterilize by autoclaving.

2.3.2 Protein purification buffer

Extraction buffer: 20 mM Tris/HCl, 500 mM NaCl, 5 mM EDTA, pH 7.8

Wash buffer: 25 mM Imidazole, 500 mM NaCl, 20 mM Tris/HCl, pH 7.8

Elution buffer: 100 mM imidazole, 500 mM NaCl, 20 mM Tris/HCl, pH 7.8

2.3.3 LB medium: 10 g Bacto-Tryptone, 5 g Bacto-yeast extract 5 g NaCl, distilled H$_2$O to 1 l

2.3.4 MS medium: 435 g/l 1/2 Murashige and Skoog salts, 0.05 % MES, 0.8 % Agar

2.3.5 1b medium: 1 M l^{-1}KNO$_3$, 0.1 M l^{-1} CaCl$_2$, 1 M l^{-1} KH$_2$PO$_4$, 10 mM l^{-1} C$_6$H$_5$FeO$_7$, trace eletnents (0.22 mM l^{-1} CuSO$_4$, 10 mM l^{-1}H$_3$BO$_4$, 0.2 mM l^{-1} CoCl$_2$, 0.1 mM l^{-1} Na$_2$MO$_4$, 0.2 mM l^{-1} ZnSO$_4$, 2 mM l^{-1} MnCl$_2$ and 0.17 mM l^{-1} Kl) and 2 g l^{-1} glucose and 1.1 % agar, before agar adding, pH was adjusted to 5.8 with KOH.

3 Results

The focus of this work were to study the chromophore structure of phytochrome, the biological function and localization of each single phytochrome in *Ceratodon purpureus*, and the phytochrome function at different temperatures.

The two locked PCB chromophores which called 15*Za*PCB and 15*Ea*PCB were using to studying the chromophore structure both *in vivo* and *in vitro* (section 3.1). *In vitro* studies four recombinant phytochrome proteins were used to assemble with locked chromophores, to study the absorbance spectral characters of those locked chromophores adducts (section 3.1.1). *In vivo* studies *Ceratodon purpureus*, *Adiantum* and *Arabidopsis thaliana* were used to study the biological functions of locked chromophores. In order to test whether locked chromophores can assemble with plants phytochrome *in vivo* or not, and to test whether phytochrome control active via red light irradiation can be initiated by locked chromophores feeding in darkness or not (section 3.1.2).

DNA interference was used to silence specific phytochrome gene/genes, and then PEB was used to stain the remaining phytochrome (section 3.2). Combine these two methods study the function and localization of each single *Ceratodon purpureus* phytochrome, in living cell.

Phytochrome functions at different temperature were also studied. Both *in vitro* and *in vivo* experiments were tested. Cph1 and its N-terminal (PAS, GAF, and PHY domains) version were used to test the *in vitro* spectral characters at different temperatures (section 3.3.1). Phytochrome controlled biological functions were tested at different temperatures under totally darkness using wild type, chromophore mutant of *Ceratodon purpureus* and wild type, phytochrome mutants of *Arabidopsis thaliana* (section 3.3.2).

3.1 *In vitro* and *in vivo* locked chromophores studies

3.1.1 *In vitro* studies

Table 3.1 shows the calculated extinction coefficient ε of different phytochrome adducts. The extinction coefficient ε is an intrinsic property of a chemical compound, which shows how strongly it absorbs light at a given wavelength. Through that a basic knowledge of chemical character of locked chromophores was given. The actual absorbance A is dependent on the path length d, the concentration c, and ε *via* the Beer–Lambert law, A = εcd, $\varepsilon=A/cd$. The lower the ε is the wilder the absorbance peak. Agp1-M15-15ZaPCB had the highest ε with a value of 10^5 followed by Agp1-M15-BV and Agp1-M15-PCB, Agp1-M15-15EaPCB, the value range were around 10^4. Same as Agp1-M15-15ZaPCB adducts, Agp1-M15CV-15ZaPCB again had the highest ε value, 2.7×10^6. All the Cph1 chromophore adducts have the same ε value, except the 15EaPCB adduct. PhyB-N651-PCB has the highest ε value compared with other PhyB-N651 phytochrome adducts. The higher the ε value is, the sharper the absorbance spectra should be look like. The sharp and higher absorbance peak is confirmed by later absorbance spectral measurement.

	Agp1-M15	M15CV	Cph1	PhyB-N651
BV	9×10^4	9×10^4	8.5×10^4	3.4×10^4
PCB	9×10^4	9×10^4	8.5×10^4	1.2×10^5
15ZaPCB	1.5×10^5	2.7×10^6	8.5×10^4	8.5×10^4
15EaPCB	5.7×10^4	5.7×10^4	5.8×10^4	8.4×10^4

Table 3.1 Calculated extinction coefficients (at λmax). Note: The extinction coefficient of protein were got by GENtle according to their protein sequence; BV 1.2×10^4 $M^{-1}cm^{-1}$, PCB 2.1×10^4 $M^{-1}cm^{-1}$, 15ZaPCB 2.6×10^4 $M^{-1}cm^{-1}$ and 15EaPCB 2.5×10^4 $M^{-1}cm^{-1}$ were either form the literature or given by the manufacturer. For Agp1-M15 and its CV mutants BV, PCB adducts, 9×10^4 $M^{-1}cm^{-1}$ were used here calculated by Lamparter (Lamparter, T. et al. 2002). ε of Cph1-PCB, PhyB-PCB are 8.5×10^4 $M^{-1}cm^{-1}$, 1.2×10^5 $M^{-1}cm^{-1}$ calculated by Lamparter were also used here (Lamparter, T. et al. 2001a)

3.1.1.1 15*Za*PCB adducts are Pr like and 15*Ea*PCB adducts are Pfr like

Four different chromophores: BV, PCB, and 15*Za*PCB, 15*Ea*PCB were used in this work. They were used to assemble with recombinant proteins Agp1-M15, Agp1-M15CV, Cph1 and PhyB-N651. The results showed that all the chromophores were assembled with recombinant proteins, details are described below.

Agp1-M15 As in previous assays (Lamparter, T. et al. 2002) BV assembled with Agp1-M15 very rapidly. The assembly was almost finished after 1 min mixing BV and Agp1-M15, only slight further increases were observed. No more spectral changes were evident 10 min after mixing. Rapid assembly was also observed for PCB, 15*Za*PCB and 15*Ea*PCB. The 15*Za*PCB spectrum has a maximum absorption at 710 nm (Figure 3.1 C), which is 14 nm red shifted in compared to the absorption maximum of the PCB adduct (Figure 3.1B 686 nm). The absorption peak of the 15*Za*PCB adduct is sharper than that of the PCB adduct. It confirms the calculated extinction coefficients as given in Table 3.1. A similar characteristic has been found for 15*Za*BV versus BV adducts of Agp1 (Inomata, K. et al. 2005a). The absorption maximum of the 15*Ea*PCB adduct is at 735 nm, which is 6 nm red shifted compared to the Pfr form of the PCB adduct (Figure 3.1 B). Red light irradiation of both locked chromophore adducts did not result in detectable spectral changes (Figure 3.9 A).
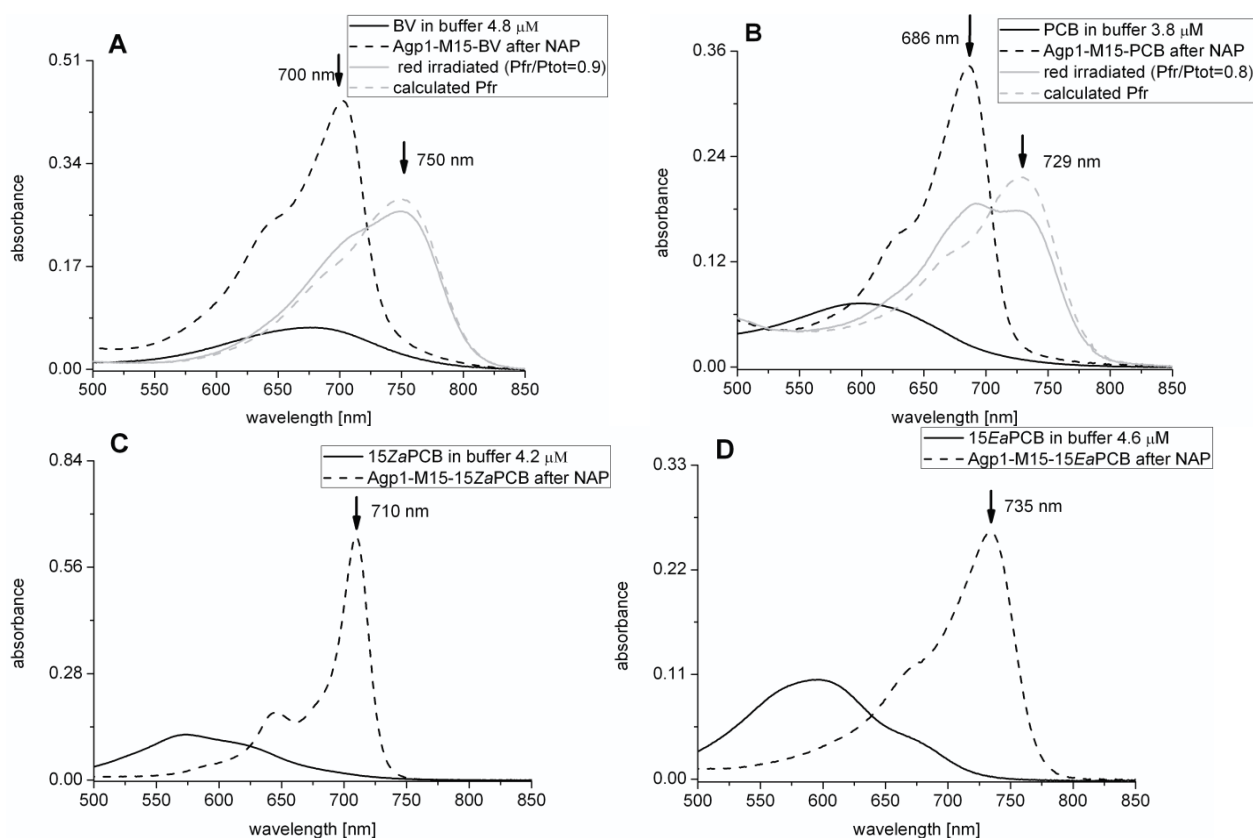
Figure 3.1 Agp1-M15 chromophore adducts. A, Absorption spectra of free BV in buffer, the BV adduct after NAP column separation in the dark adapted Pr form, after red light irradiation, and of calculated Pfr. B, Spectra of free PCB, the PCB adduct after NAP column separation in the dark adapted Pr form, after red light irradiation, and of calculated Pfr. C, Spectra of free 15*Za*PCB and the 15*Za*PCB adduct after NAP column separation. D, Spectra of free 15*Ea*PCB and the 15*Ea*PCB adduct after NAP column separation. The spectra of free chromophores in A to D are recorded in the same buffer as the proteins and are calculated to the estimated concentration of the holoprotein. (Concentrations are given in the panels). In A and B, the estimated Pfr/P_{tot} contents of the red irradiated samples are given. The spectra of calculated Pfr were drawing using the formula (Red light irradiated spectra - (1 − Value $_{Pfr/Ptot}$) × Pr) / Value $_{Pfr/Ptot}$, the Value $_{Pfr/Ptot}$ were chosen from 0.5 to 0.9 till typical Pfr spectra showed out.

Agp1-M15CV The assembly of Agp1-M15CV with BV was characterized by spectral changes during 225 min. Whereas early spectra reveal a characteristic peak around 701 nm and are comparable with the BV adduct of Agp1-M15, continued assembly is characterized by an increase in the 670 nm range (Figure 3.2 A). The final adduct consists apparently of two spectral species which might be covalent and non-covalent adducts. The covalent attachment of BV to Cys249 is maybe the cause for spectral changes observed during longer incubation times. The reason for this incomplete covalent attachment is then the alteration of the chromophore

41

binding site from the N-terminal domain to the GAF domain. Red light irradiation results in an absorption increase at 750 nm and a decrease at 701 nm and 672 nm (Figure 3.2 B). The photoproduct is a species which has only one absorption maximum in the red spectral range. When Agp1-M15CV was assembled with PCB, a uniform spectral species with an absorption maximum at 655 nm was obtained. Assembly was completed ca. 60 min after mixing. During this incubation time, a transient species absorbing at longer wavelengths was detected (Figure 3.2 C). The transition from longer to shorter wavelengths absorption maxima is indicative for covalent bond formation, which results in the loss of the ring A ethylidene double bond. The Pfr form which is obtained after photoconversion has a maximum around 690 nm (Figure 3.2 D). Assembly of Agp1-M15CV with both locked chromophores followed the same principle as the assembly with PCB: the formation of assembly intermediates with longer wavelengths absorption maxima are followed by transitions to shorter wavelengths (Figure 3.2 E, G). This again is indicating covalent bond formation. With locked chromophores, the assembly intermediates are even more pronounced than with PCB. The absorbance spectrum of the Agp1-M15CV 15*Za*PCB adduct is in the Pr form with a 23 nm red shift at the maximum absorbance peak compared to the PCB adduct. The same situation was shown by 15*Ea*PCB and PCB adducts after red light irradiation. With red shifts of approximately 20 nm (Figure 3.2 D, H).
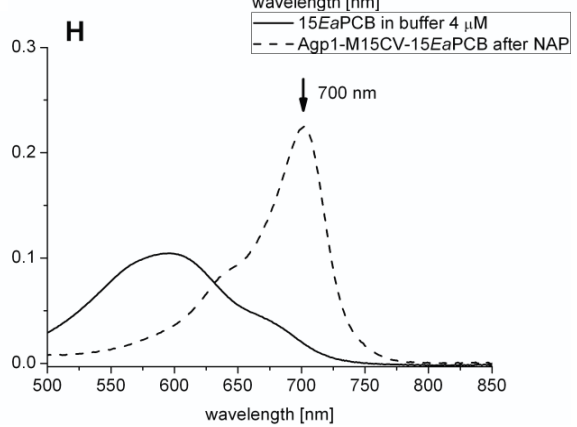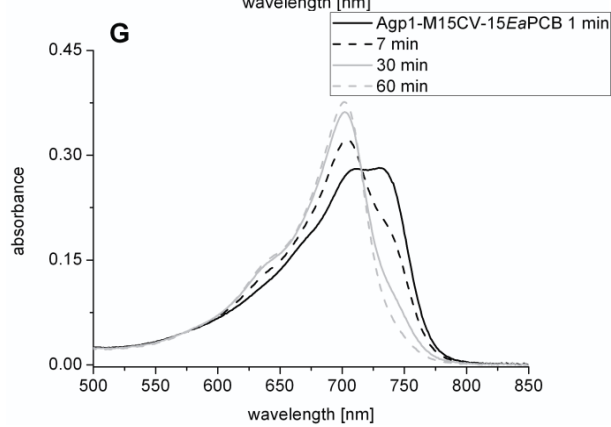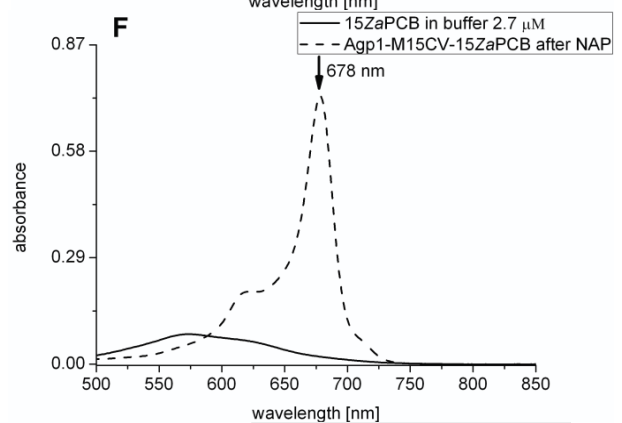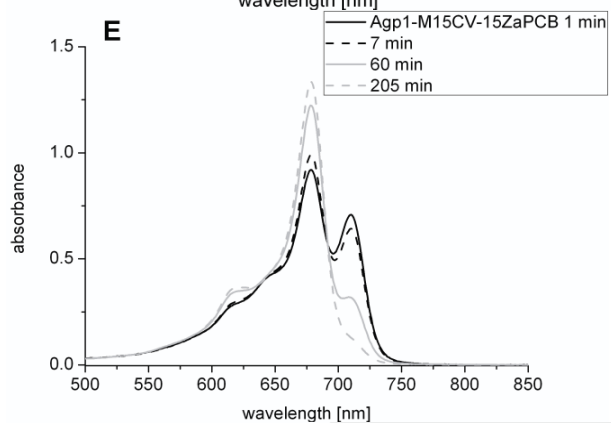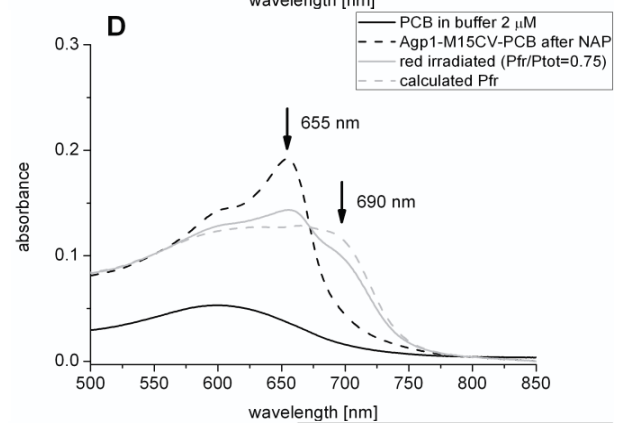
Figure 3.2 Agp1-M15-CV chromophore adducts. A, Absorption spectra during the assembly with BV, recorded after mixing protein and BV at indicated time points. B, Spectra of free BV in buffer, the BV adduct after NAP column separation in the dark adapted Pr form and after red irradiation. C, Spectra during the assembly with PCB, recorded after mixing protein and PCB at indicated time points. D, Spectra of f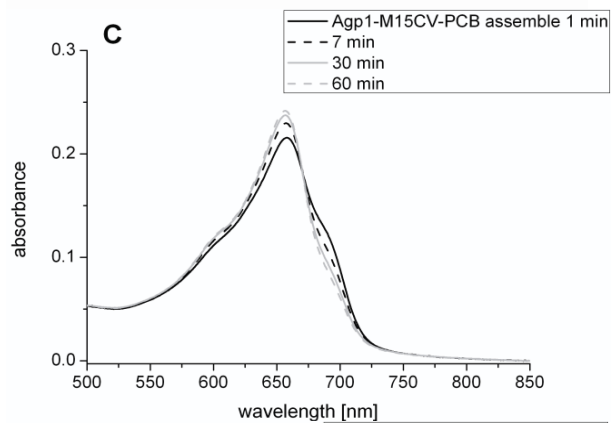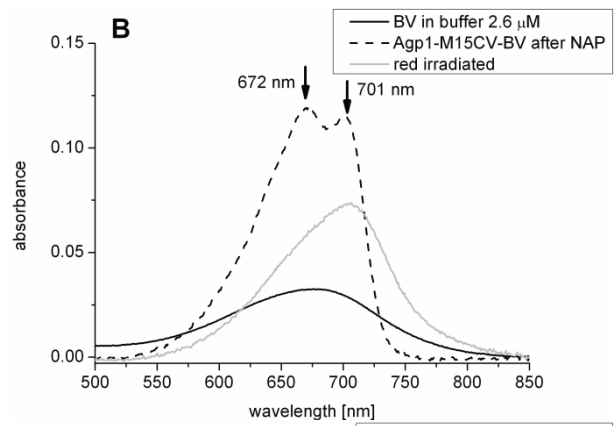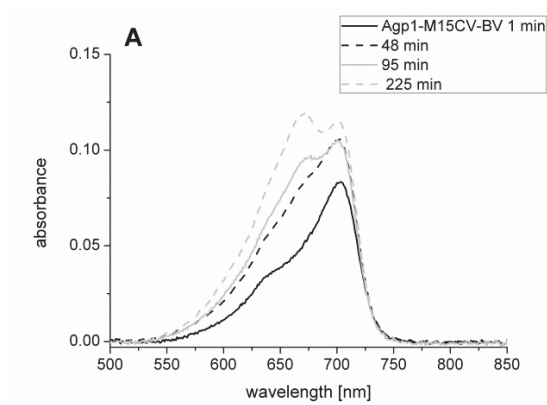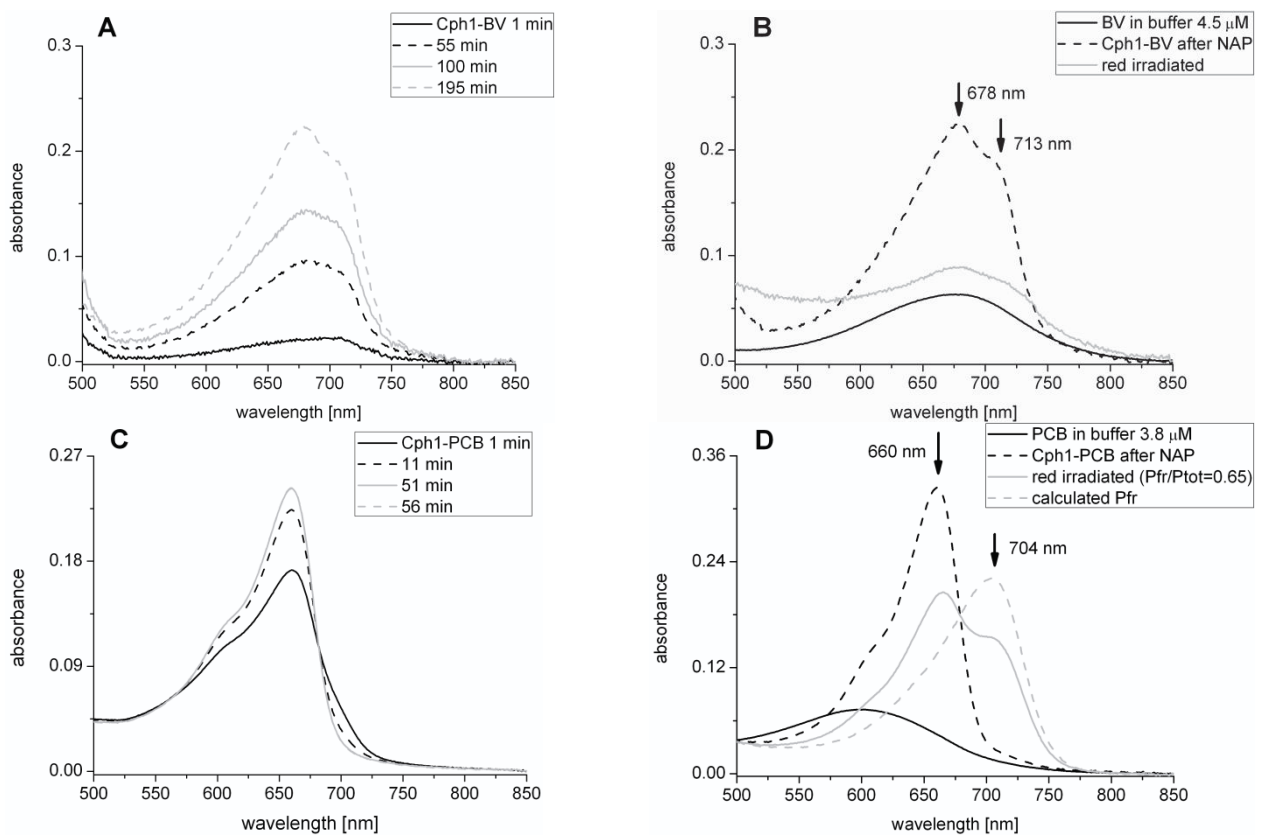ree PCB, the PCB adduct after NAP column separation in the dark adapted Pr form, after red irradiation and of the calculated Pfr form. E, Spectra during the assembly with 15ZaPCB, recorded at the indicated time points. F, Spectra of free 15ZaPCB and the 15ZaPCB adduct after NAP column separation. G, Spectra during the assembly with 15EaPCB recorded at the indicated time points. H, Spectra of free 15EaPCB and the 15EaPCB adduct after NAP column separation. The spectra of free chromophores in B, D, F and H are recorded in the same buffer as the proteins and are calculated to the estimated concentration of the holoprotein. (Concentrations are given in the panels). In D, the estimated Pfr/P$_{tot}$ content of the red irradiated sample is given in the panel. The spectra of calculated Pfr were drawing using the formula (Red light irradiated spectra - (1 − Value $_{Pfr/Ptot}$) × Pr) / Value $_{Pfr/Ptot}$, the Value $_{Pfr/Ptot}$ were chosen through till nice spectra showed out 0.5 to 0.9.

Cph1 The same set of chromophores was tested with the cyanobacterial phytochrome Cph1 from the *Cyanobacterium Synechocystis* PCC 6803. Details on the assembly of Cph1 with PCB have been reported before (Borucki, B. et al. 2003). It has been shown that Cph1 also interacts with BV (Lamparter, T. et al. 2001a). The PCB binding assay in our present experiments is in line with previous studies: absorption changes were apparently complete within 1 h after mixing chromophore and protein, and an assembly intermediate which absorbs at longer wavelengths is detected (Figure 3.3 C). Pr and Pfr had maxima at 660 and 704 nm, respectively. The absorption spectrum that was obtained with BV differs slightly from previous studies (Lamparter, T. et al. 2001b) as it revealed a 678 nm peak and a shoulder at 713 nm (Figure 3.3 B). In addition the adduct was photoactive (Figure 3.3 B). Red light irradiation resulted obviously in a loss of protein bound chromophore, since the final absorption spectrum was very similar to that of the free chromophore. The locked chromophores also assembled with Cph1. However, the spectra that were measured during and after completion of assembly were complex and did not follow our expectations. When Cph1 was mixed with 15ZaPCB, the adduct revealed two peaks in the long wavelength range with maxima at 678 nm and at 590 nm (Figure 3.3 F), indicating that the adduct contains 2 spectral species which differ in their chromophore conformation. The 678 nm maximum was again red shifted as compared to the Cph1-PCB Pr state and represents the covalent adduct in the Pr form. The absorption in this spectral region

44

increased with incubation time. The 590 nm peak decreased during the assembly and finally reached a balance with 678 nm peak, which finally got almost the same absorbance value. Zn^{2+}-fluorescence suggests that the 15*Za*PCB chromophore is covalently bound to the protein (Figure 3.7 E). The adduct was also subjected to SDS NAP column separation (Figure 3.7 C). In this assay, the chromophore / protein ratio was not affected by the size separation, indicating that the chromophore of both spectral species is covalently bound. Irradiation with red light induced no spectral changes of the adduct (Figure 3.9 C). Cph1-15*Ea*PCB revealed even more complex spectra with three peaks at 600, 663 and 716 nm (Figure 3.3 G).
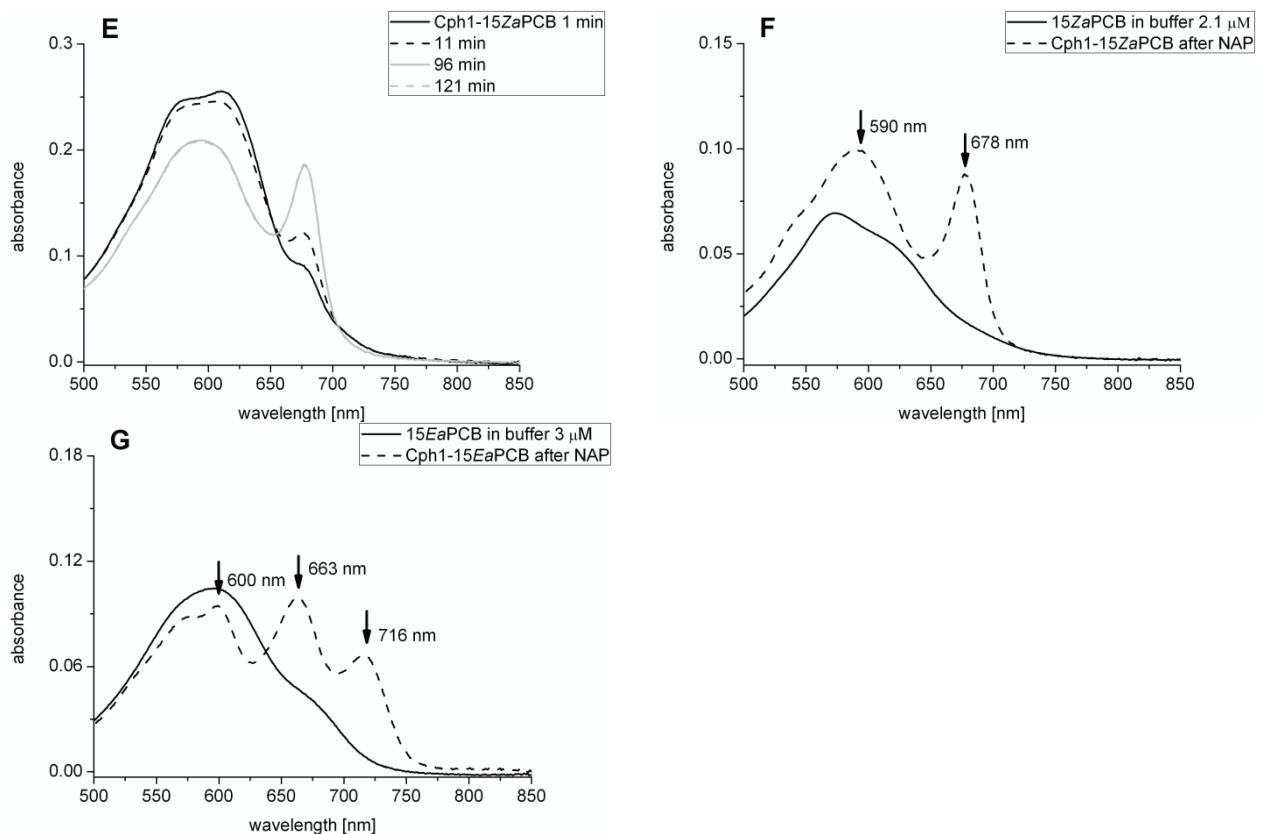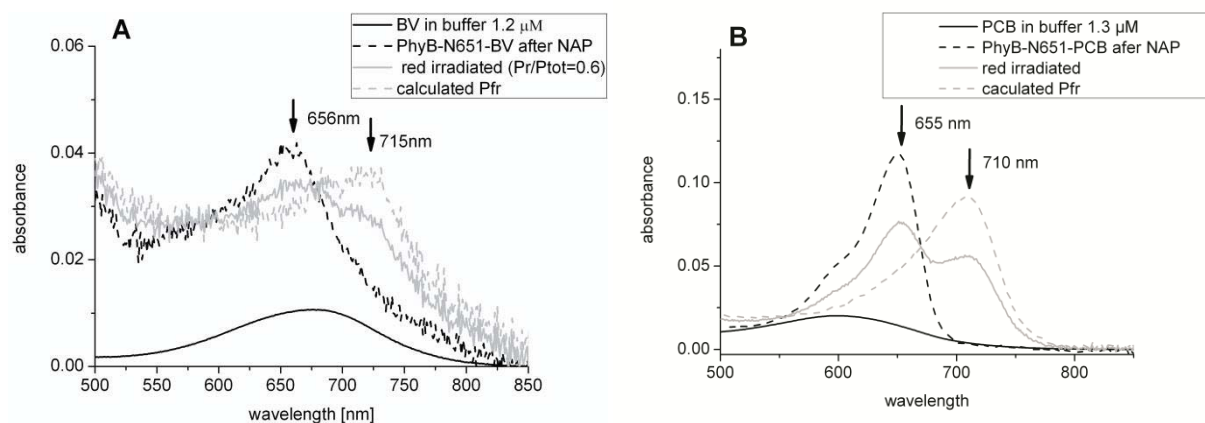
Figure 3.3 Cph1 chromophore adducts. A, Absorption spectra during the assembly with BV, recorded after mixing protein and BV at indicated time points. B, Spectra of free BV in buffer, the BV adduct after NAP column separation in the dark adapted Pr form and after red irradiation. C, Spectra during the assembly with PCB recorded after mixing protein and PCB at indicated time points. D, Spectra of free PCB in buffer, the PCB adduct after NAP column separation in the dark adapted Pr form, after red irradiation, and of the calculated Pfr form. E, Spectra during the assembly with 15*Za*PCB, recorded at the indicated time points. F, Spectra of free 15*Za*PCB in buffer and the 15*Za*PCB adduct after NAP column separation. G, Spectra of free 15*Ea*PCB in buffer and the 15*Ea*PCB adduct after NAP column separation. The spectra of free chromophores in B, D, F and H are recorded in the same buffer as the proteins and are calculated to the estimated concentration of the holoprotein. (Concentrations are given in the panels). In D, the estimated Pfr/P_{tot} content of the red irradiated sample is given. The spectra of calculated Pfr were drawing using the formula (Red light irradiated spectra - (1 – Value $_{Pfr/Ptot}$) × Pr) / Value $_{Pfr/Ptot}$, the Value $_{Pfr/Ptot}$ were chosen through till nice spectra showed out 0.5 to 0.9.

Plant phytochrome PhyB-N651 When recombinant PhyB-N651 was mixed with BV, a low concentration of BV remained bound to the protein after the final NAP column separation. This adduct is photoactive. This result is in accordance with Li, that BV is bound to plant phytochrome (Li, L. M. et al. 1995), and with Jorissen, who showed photochromicity for these

46

adducts (Jorissen, H. J. et al. 2002). The absorption maximum of the PCB adduct is at 655 nm and the adduct photo-converts into Pfr with a maximum at 710 nm after red light irradiation (Figure 3.4 B). The 15*Za*PCB chromophore assembled also with PhyB-N651, and the absorption changes were apparently completed after 20 min. The spectrum of the adduct resembles the Pr spectrum of PhyB-N651-PCB. The absorption maximum of 670 nm is 15 nm red shifted vs. the absorption maximum of PhyB-N651-PCB (Figure 3.4 B). Such a red shift is observed for all 15*Za* adducts that have been analyzed here and in previous studies (Inomata, K. et al. 2005b). The assembly with 15*Ea*PCB was also completed after ca. 20 min. This adduct has an absorption maximum at 715 nm, in accordance with the Pfr maximum of PhyB-N651-PCB. The peak absorption is only 1.3 times higher than that of the 670 nm shoulder (Figure 3.4 E). In this respect, the spectrum differs from other 15*Ea* adducts, in which the peak is ca. 2 times higher than the shoulder.

Despite minor spectral differences between the locked chromophore adduct and the Pr and Pfr form of PhyB, the spectral similarities suggest that the 15*Za* chromophore imposes a Pr and the 15*Ea* chromophore imposes a Pfr conformation of the protein. It should be noted that the assembly of PhyB-N651 was less efficient than the assembly of the other proteins used in the present study. Since the low efficiency was found for all chromophores, it assumes that it reflects an adverse folding property of the recombinant proteins or inappropriate buffer conditions.
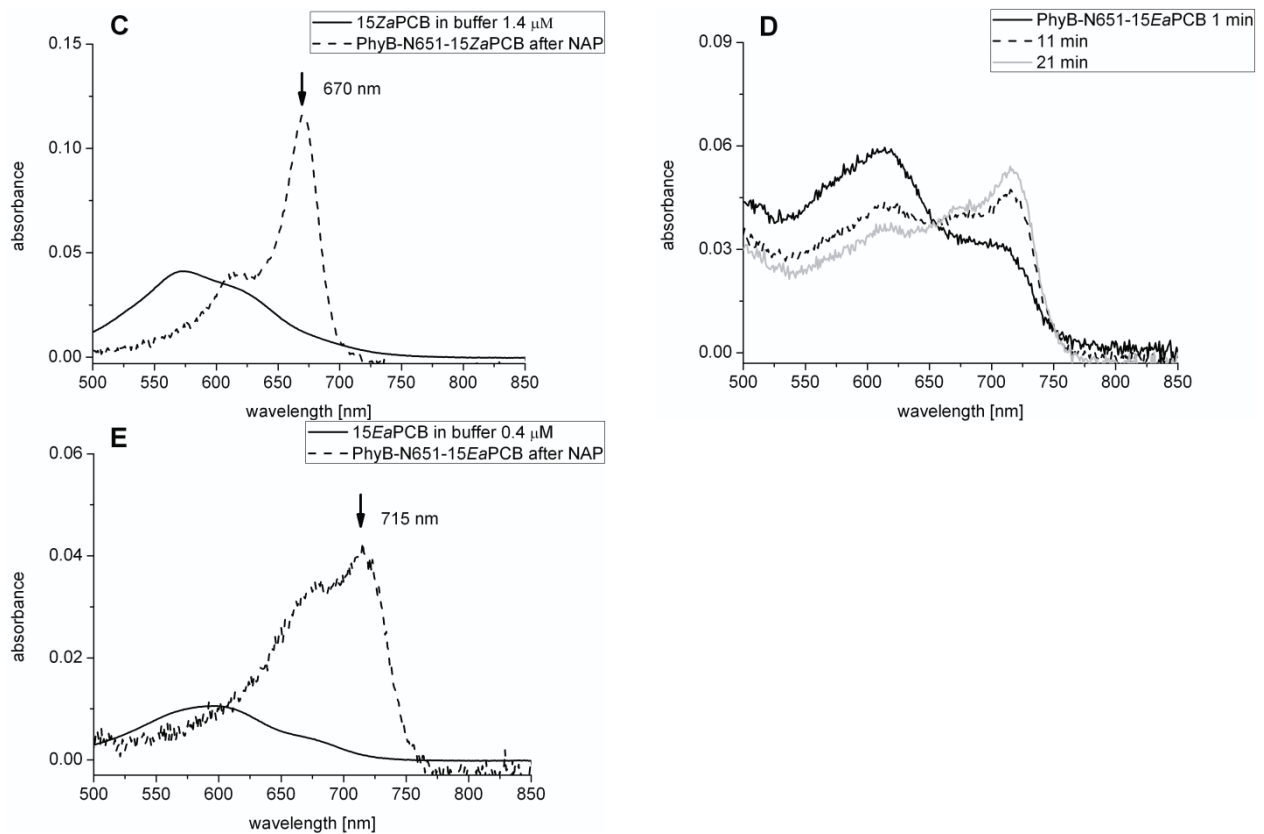
Figure 3.4 PhyB-N651 chromophore adducts. A, Absorption spectra of free BV in buffer, the BV adduct after NAP column separation in the dark adapted Pr form, after red light irradiation, and of calculated Pfr. B, Spectra of free PCB, the PCB adduct after NAP column separation, in the dark adapted Pr form, after red light irradiation, and of calculated Pfr. C, Spectra of free 15*Za*PCB and the 15*Za*PCB adduct after NAP column separation. D, Spectra of the assembly with 15*Ea*PCB recorded at the indicated time points after mixing. E, Spectra of free 15*Ea*PCB and the 15*Ea*PCB adduct. The spectra of free chromophores in A, B, C and E are recorded in the same buffer as the proteins and are calculated to the estimated concentration of the holoprotein. (Concentrations are given). In A and B, the estimated Pfr/P_{tot} contents of the red irradiated samples are given. The spectra of calculated Pfr were drawing using the formula (Red light irradiated spectra - (1 − Value $_{Pfr/Ptot}$) × Pr) / Value $_{Pfr/Ptot}$, the Value $_{Pfr/Ptot}$ were chosen through till nice spectra showed out 0.5 to 0.9.

3.1.1.2 Locked chromophores form covalent bonds with plant phytochrome

In order to find out whether the chromophore adducts measured above can form covalent bonds or not, SDS test was performed. According to the absorbance spectra of SDS treated samples before/after after NAP column separation, covalent or non-covalent bond can be detected. If the absorption spectra do not change, before and after NAP column separation, means chromophore can covalent bond to protein, otherwise not. SDS-Zn^{2+} fluorescence, another efficient way to check the covalent bond, give more directly information, the covalent bond will show fluorescence signal on coomassie gel, not, if there is non-covalent bond. That is because Zn^{2+} can form a covalent bond with chromophore and showing fluorescent signal, if the chromophore also covalent bind to protein, in SDS-PAGE gel, at the position of protein, a fluorescent signal should be detected.

Agp1-M15 Figure 3.5 shows that only BV formed a covalent bond with Agp1-M15, others didn't. This is accordingly with our suggestion, if there is no *Cys* chromophore binding site at the GAF domain, there should be non-covalent binding of PCB, 15*Za*PCB and 15*Ea*PCB. Covalent binding can be detected by the addition of SDS to the sample and run a NAP column later. The none covalently bound chromophore is then lost during the NAP separation, seen in the spectrum by the loss of its absorption peak. The absorption changes compared to the normal absorption due to the addition of SDS. Zn^{2+} fluorescence showed the same results as the SDS NAP column assay. Agp1-M15-BV was the only adduct forming a covalent bond, of other BV-adducts. Fluoresce signal was detected.
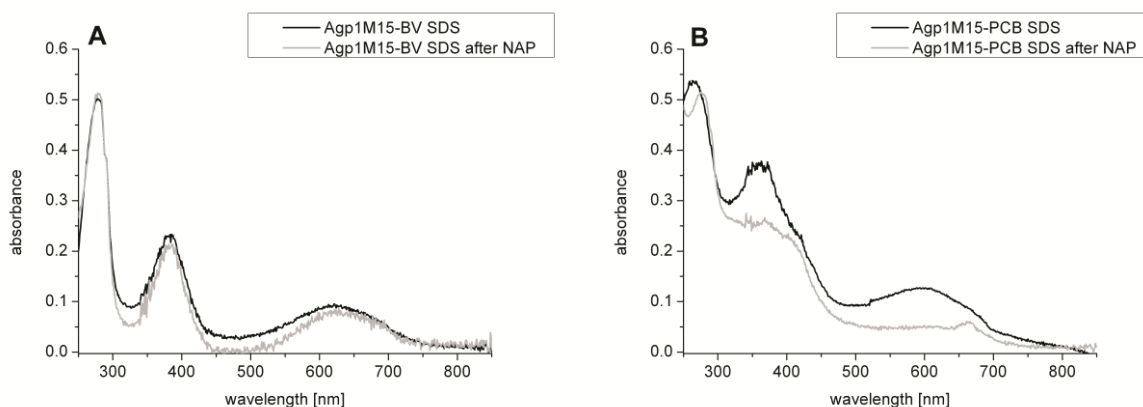
Figure 3.5 SDS-NAP spectra analysis of Agp1-M15 chromophore adducts and Zn^{2+} fluorescence. A, Agp1-M15-BV in SDS buffer before and after the NAP. B, Agp1-M15-PCB in SDS buffer before and after the NAP. C, Agp1-M15-15ZaPCB in SDS buffer before and after the NAP. D, Agp1-M15-15EaPCB in SDS buffer before and after the NAP. E, Agp1-M15-BV, PCB, 15ZaPCB, and 15EaPCB adducts, SDS-PAGE and Zn^{2+}-fluorescence; the gel was stained with Coomassie (left) and subjected to Zn^{2+}-fluorescence (right).

Agp1-M15CV PCB, 15ZaPCB and 15EaPCB formed a covalent bond with Agp1-M15CV except BV. The SDS treated protein-chromophore adducts were pass through NAP 10 column. The absorbance spectra before and after NAP column were almost same in the case of locked 15ZaPCB and 15EaPCB adducts, only a little bit peak lost at blue range for PCB. Although Zn^{2+} fluorescence showed a weak fluorescence signal of 15ZaPCB (Figure 3.6 E), this might be due to a general weaker binding of Zn^{2+} to 15ZaPCB compared with PCB and 15EaPCB. Nonetheless covalent binding were detected for both locked chromophore adducts.
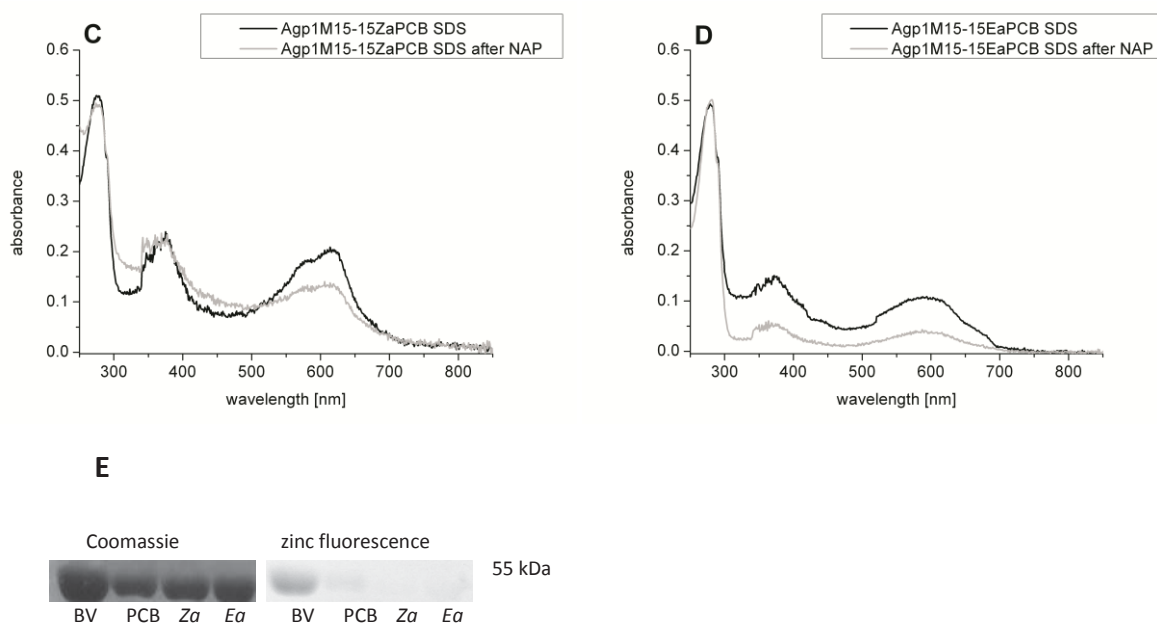
Figure 3.6 SDS-NAP spectra analysis of Agp1-M15CV chromophore adducts and Zn^{2+} fluorescence. A, Agp1-M15CV-BV in SDS buffer before and after the NAP. B, Agp1-M15CV-PCB in SDS buffer before and after the NAP. C, Agp1-M15CV-15*Za*PCB in SDS buffer before and after the NAP. D, Agp1-M15CV-15*Ea*PCB in SDS buffer before and after the NAP. E, Agp1-M15CV-BV, PCB, 15*Za*PCB, and 15*Ea*PCB adducts, SDS-PAGE and Zn^{2+}-fluorescence; the gel was stained with Coomassie (left) and subjected to Zn^{2+}-fluorescence (right).

Cph1 Although the absorbance spectra of Cph1 locked chromophore adducts were not in accordance with PCB and BV adducts, comparing the SDS treated denatured samples before and after NAP column spectra showed, that no absorbance peak reduces, indicates Cph1-15*Ea*PCB and 15*Za*PCB adducts all the peak shows in the absorbance spectra (Figure 3.3 F, G) were covalent bond. Zn^{2+} fluorescence gave the same results: except BV all chromophores

formed covalent bonds. Again the 15*Za*PCB adduct had a lower Zn^{2+} fluorescence intensity compared with the others chromophore adducts.
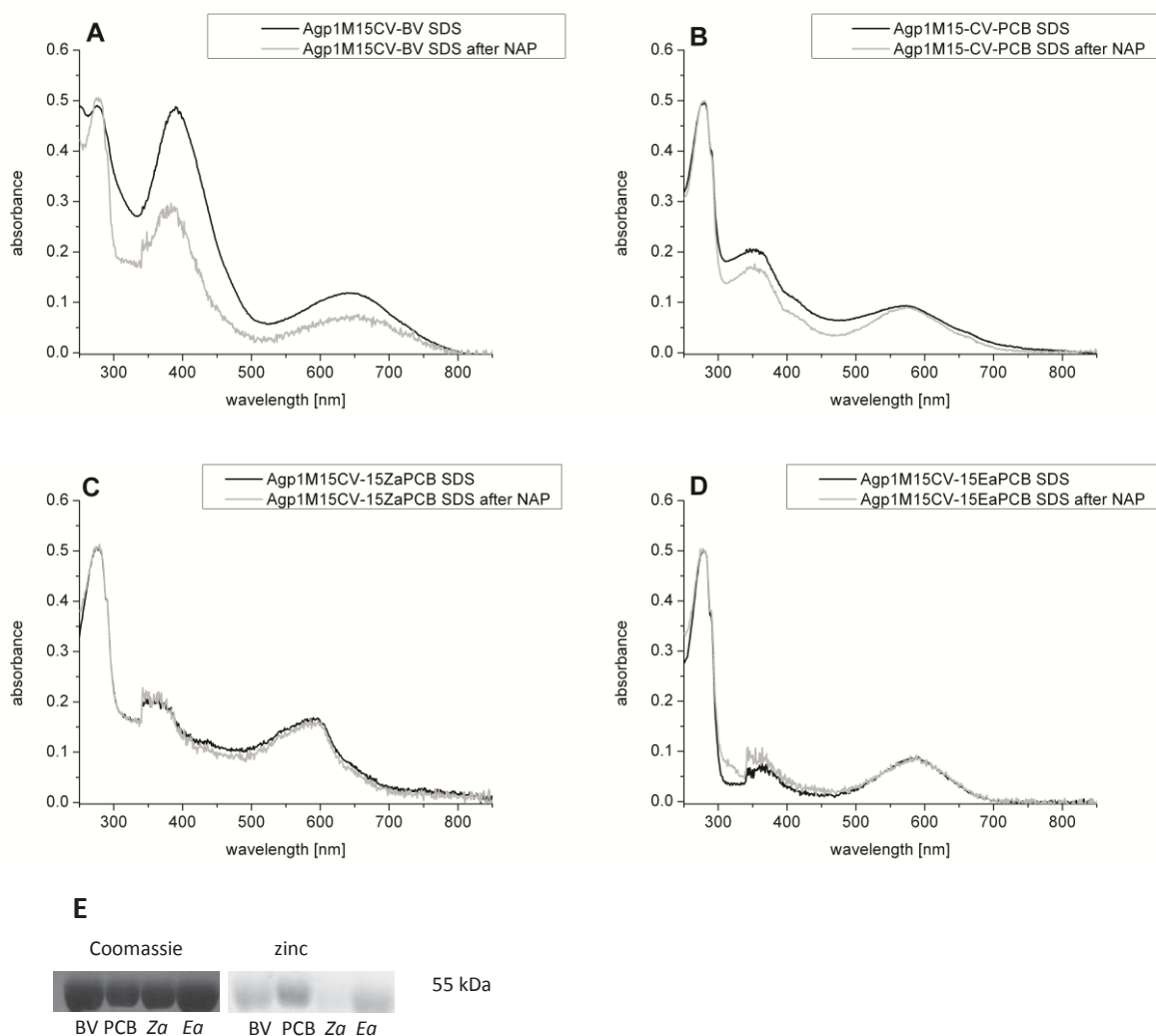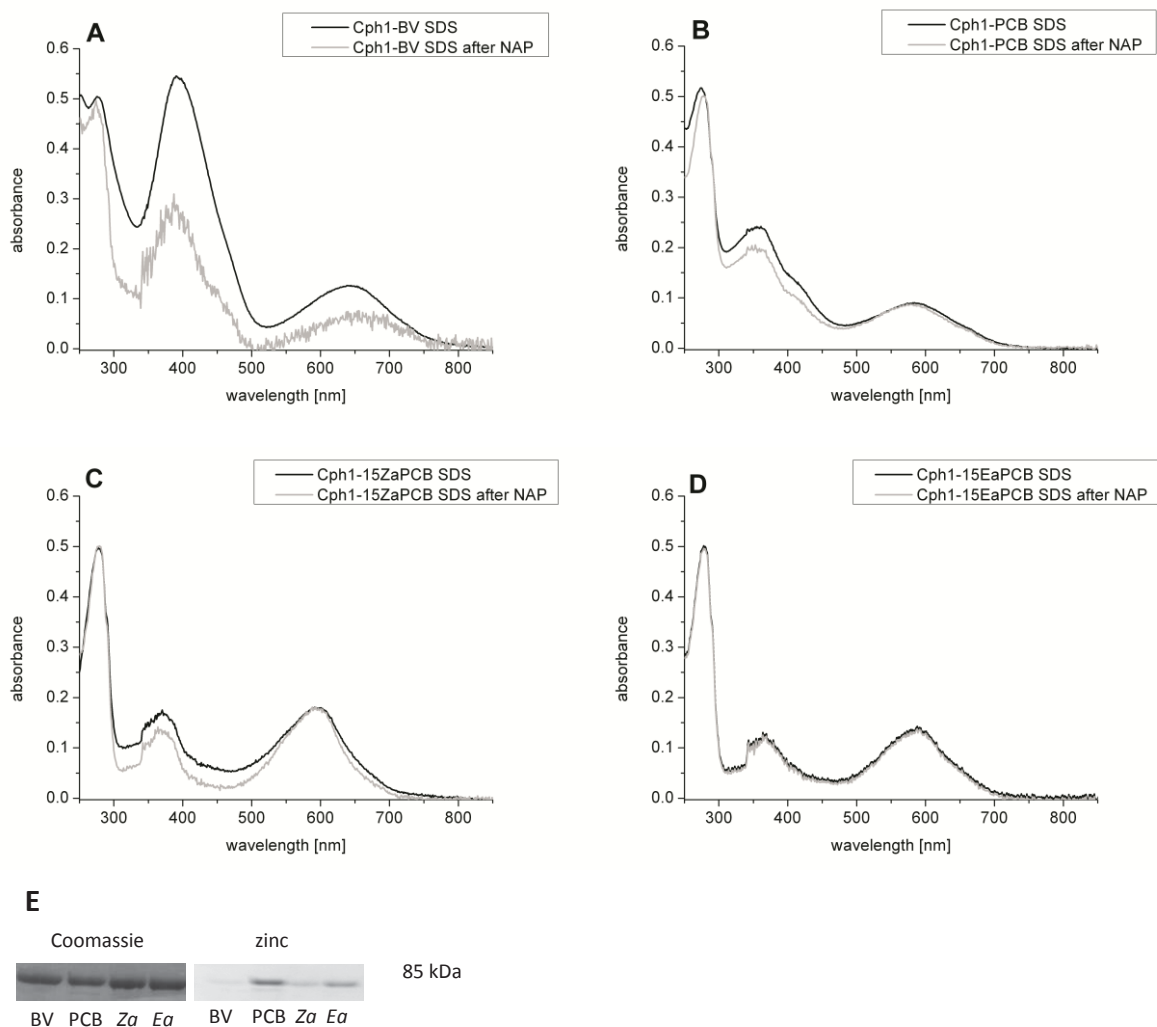

Figure 3.7 SDS-NAP spectra analysis of Cph1 chromophore adducts and Zn^{2+} fluorescence. A, Cph1-BV in SDS buffer before and after the NAP. B, Cph1-PCB in SDS buffer before and after the NAP. C, Cph1-15*Za*PCB in SDS buffer before and after the NAP. D, Cph1-15*Ea*PCB in SDS buffer before and after the NAP. E, Cph1-BV, PCB, 15*Za*PCB, and 15*Ea*PCB adducts, SDS-PAGE and Zn^{2+}-fluorescence; the gel was stained with Coomassie (left) and subjected to Zn^{2+}-fluorescence (right).

PhyB-N651 Comparing the absorbance spectra of SDS treat samples before and after NAP column separation, the covalent bond is strong in the PCB and the 15*Ea*PCB adducts and a little bit weaker with 15*Za*PCB, because of the slight loss of the peak in the red range. No covalent bond were detected in BV adduct. Zn^{2+} fluorescence results prove the SDS-NAP column results; all the chromophores except BV form the covalent bond with plant phytochrome.
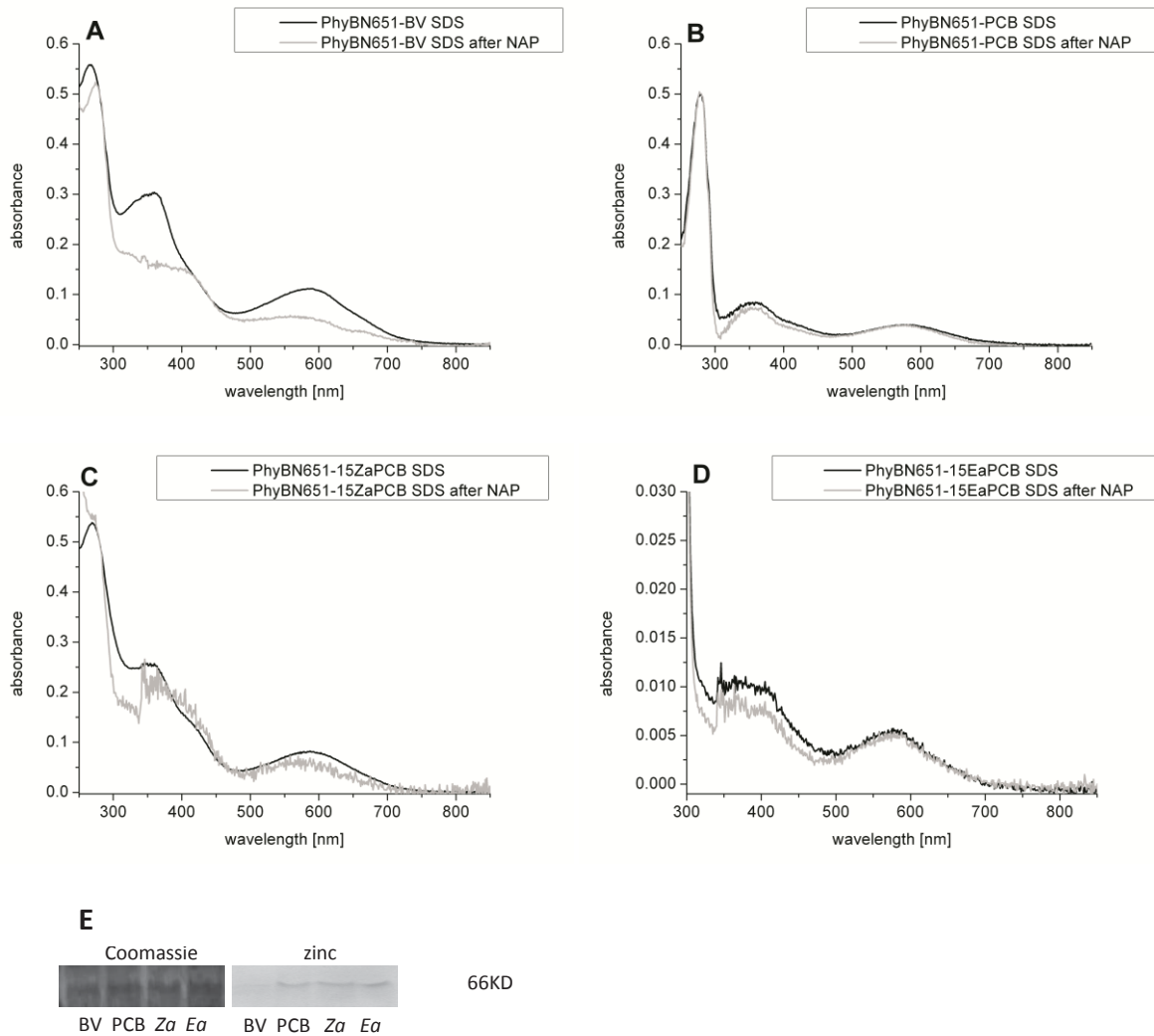
Figure 3.8 SDS-NAP spectra analysis of Phytochrome adducts and Zn^{2+} fluorescence. A, PhyB-N651-BV mixed with SDS before and after the NAP. B, PhyB-N651-PCB mixed with SDS before and after the NAP. C, PhyB-N651-15*Za*PCB mixed with SDS before and after the NAP. D, PhyB-N651-15*Ea*PCB mixed with SDS before and after the NAP. E, Adducts wit BV, PCB, 15*Za*PCB, and 15*Ea*PCB, SDS-PAGE; the gel was stained with Coomassie (left) or subjected to Zn^{2+}-fluorescence (right).

3.1.1.3 Locked chromophore adducts have no photoconversion

Red or far red light were used to irradiate the phytochrome adducts to check whether the locked derivatives have photoconversion abilities or not. Samples used were fully assembled with a protein concentration of between 1 to 6 μM. They were illuminated with red and far red light, subsequently. Figure 3.9 shows that both the locked chromophore adducts cannot undergo photoconversion, no data A detect, compared with PCB adduct.
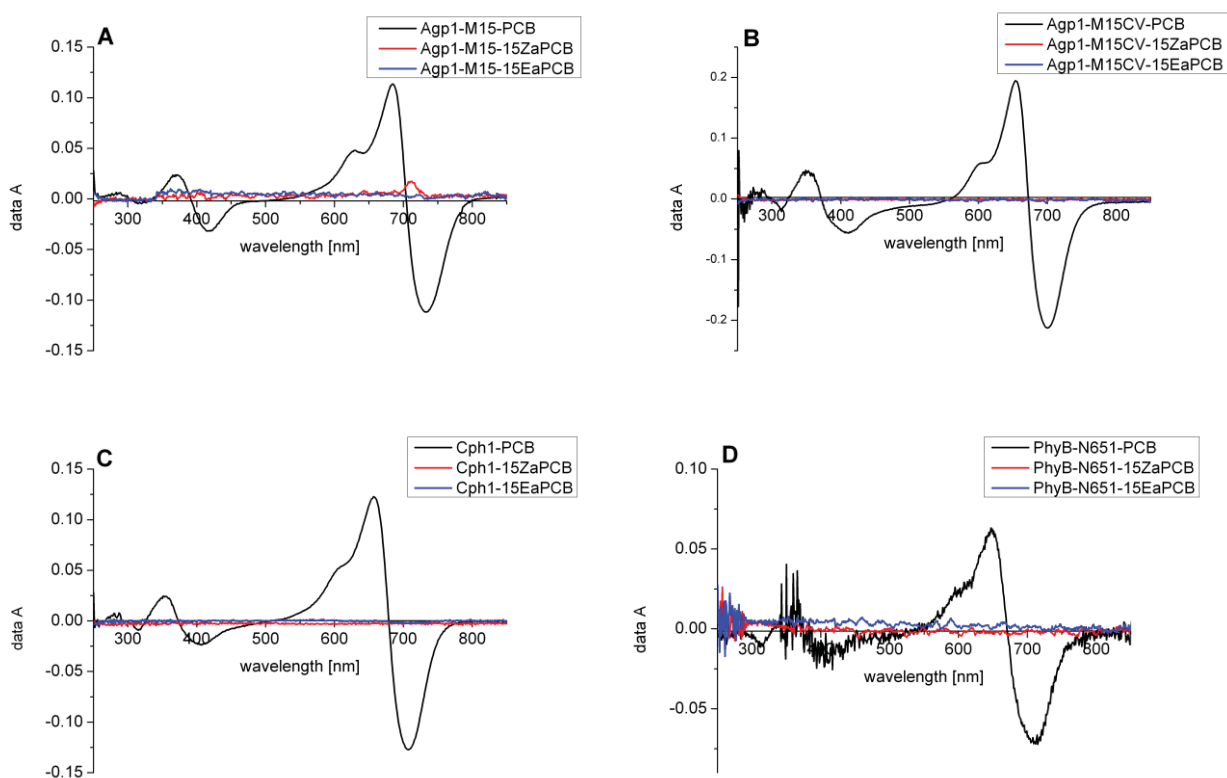
Figure 3.9 Difference spectrum of phytochrome chromophore adducts. Difference spectra is generated by far red irradiated sample minus red light irradiated sample, which shows the photoconversion ability. A, Difference spectra of Agp1-M15 with PCB, 15*Za*PCB and 15*Ea*PCB adducts. B, Difference spectra of Agp1-M15CV with PCB, 15*Za*PCB and 15*Ea*PCB adducts. C, Difference spectra of Cph1 with PCB, 15*Za*PCB and 15*Ea*PCB adducts. D, Difference spectra of PhyB-N651 with PCB, 15*Za*PCB and 15*Ea*PCB adducts.

3.1.1.4 Strong fluorescence of 15*Za*PCB

Very weak fluorescence signal is detected on wild type Agp1 and Agp2 phytochrome at room temperature. When locked BV chromophores or Agp1, Agp2 mutants were used, in which block the photoconversion, strong fluorescence signal can be detected (Zienicke, B. et al. 2011b). In my work locked 15*Za*PCB and 15*Ea*PCB chromophores which cannot undergo photoconversion (Figure 3.9) were used to assemble with recombinant proteins: Agp1-M15, Agp1-M15CV, Cph1, and PhyB-N651 to test the fluorescence signal in *vitro*. Figure 3.10 below shows the emission-excitation spectra of locked PCB chromophore adducts.

Fluorescence spectra of 15*Za*PCB adduct was first test. In the emission spectra of Agp1-M15-15*Za*PCB adduct at room temperature, the maximum is located in the range of 709 nm to 715 nm, in particular, at 712 nm, as showing on Figure 3.10 A. Excitation spectra of Agp1-M15-15*Za*PCB adduct had maximum at 707 nm (Figure 3.10 A). λ e for the emission spectra was 690 nm, λ m for the excitation spectra was 725 nm. For Agp1-M15CV-15*Za*PCB the emission peak is blue shift compared with Agp1-M15-15*Za*PCB, at 686 nm (Figure 3.10 B). The fluorescence counts of excitation spectra at maximum wavelength (679nm) were a little bit lower than the emission spectra (Figure 3.10 B). For Cph1-15*Za*PCB the emission maximum was at 687 nm, excitation maximum was at 681 nm, with the fluorescence counts of 1.25×10^8 (Figure 3.10 C). Both the maximum and the fluorescence counts were identically compared with Agp1-M15CV-15*Za*PCB. PhyB-N651-15*Za*PCB had a maximum emission at 677 nm, even blue shift with Cph1 and Agp1-M15CV adducts, shows the different character of those adducts. Excitation maximum of PhyB-N651-15*Za*PCB was 675 nm, with 7.5×10^7 fluorescence count (Figure 3.10 D). According to those results I conclude that all 15*Za*PCB adducts had fluorescence signals, no matter if they form covalent bonds or not, but the intensity of the fluorescence signal was different between covalent and non-covalent adducts. The fluorescence spectra shows covalent bond results in a strong fluorescence signal (Figure 3.10 A-D), except Agp1-M15 non-covalent bond with 15*Za*PCB; others had covalent bond (Figure 3.5-3.8). So I could show that fluorescence signal can enhance through covalent bound. The intensity of the fluorescence signal was somehow also dependent on the apoprotein. Three times stronger fluorescence

signals were detect for Agp1-M15CV-15*Za*PCB and PhyB-N651-15*Za*PCB compared to Agp1-M15-15*Za*PCB. A much stronger signal was found in the Cph1 -15*Za*PCB adduct more than 5 times compared to Agp1-M15-15*Za*PCB, might because of the molecular weight of Cph1. In one of the old publication they also discussed the molecular weight of pigment might affect the fluorescence of phytochrome (Sineshchekov. V. A, 1995).

Later I measured the fluorescence signal of 15*Ea*PCB adducts, but in all 15*Ea*PCB adducts only a weak fluorescence signal can be detected in Agp1-M15CV-15*Ea*PCB adduct, around 4×10^6 fluorescence counts at the maximum of emission spectra, almost 20 times lower compared with Agp1-M15CV-15*Za*PCB adduct.
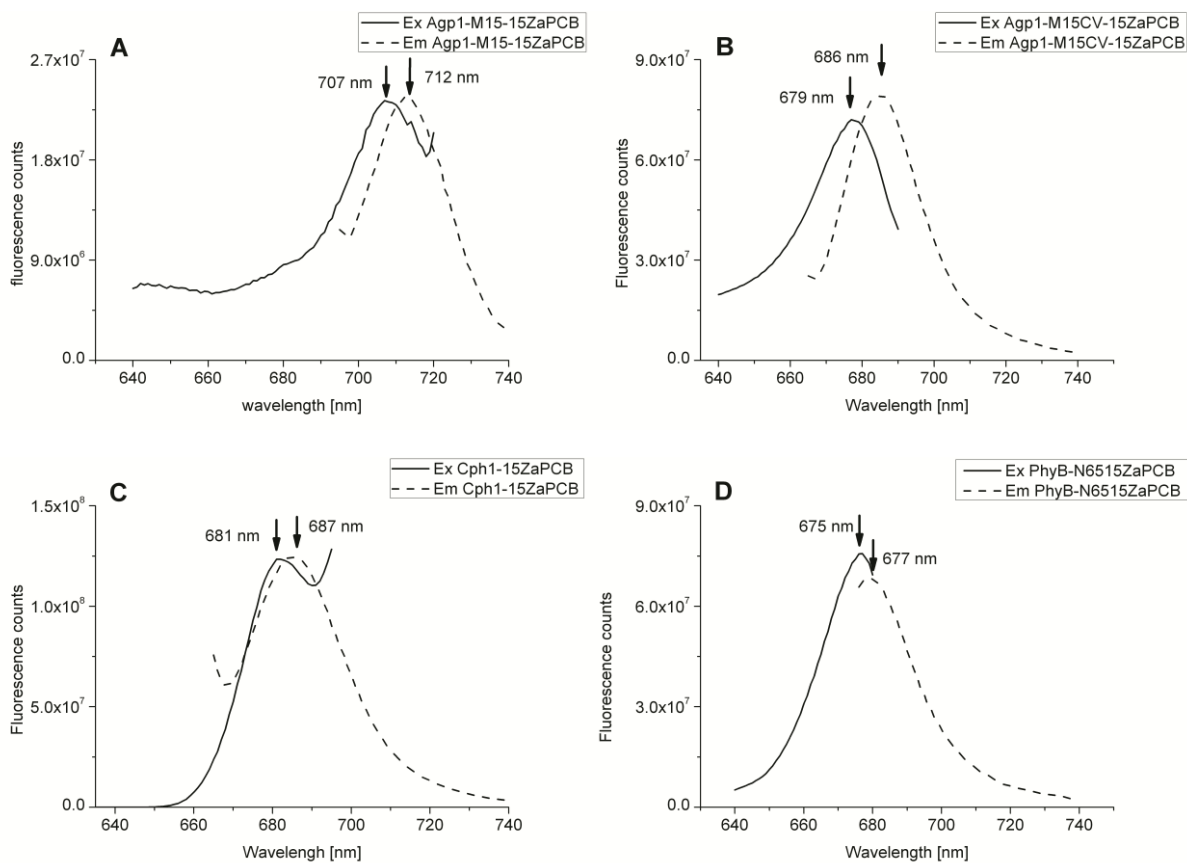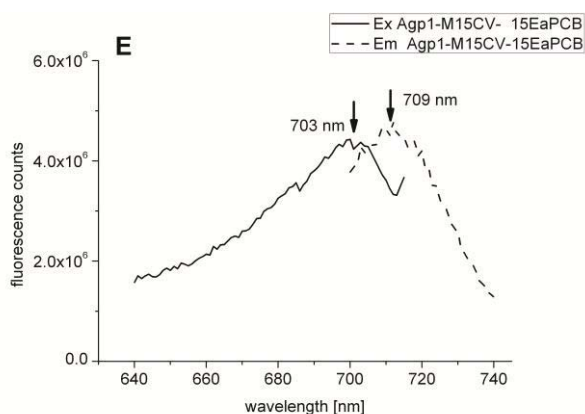
Figure 3.10 Emission-excitation fluorescence spectra of locked chromophore adduct. A, Agp1-M15-15*Za*PCB fluorescence spectra, emission spectra under excitation at λ e=690 nm, excitation spectra, emission wavelength monitored, λ m=735 nm. B, Agp1-M15CV -15*Za*PCB fluorescence spectra, emission spectra under excitation at λ e=665 nm, excitation spectra, emission wavelength monitored, λ m=695 nm. C, Cph1 -15*Za*PCB fluorescence spectra, emission spectra under excitation at λ e=660 nm, excitation spectra, emission wavelength monitored, λ m=700 nm. D, PhyB-N651-15*Za*PCB fluorescence spectra, emission spectra under excitation at λ e=660 nm, excitation spectra, emission wavelength monitored, λ m=695 nm. E, Agp1-M15CV -15*Za*PCB fluorescence spectra, emission spectra under excitation at λ e=680 nm, excitation spectra, emission wavelength monitored, λ m=720 nm

Cph1-PEB adducts as a reference for new phytochrome chromophore adducts, were measured by Zienicke.B. The quantum yield of PEB-Cph1 is 0.54. (Zienicke, B. et al. 2011b). Table 3.2 shows the quantum yield of locked chromophore adducts mentioned before. Because of the non-covalent bond, Agp1-M15-15*Za*PCB adduct only had a weak quantum yield. The quantum yield was 0.003 which was almost 10 times lower than Agp1-M15CV-15*Za*PCB, but compared with its natural chromophore Agp1-M15-BV it is about 15 times higher (Zienicke, B. et al. 2011b). The quantum yield of Agp1-M15CV, Cph1 and PhyB-N651-15*Za*PCB adducts were in the same magnitude. For Cph1 it is slightly stronger than the other two. The stronger quantum yield may be because of the covalent bond. The quantum yield of Agp1-M15CV-15*Ea*PCB, was only 0.003, which was the same as for Agp1-M15-15*Za*PCB but much lower than for other covalent 15*Za*PCB adducts. Lower quantum yield of 15*Ea*PCB adducts, indicated the low Pfr fluorescence.

Stokes shift give the information of the peak shift from absorbance to emission of a same electronic transition. When a system absorbs a photon, it enters an excited state. Emit a photon is one way for the system to relax, when the emitted photon has less energy than the absorbed photon, this energy difference is called the Stokes shift. The less the energy loss through emit the photon the less of the value of stokes shift. Table 3.2 shows that the stokes shift of non-covalent bond was small then covalent bond, 2 nm for Agp1-M15-15*Za*PCB, 7 to 9 nm for other covalent adducts.

According to the results, the stronger fluorescence of 15*Za*PCB adducts and the weaker fluorescence of 15*Ea*PCB makes them both possible to work as intracellular marker. *In vivo* fluorescence signal are discussed in section 3.2.2.4.

	Quantum yield	Stock Shift (nm)	Em (nm)	Ex (nm)	Ab (nm)
Agp1-M15-15*Za*PCB	0.003	2	712	707	710
Agp1-M15CV-15*Za*PCB	0.028	7	686	679	679
Cph1-15*Za*PCB	0.050	9	687	681	678
PhyB-N651-15*Za*PCB	0.010	7	679	677	670
Agp15CV-15*Ea*PCB	0.003	8	709	703	701
Fluorescein	0.950	26	516	489	490
Cph1-PEB	0.537	10	590	579	580

Table 3.2 Quantum yield and stock shift of locked chromophore adducts.

3.1.2 *In vivo* studies

According to the *in vitro* studies results, locked chromophores can assemble with plant phytochrome and form covalent bond. The absorbance spectra of 15*Za*PCB adduct corresponds spectrally more like the Pr form and 15*Ea*PCB adduct spectral more like the Pfr form. But can these chromophores assemble also *in vivo*? And if so, can 15*Ea*PCB induce phytochrome responses in darkness?

Ceratodon purpureus

3.1.2.1 15*Ea*PCB induced chlorophyll synthesis in darkness

In the next steps, I tested the effect of locked chromophores on *Ceratodon purpureus* filaments. It has been found that red light induces via phytochrome chlorophyll synthesis in *Ceratodon purpureus* filaments (Lamparter, T. et al. 1997a). Dark grown filaments of the phytochrome-chromophore deficient mutant *ptr116* were incubated on medium containing BV, PCB, PEB, 15*Za*PCB or 15*Ea*PCB and chlorophyll synthesis levels were assayed in the tip cell by confocal laser scanning microscopy. Untreated wild type (wt4) filaments were taken as a control. During the last 24 h before the measurements, filaments were either kept in darkness or irradiated continuously with red light. Red light increased chlorophyll synthesis levels in the wt4 but not in *ptr116 t*ip cells. In the presence of BV or PCB, red light induced an increase of chlorophyll also in the *ptr116* tip cells (Figure 3.11). These results are in accordance with earlier studies (Lamparter, T. et al. 1997a). Feeding with 15*Ea*PCB resulted in an increase of chlorophyll in darkness to levels in the range of red light treated *ptr116* cells grown on PCB or BV (Figure 3.11). No differences can be found between the 15*Ea*PCB light and dark treated samples. The chlorophyll synthesis level was a little bit induced by the PEB and 15*Za*PCB treatment. which may be because of the feedback effect because the chromophore and chlorophyll sharing the same synthesis pathway (Terry, M. J. and Kendrick, R. E. 1999). From these results I conclude that 15*Ea*PCB results in the formation of an active Pfr equivalent in the cell, which in turn induces chlorophyll synthesis in darkness. The strong effect of 15*Ea*PCB on chlorophyll synthesis shows that in *Ceratodon purpureus* and most likely also in other mosses, all enzymes of the chlorophyll biosynthesis pathway are active in darkness, see discussion (section 4.4.3). The size of chloroplasts in 15*Ea*PCB treated tip cells were not changed, only much more chloroplast were observed compared to dark grown samples (Figure 3.11 C, F). According to former studies, both size and replication of chloroplasts is red and far red reversible. So our 15*Ea*PCB seems to works mainly on the replication of chloroplasts (Kasperbauer, M. J. and Hamilton, J. L. 1984, Lamparter et al, 1997).
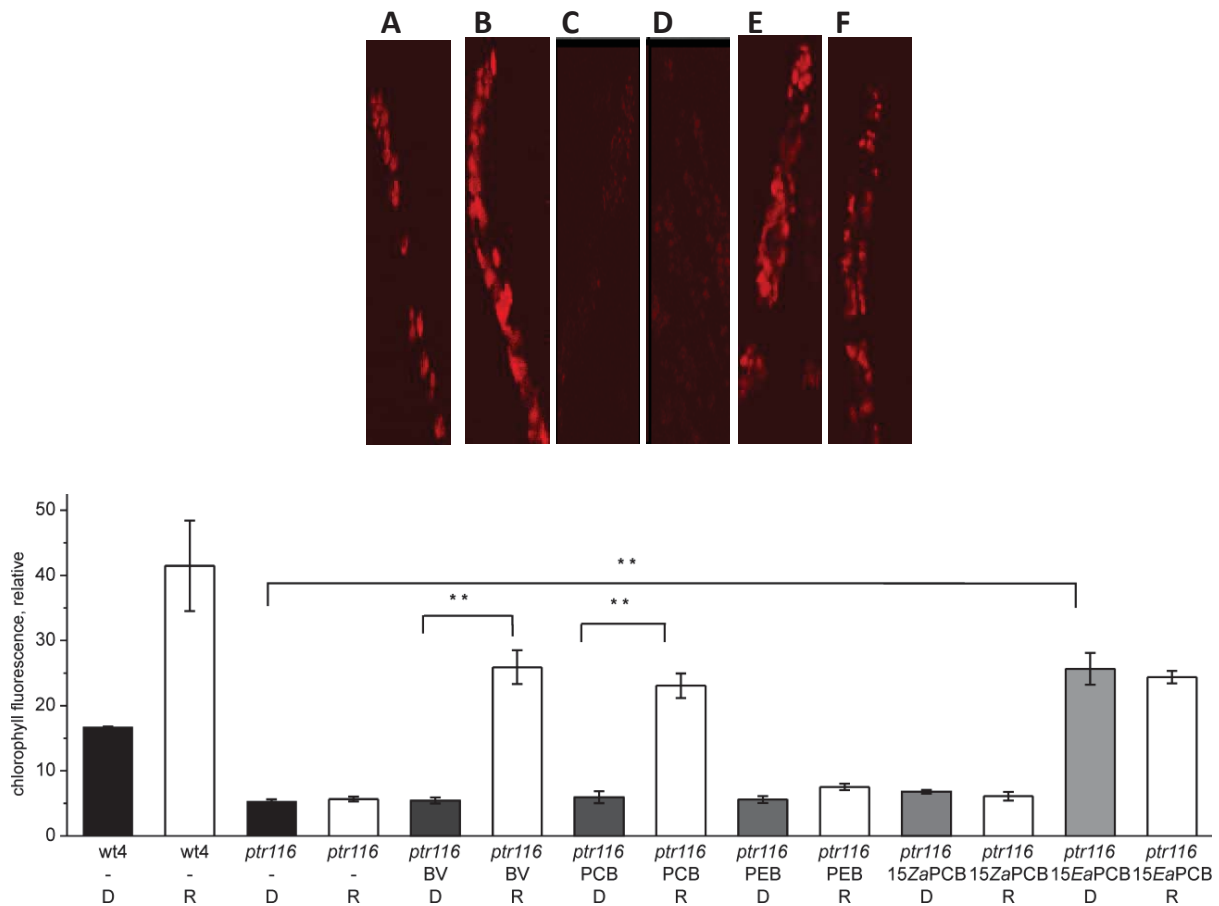
Figure 3.11 Effect of chromophore on chlorophyll fluorescence of protonemal tip cells of *Ceratodon purpureus* wt4 and *ptr116* mutant. All filaments were grown for a total of 7 days. Red light irradiations and chromophore treatments were performed during the last day. A to F, fluorescence images of typical tip cells recorded with the same parameter settings. A, dark grown wild type wt4. B, red light irradiated wt4. C, dark grown mutant *ptr116*. D, red irradiated *ptr116*. E, red light irradiated *ptr116* on BV. F, dark grown *ptr116* on 15*Ea*PCB. G, relative chlorophyll fluorescence of tip cells. Moss strains (wt: wt4), light treatment (R: red / D: darkness) and chromophore treatment is indicated under each bar. Mean values of 30 or more cells from 3 experiments ± SE. In some cases (see brackets above the bars) Student's *t*-test was performed for significance, **P < 0.01.

Figure 3.12 Effect of 15*Ea*PCB on chlorophyll content of *Ceratodon purpureus* K1 tip cells. All filaments were grown for a total of 3 days. Red light irradiations and chromophore treatments were performed during the last day. A to C, fluorescence of typical tip cells. A, dark grown. B, red light treated. C, dark gr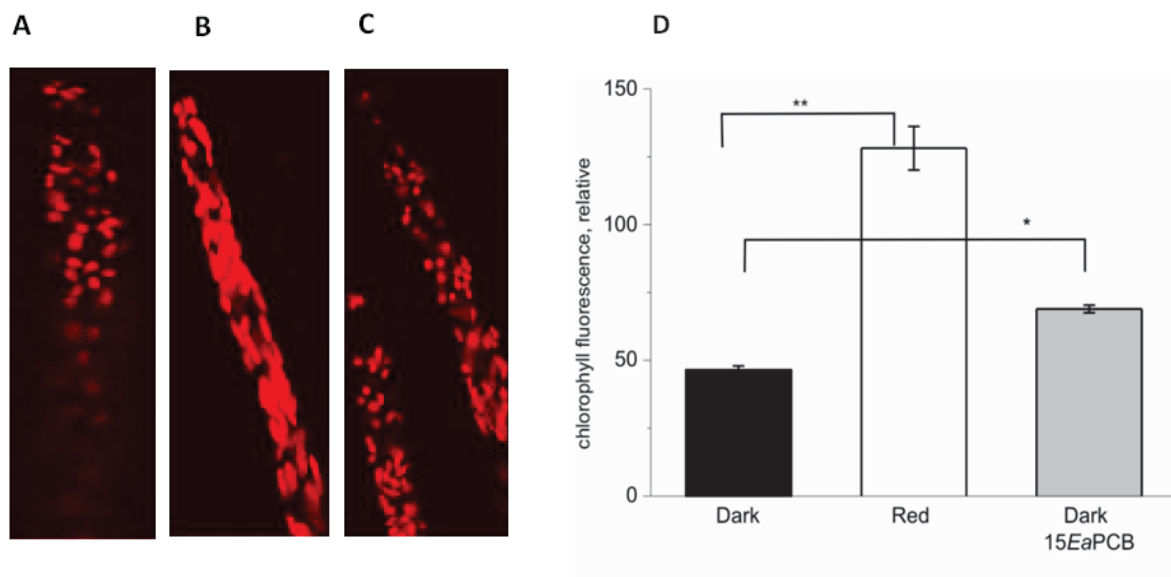own on 15*Ea*PCB. D, quantification of relative chlorophyll fluorescence, mean values of 30 or more tip cells from 3 experiments ± SE. Asterisks denote Student's *t*-test significance, *$P < 0.05$, **$P < 0.01$.

Subsequent experiments were performed with a newly isolated wild type strain, termed K1. When protonemata were incubated on medium with 15*Ea*PCB, chlorophyll synthesis level was increased over the untreated control in darkness. This result shows that the inductive effect can also be induced in wild type cells. It is expected that 15*Ea*PCB competes with the natural chromophore PΦB for incorporation into holo phytochrome. In earlier experiments (Boese, G. et al. 2004a), wt4 and *ptr116* were fed with PEB, which is also incorporated into phytochrome and produces fluorescent adducts. In this work, the PEB chromophore was incorporated into about one fourth of the phytochrome molecules in wild type cells. The relative increase of the chlorophyll level by 15*Ea*PCB in the K1 wild type was not as strong as in *ptr116* or the induction by red light. This is most certainly the result of only partial 15*Ea*PCB incorporation into phytochrome, due to competition with the internal chromophore. Quite interestingly, the 15*Ea*PCB induced increase of chlorophyll content is about one fourth of the red light induced increase. This correlates well with the ca 25% chromophore incorporation into wild type cells rate mentioned above.

3.1.2.2 15*Ea*PCB induced branch formation in darkness

It has been shown that the formation of side branches is induced by phytochrome (Kagawa, T. et al. 1997). I thus tested the effect of 15*Ea*PCB on branch formation (Figure 3.13). Here, untreated cells had a branch formation rate of about 6 %, which increased to 100 % in red light (Figure 3.13 D), i.e. under these conditions all filaments form side branches in the region of the upper 5 cells. Feeding 15*Ea*PCB to dark growing filaments resulted in a branch formation rate of 26 %, which is significantly higher than the rate of the untreated dark control. As above, the increase correlates roughly with the proposed incorporation rate of 15*Ea*PCB.
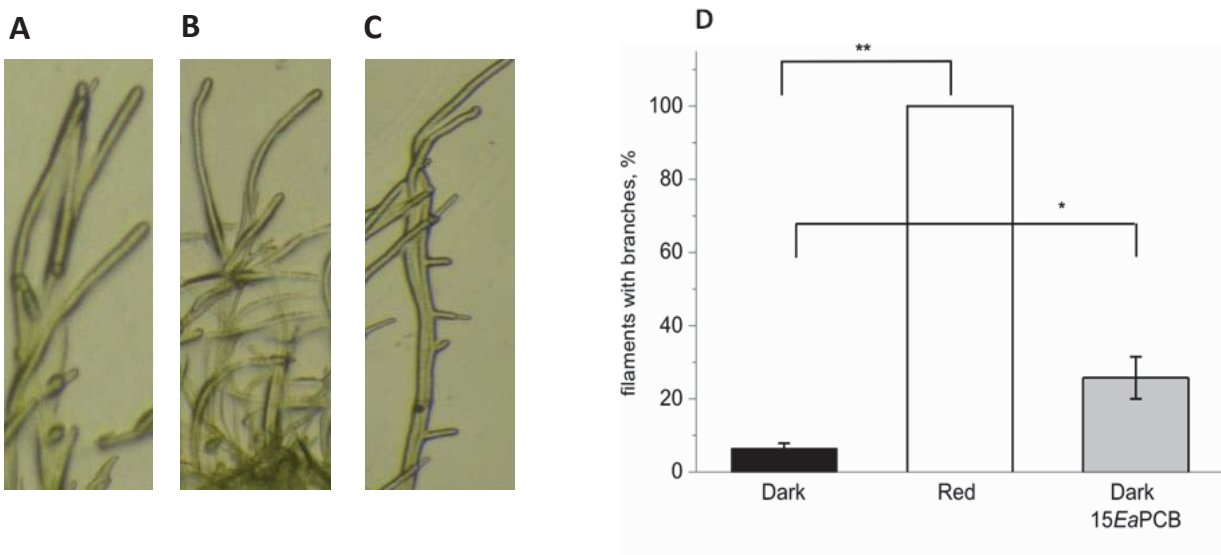
Figure 3.13 Effect of 15*Ea*PCB on branch formation of *Ceratodon purpureus* K1. All filaments were grown for a total of 3 days. Red light irradiations and chromophore treatments were performed during the last day. A, dark grown filaments. B, red light treated filaments. C, dark grown filaments on 15*Ea*PCB. D, calculated branch formation rate, mean values of 30 or more filaments from 3 experiments ± SE. Asterisks denote Student's *t*-test significance, * $P < 0.05$, **$P < 0.01$.

3.1.2.3 15*Ea*PCB disturbed gravitropism in darkness

The gravitropism response of *Ceratodon purpureus* filaments growing in darkness is inhibited by red light via phytochrome (Lamparter, T. et al. 1998). Since red light also induces the phototropic response, a direct effect of phytochrome on gravitropism could only be analyzed with Class II mutants in which phototropism is specifically inhibited (Esch, H. et al. 1999). In our present experiments with K1, in which the filaments were re-oriented by 90° after initial growth and analyzed 48 h later, the tip cells of dark growing filaments were aligned according to the new growth direction. When these filaments were irradiated with red light after reorientation, the final growth direction was random (Figure 3.14 B). This effect is in accordance with earlier studies that had been performed with wt4 (Lamparter, T. et al. 1998). It should be noted that in the setting of the experiment the phototropic response is impaired because irradiation occurs through the cellophane on which the filaments grow. The curvatures of dark growing filaments that were either kept on standard medium or exposed to medium with 15*Za*PCB or 15*Ea*PCB were quantified, whereas the curvatures of filaments grown in red light were not further quantified. A curvature of almost 90 ° of the tip were obtained for untreated filaments and for filaments grown on 15*Za*PCB and 15*Ea*PCB. However, the curvature of these filaments measured 200 µm behind the tip was only 45 ° in the case of 15*Ea*PCB treated filaments, as compared to almost 90 ° in the case of untreated filaments or filaments grown on 15*Za*PCB (Figure 3.14 D). This shows that after reorientation, the tip cell finds its new growth direction later when 15*Ea*PCB is present in the medium. As there is no difference between 15*Za*PCB treated and control sample, in the same time moss filaments grow normal on the 15*Ea*PCB plates, I concluded that 15*Ea*PCB reduces the sensitivity of the gravitropic response, most likely via its incorporation into phytochrome and formation of Pfr.
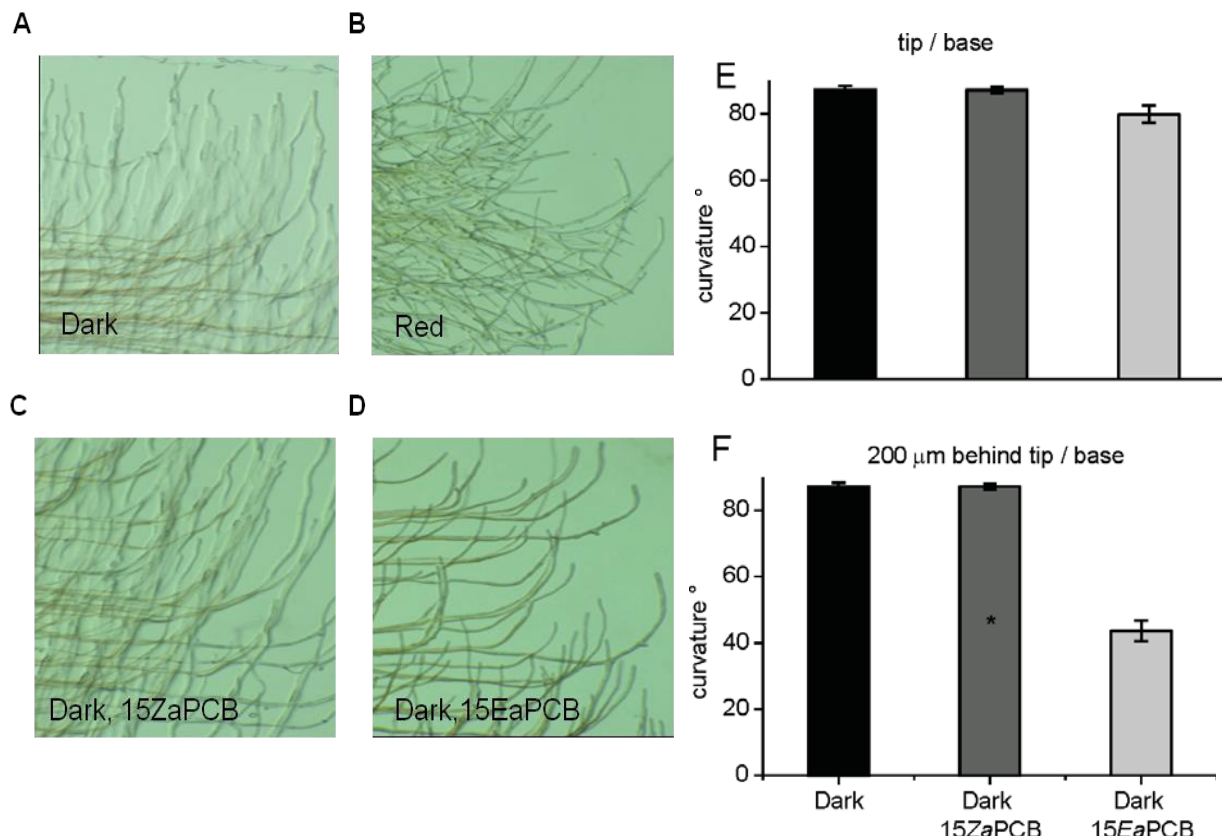
Figure 3.14 Effect of chromophores on the gravitropic response of *Ceratodon purpureus* K1. Filaments grown for 3 d in darkness were re-oriented by 90 °C and kept for another 48 h in darkness or in red light on medium with or without chromophore. A, dark grown filaments. B, red light irradiated filaments. C, dark grown filaments on 15*Za*PCB. D, dark grown filaments on 15*Ea*PCB. E, tip to base curvature and F, curvature between the filament 200 μm behind the tip and the base, of dark grown filaments on medium without chromophore, with 15*Za*PCB or 15*Ea*PCB. Mean values of 30 or more filaments from 3 experiments ± SE. The difference in F between 15*Ea*PCB treated filaments and the control is significant with *P < 0.05.

Adiantum capillus-veneris

3.1.2.4 15*Ea*PCB induced spore germination

Spore germination of ferns is another phytochrome response that can be monitored at the cellular level (Furuya, M. 1983, Haupt, W. 1992). Here, I tested for the effect of 15*Ea*PCB on *Adiantum capillus-veneris* spore germination. The dark germination rate was in the range of 2 %,

whereas 49 % of the spores germinated upon red light treatment (Figure 3.15 D). Feeding of 15*Ea*PCB resulted in a spore germination rate of 5 %. In most of the 15*Ea*PCB treated spores, only the tip emerged out of the spore envelope, indicating that germination was induced later than red light treatments. Protonema filaments were clearly visible after red light treatment. The weak induction might result from insufficient chromophore uptake by spore or because the chromophore is less efficiently incorporated into the phytochrome molecules.
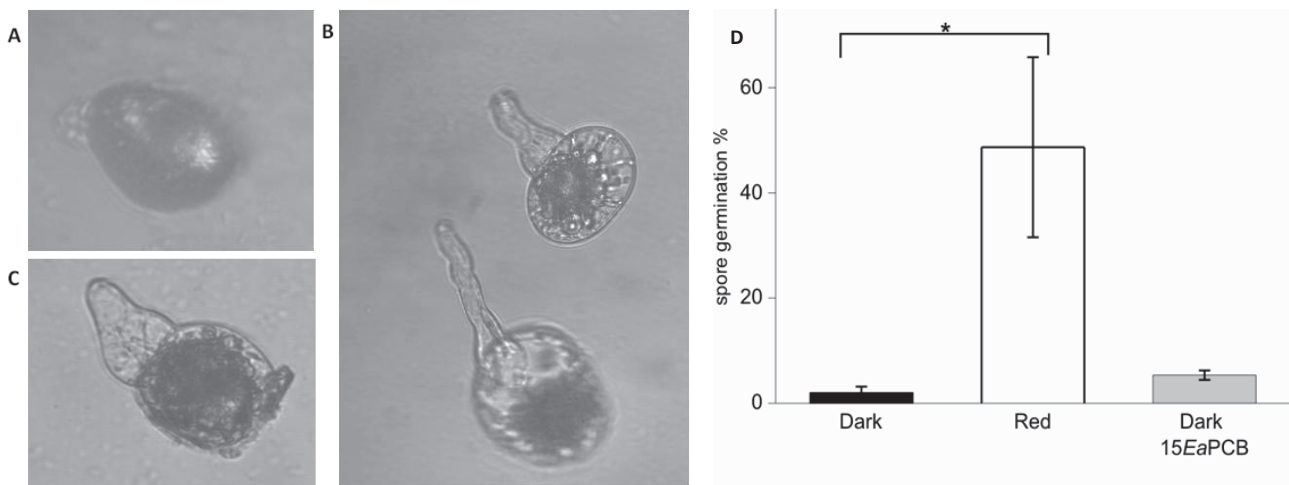
Figure 3.15   Effect of 15*Ea*PCB on *Adiantum venustum* spore germination. All spores were kept for a total of 7 days in darkness. A, non-germinated spore of dark control. B, germinated spore which was kept for the final 3 d in red light treatment C, germinated spore which was kept for the final 3 days on 15*Ea*PCB. D, calculated spore germination rate, mean values of 300 or more spores from 3 experiments ± SE. Asterisks denote Student's *t*-test significance, * P < 0.05

Arabidopsis thaliana

3.1.2.5 15*Ea*PCB induced seed germination

Chromophore feeding studies were performed also with *Arabidopsis thaliana*. The *hy*1 and *hy*2 mutants are defective in the synthesis of endogenous chromophore, due to defects in the conversion of heme to BV (Muramoto, T. et al. 1999) or BV to phytochromobilin (Kohchi, T. et al. 2001), respectively. Under conditions described in the Methods section, seed germination of *Arabidopsis* wild type was induced by red light to almost 100 %. The dark germination rate was in the range of 2 %. Feeding with BV under dark or red conditions had no impact on

germination rates compared with the dark or red light control seeds. With 15ZaPCB, germination rate was almost the same as in the dark control, but 15EaPCB feeding resulted in a significantly increased germination rate to ca 18 % (Figure 3.16).

The dark germination rate of *hy1* mutant was in the range of 18 %, thus significantly higher than those of the wild type. Same results were also found by for *phyB* mutant (Kendrick, R. E. and Cone, J. W. 1985, Poppe, C. and Schaefer, E. 1997, Tsuchiya, Y. et al. 2010). The higher dark germination rate could result from cultivation after mutant isolation. The *hy*1 stock might be enriched for second site mutants with higher dark germination rates. Due to the lack of the phytochrome chromophore, red light treatment of *hy1* seeds did not result in an increase of germination. However, seed germination was induced by red light to ca. 60 % when seeds were incubated on BV, whereas BV did again not stimulate seed germination in darkness. Feeding with 15ZaPCB did again not result in an increased dark germination, whereas 15EaPCB increased germination to ca. 40 % (Figure 3.16).
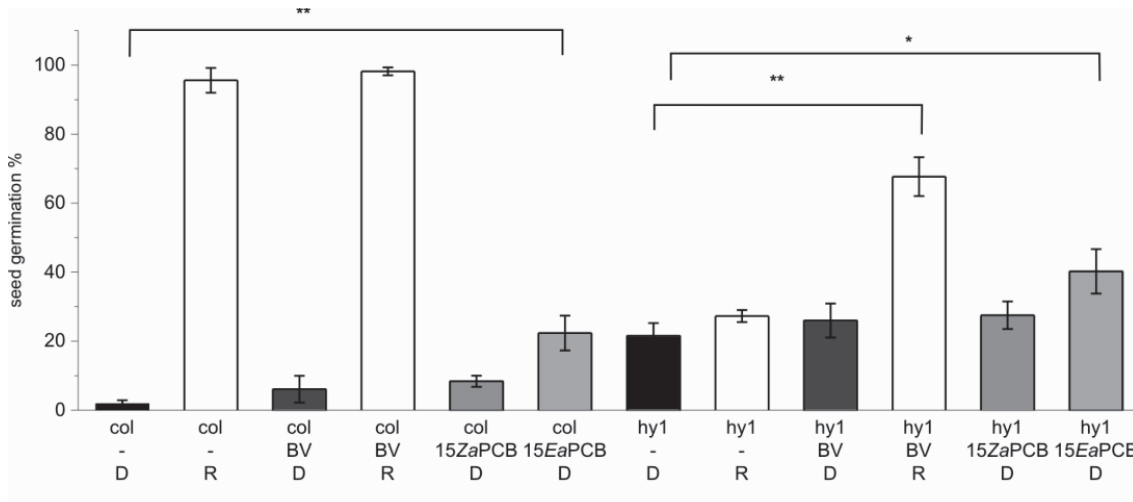

Figure 3.16 Effect of light and chromophores on *Arabidopsis* seed germination. The strain (col: Columbia wild type, hy1: *hy1* mutant), chromophore and light treatments (D: darkness, R: red light) are given under each bar. Mean values of 150 or more seeds from 3 experiments ± SE. Asterisks denote Student's *t*-test significance, * P < 0.05, **P < 0.01.

3.1.2.6 15*Ea*PCB inhibited hypocotyl elongation and induced cotyledon opening

Red light inhibits hypocotyl elongation via phytochrome. Under our test conditions, the mean length of dark grown *Arabidopsis* wild type hypocotyl was 11.1 mm, and 6.5 mm in red light. Again, the 15*Za*PCB chromophore had no effect, whereas feeding with 15*Ea*PCB resulted in a significant reduction to 10.0 mm (Figure 3.17 D). Hypocotyl of dark grown *hy1* and *hy2* mutants had a mean length of 12.0 mm and 13.9 mm, respectively. In both mutants, red light irradiation did not result in a significant reduction of the hypocotyl length. When the *hy1* and *hy2* mutants were grown on BV, red light reduced the hypocotyl to 6.2 and 7.9 mm, respectively. The fact that BV feeding of *hy2* results in a complete rescue of phytochrome responses is striking, because the mutation results in a block of conversion of BV to PÖB. Feeding of 15*Za*PCB did not change the hypocotyl length of *hy1* and *hy2*, whereas growth on 15*Ea*PCB reduced the hypocotyls lengths significantly to 10.6 and 12.9 mm, respectively. Thus, 15*Ea*PCB feeding induces a Pfr response in both mutants, but again not to the same extent as BV and red light (Figure 3.17 D).

A similar pattern of chromophore induction was found for cotyledon opening. Under our test conditions, the cotyledon opening rate of dark grown wild type seedlings were close to zero, and upon red light irradiation the rate was 52 %. With 15*Ea*PCB in darkness, the induction was 21 %, whereas no induction was found with 15*Za*PCB (Figure 3.17 E). In the *hy1* and *hy2* mutant red light alone did not result in a significant induction of cotyledon opening, whereas red light and BV together resulted in rates of 65 % and 71 %, respectively. In both chromophore deficient mutants, the mean cotyledon opening was insignificantly increased by 15*Za*PCB. Feeding with 15*Ea*PCB stimulated cotyledon opening to 33 % and 59 %, respectively.

A   B   C

D
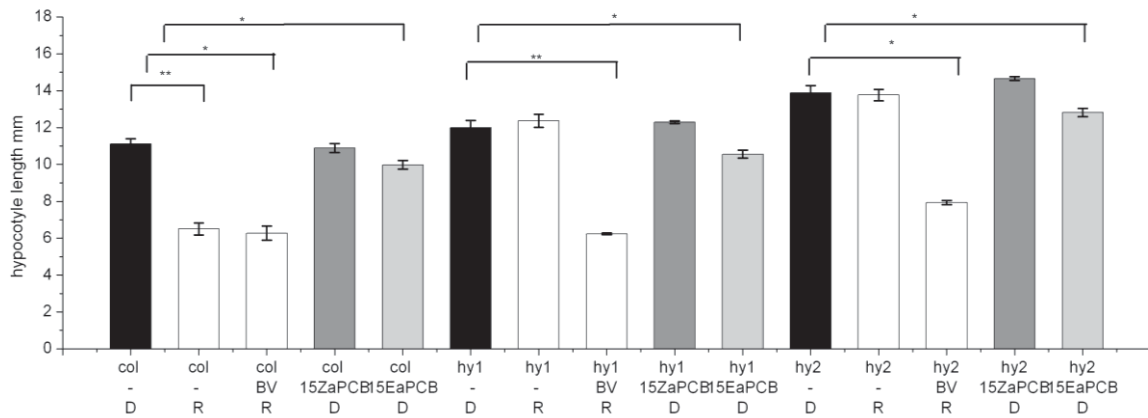
E
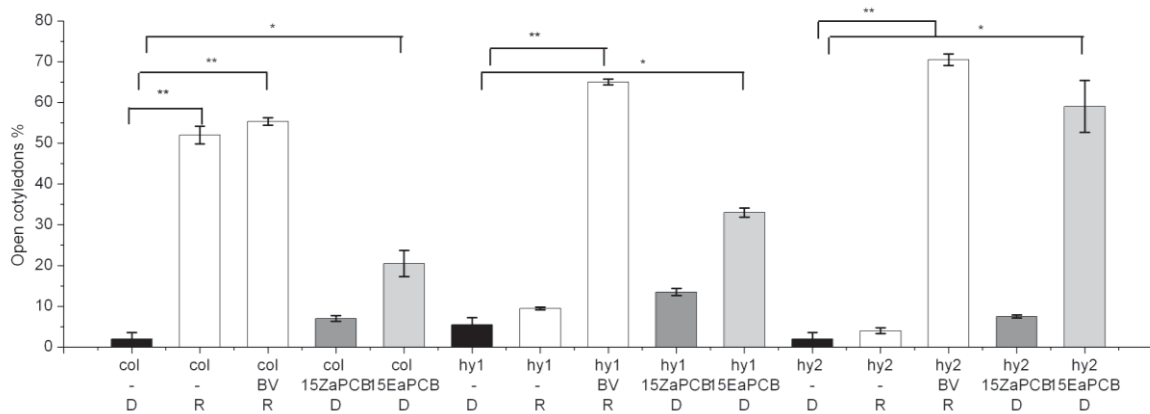
Figure 3.17 Effect of light and chromophores on *Arabidopsis* hypocotyl growth and cotyledon opening. A, B, C *Arabidopsis* seedlings of (A) WT col, (B) *hy*1 and (C) *hy*2 in darkness without (right) or with 15*Ea*PCB treatment (left). D, Hypocotyl length. The strains (col: Columbia wild type, hy1: *hy1* mutant, hy2: *hy2* mutant), chromophores and light treatment (D: darkness, R: red light) are given under each bar. Mean values of 40 or more seedlings from 3 experiments ± SE. Asterisks denote Student's *t*-test significance, * P < 0.05, **P < 0.01. E, Cotyledon opening rate; Mean values of 40 or more seedlings from 3 experiments ± SE. Asterisks denote Student's *t*-test significance, * P < 0.05, **P < 0.01.

3.1.2.7 15*Ea*PCB disturbed hypocotyl gravitropism response

Irradiation of *Arabidopsis* seedlings results in a randomization of the gravitropic response. This effect is mediated through phyA and phyB which induce VLFR and LFR responses, respectively.

In order to find out whether 15*Ea*PCB can induce this VLFR response, I compared chromophore-treated with far red treated seedlings. The results are summarized in Figure 3.18 as histograms. In darkness, 93 % of wild type seedlings had a vertical growth direction (0 to 20 ° deviation from the vertical). Far red treatment reduced the frequency of this group to 64 % and stimulated a more random growth direction. BV feeding and feeding with 15*Za*PCB (here darkness only) had no effect on the gravitropic response of the wild type. Feeding with 15*Ea*PCB resulted in a randomization of gravitropism to an extent comparable with the far red irradiated control.

Dark grown *hy1* seedlings had a more randomized growth direction as compared to the wild type. This difference is striking, but is also found for the BV treated dark grown seedlings. A far red treatment of *hy1* resulted in a more straight growth direction, indicating that some residual active Pfr was reverted into Pr. (Note that the *hy1* mutants most likely contain low levels of spectrally active phytochrome.) Far red / BV treated *hy1* seedlings had a randomized growth direction, and the effect of far red was even stronger than in the wild type. *hy1* seedlings treated with 15*Za*PCB had a growth pattern similar to the untreated control. With 15*Ea*PCB, gravitropism was again randomized. These results clearly show that 15*Ea*PCB induces VLFR responses to about the same extent as a far red treatment.
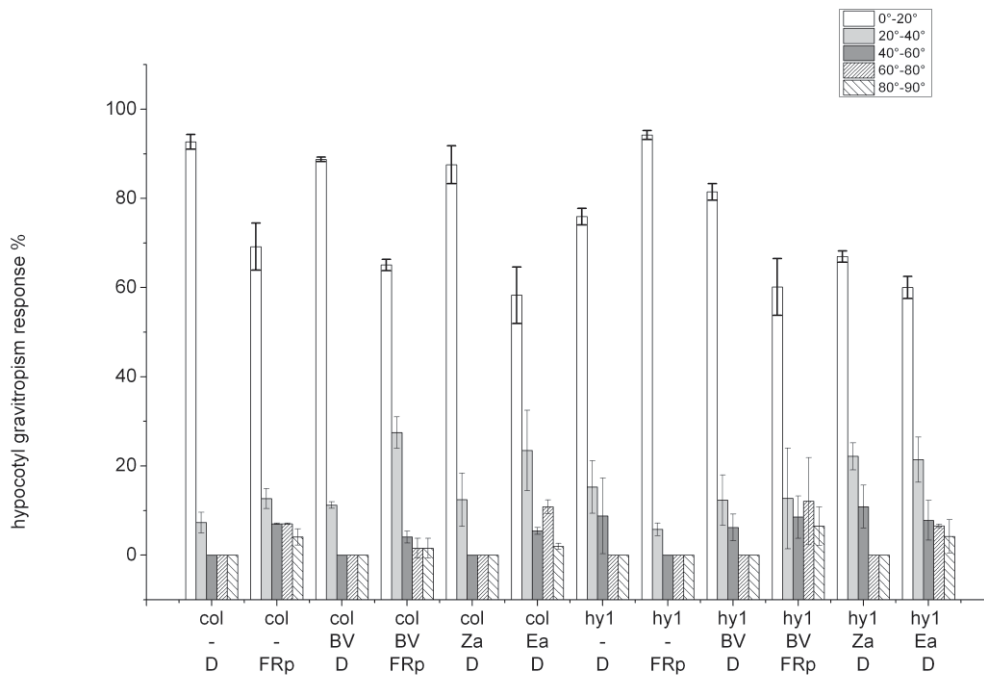
Figure 3.18 Effect of light and chromophores on *Arabidopsis* gravitropism response. Vertical growth is defined as 0 °. The fractions of seedlings that belong to groups from 0 ° - 20 °, 20 ° - 40 °, 60 ° - 80 ° or 80 ° - 90 ° were estimated. For each single treatment, 50 or more seedlings were used. Mean values of 2 independent experiments ± SE.

3.1.2.8 15*Ea*PCB regulated gene expression

We also tested whether mRNA levels of three selected phytochrome regulated genes are affected by 15*Ea*PCB chromophore treatment. Early light-induced proteins (ELIPs) are transiently induced during greening of etiolated seedling. ELIP2, one of the ELIPs proteins are thylakoid proteins which are transiently induced during greening of etiolated seedlings, and which expression is under phytochrome control (Rossini, S. et al. 2006). In our case the ELIP2 was induced by red light treatment and 15*Ea*PCB, both treatments can significantly increase the ELIP2 level. LHB1B2, Photosystem II type I chlorophyll a/b-binding protein, is also regulated by phytochrome. In our case the LHB1B2 was induced by red light treatment and 15*Ea*PCB treatment by 2.3 and 1.6-fold, respectively, after a 24 h treatment. PIL1, PHYTOCHROME-INTERACTING FACTOR 3-LIKE 1 (PIL1) was used as a known early-response gene whose

expression is robustly repressed by exposure to light (Hwang, Y. S. and Quail, P. H. 2008). Figure 3.19 indicated that abundance of PIL1 mRNA declines 4 times below the dark treatment when exposed to continuous red light for 24 h, and 2 times below when incubating plants 24 h with 15*Ea*PCB.
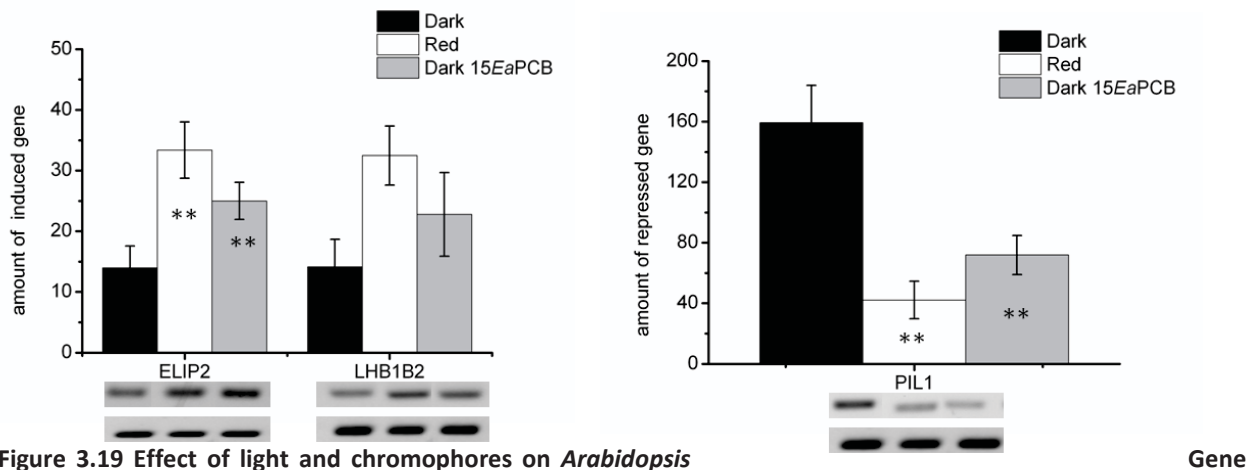
Figure 3.19 Effect of light and chromophores on *Arabidopsis* Gene expression. A, ELIP2 and LHB1B2 genes induced by Red light and 15*Ea*PCB treatment. Upper level gels: transcripts of interest, lower level gels reference gene PP2A. From left to right are red light treated sample, dark and 15EaPCB treated samples. Mean values of two biological repeats and at least two times technical repeats ± SE. B, PIL1 gene repressed by red light and 15*Ea*PCB treatment.

3.2 *Ceratodon purpureus* phytochrome function and localization

3.2.1 Function

DNA interference which shows to be a useful method to silence is used, this method is also proven to be very efficiency for multigene silencing (Akamatsu, T. and Taguchi, H. 2001, Bonnassie, S. et al. 1990, Bruecker, G. et al. 2005, Cove, D. J. et al. 2009b, Forsburg, S. L. 2003, Kawai-Toyooka, H. et al. 2004). In all DNA interference studies protoplasts of *Ceratodon purpureus* wild type K1 were used, which were first grown under continuous white light for 5 d. Then protoplasts were isolated, transformed with foreign DNA fragments and regenerated. Regenerated filaments were then screened for the desired phytochrome controlled phenotype, like phototropism and branch formation.

3.2.1.1 Heme oxygenase interference disturbed phytochrome function

Heme oxygenase is one of the enzymes which are responsible for chromophore synthesis. It reduces the heme to biliverdin. If heme oxygenase function is disturbed the chromophore synthesis pathway is inhibited and therefore no chromophore can be synthesized. Using different parts of foreign heme oxygenase genes one can disturb inner heme oxygenase gene expression. N-terminal, C-terminal DNA fragments as well as the full-length heme oxygenase genes were used to silence heme oxygenase expression in moss filaments. In all three cases aphototropic phenotype moss filaments were found under unilateral red light. No big differences were observed between the different DNA treatments; both efficiency and effect were almost the same. Figure 3.20 shows images of regenerated moss filaments after DNA interference; one can clearly see that the transformed moss filaments were not growing towards the light. The transformation efficiency was quantified according to the formula: Transformation rate = the number of aphototropic filaments/the totally number of filaments. Calculated data is shown in Table 3.3. The transformation rates of all fragments are around 20 %.
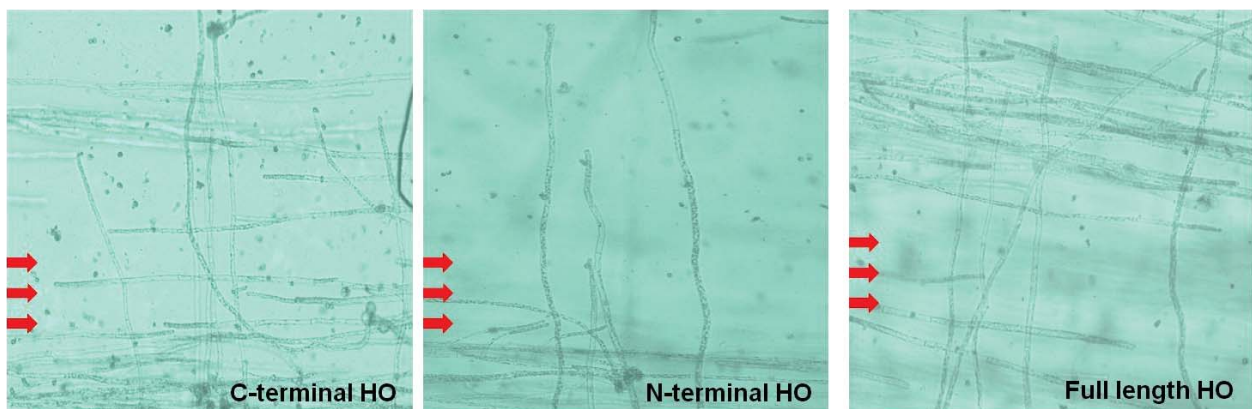
Figure 3.20 Phototropic responses after heme oxygenase gene interference of new regenerate filaments

3.2.1.2 Special phytochrome gene interference disturbed function

Single or double phytochrome genes of *Ceratodon purpureus* were also used for DNA interference. CerpuPhy2 silence in filaments causes much more branch under red light in single filament compared to the control. Also the numbers of filaments having branch were elevated.

72

The transformation rate was more than 10 %. In this case the transformation rate calculated using formula below: Transformation rate = the number of phenotype filaments/the totally number of filaments. New regenerated filaments had more branches then the controls, which normally had no branch or less than 3 in one single filament. In contrast CerpuPhy2 silenced filaments had 3 to 5 branch in each filament (Figure 3.21). Both, the newly regenerated filaments and their branch showed phototropic response.

Disturbed CerpuPhy3 gene caused the loss of the phototropic response. Almost 75 % of the filaments regenerated from transformed protoplasts grew randomly compared to the control (Figure 3.21). The phenotype of this mutant looks like the Class II mutant, mentioned before, with random growth filaments under red light. The CerpuPhy4 interference did not show any phenotype in our experiments, which is not in accordance with Mittmann' results: phy4 is responsible for phototropic response. The reason could be the N-terminal part of CerpuPhy4 might be not enough to induce gene silence. Later studies should test the silencing efficiency of the full-length CerpuPhy4 gene.
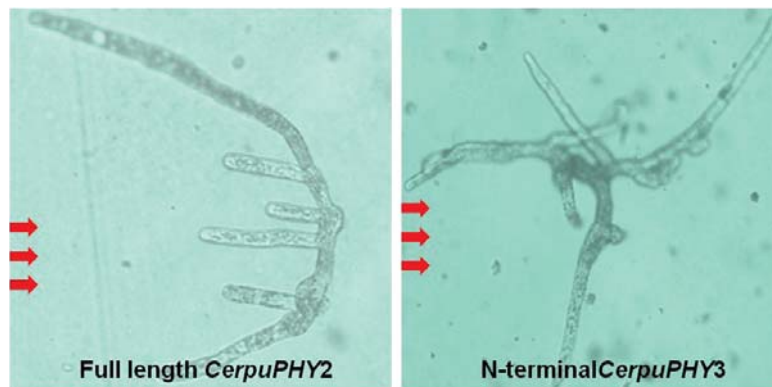

Figure 3.21 Phenotype of gene silencing by DNA interference with PHY2, PHY3

Table 3.3 shows the transformation rate of different gene fragments. The transformation rate of CerpuPhy3 was the highest compared with others, 75 % new generated filaments showed random grown phenotype under unilateral red light. Then the heme oxygenase DNA fragments had about 20 % transformation rate, followed by the full length CerpuPhy2 gene. The different transformation rates might because of the different length of coding sequence used in DNA interference. In early studies on fern also show that, the transformation rate is affect by the length of coding sequence (Kawai-Toyooka, H. et al. 2004).

	phenomenon	efficiency
CerpuPhy2	more branches	10 %
CerpuPhy3	random growth	70 %
CerpuPhy4	no phenotype	
CerpuPhy2phy3heme	random growth	10 %
CerpuPhy2phy4heme	no phenotype	
Full-length Heme	aphototropism	25 %
N-Terminal Heme	aphototropism	22 %
C-Terminal Heme	aphototropism	20 %

Table 3.3 Calculated transformation rate of different DNA interference fragments.

3.2.2 Intracellular localization

3.2.2.1 CerpuPhy3 might be membrane attached

Localization studies were test by PEB staining. After incubation with PEB phytochrome can form a covalent bond with PEB and show fluorescence upon irradiation. Using the filaments got from DNA interference experiments, the localization of phytochrome were checked using PEB, which has a high fluorescence when assembled with phytochrome. This is caused by a missing the double bond at C15 and C16. Because of the low or no expression of other phytochromes in the mutant filaments described above, PEB staining was used to test the remaining phytochrome in the cell. PEB signal was detected in the cytoplasm when CerpuPhy2, CerpuPhy3 and heme oxygenase were used at same time for silencing, at the same time. In the case when CerpuPhy2, CerpuPhy4 and heme were used for DNA interference, PEB signal was seen only on the cell

membrane (Figure 3.22), which directly indicated that CerpuPhy3 might be membrane attached. Together with the phonotype studies of CerpuPhy3, which shows the randomly grow under red light, indicated CerpuPhy3 maybe connected to the cell membrane. The possibility of membrane localization of CerpuPhy1 or 4 cannot be excluded. In CerpuPhy2,4 and heme treble mutants, maybe the expression of Phy1 and Phy4 not totally inhibit, there is still some gene expression, that makes the PEB staining signal, but not enough to control response. To make sure CerpuPhy3 or any phytochrome is a membrane attached phytochrome, gene expression levels of those mutants need to be test.
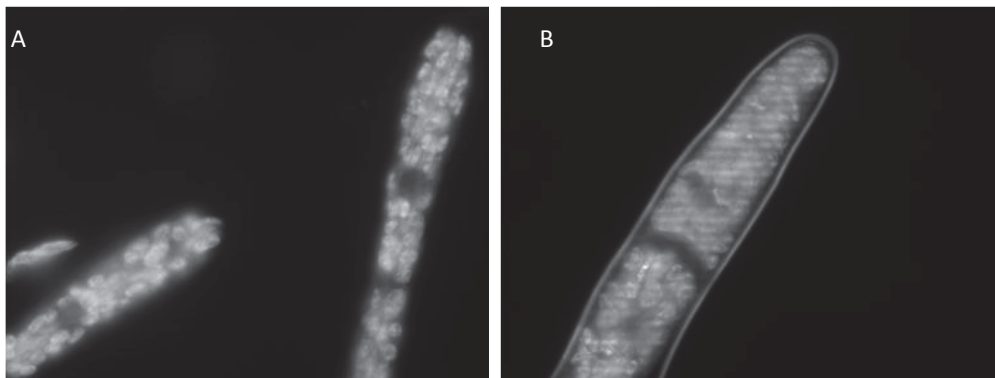
Figure 3.22 Fluorescence of PEB signal on CerpuPhy2Phy4heme triple DNA interference mutant. phy2phy4heme triple mutants filaments A, control. B, PEB staining

3.2.2.2 Protoplast PEB staining shows membrane phytochrome signal

The fluorescence signal seen in Figure 3.22 might also be in the cell wall and not in the cell membrane. To get rid of the effect of cell wall fluorescence, protoplast was used to test the phytochrome location. Protoplasts were incubated with PEB for 2 h. Because of the contamination of the phy2phy4heme mutant, no more experiments continuous with that. For later experiments either wild type K1, or newly generated *ptr201* mutant were used.

From the Figure 3.23 it can be seen that without PEB staining no phytochrome signal can be seen in both the K1 and the *ptr201* mutant (Figure 3.23 b, f). After 2 h PEB staining, phytochrome signal was detected both in the cytosol and plasma membrane (Figure 3.23 d, h) especially in wild type protoplast the signal of membrane phytochrome was much stronger (Figure 3.23 d).
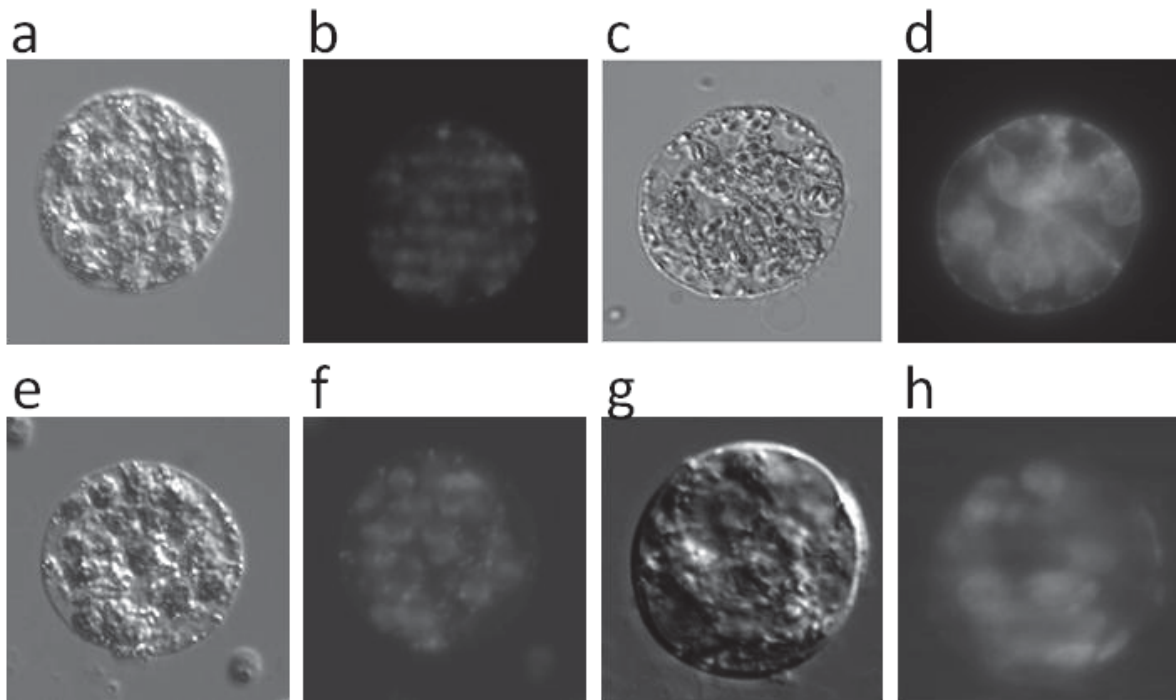
Figure 3.23 Phytochrome-PEB fluorescence signals in moss protoplasts. a-d, K1 protoplast transmission and phytochrome-PEB fluorescence images. a-b, Control without any chromophore treatment. c-d, incubated with PEB for 2 h. e-h, *ptr201* protoplast transmission and phytochrome-PEB fluorescence images. e-f, Control without any chromophore. g-h, incubated with PEB for 2 h.

3.2.2.3 Eight hours are sufficient for phytochrome-PEB binding

To answer the question how long it takes the PEB to enter the cell and bind to the phytochrome. Time course experiments were performed. Figure 3.24 shows the time course of PEB staining efficiency. There was an increase of the PEB fluorescence from 2 h to 8 h (Figure 3.24). After 8 h there is no further change when using K1 filaments, whereas with *ptr201* the PEB signal already reached the highest level after 2 h. No more changes were detected after that. The slow and

low intensity of PEB signal using the wild type indicated, there might be a competition in K1 with the nature chromophore, whereas direct binding occurs in *ptr201* within a short time and strong fluorescence (Figure 3.24 e-h).
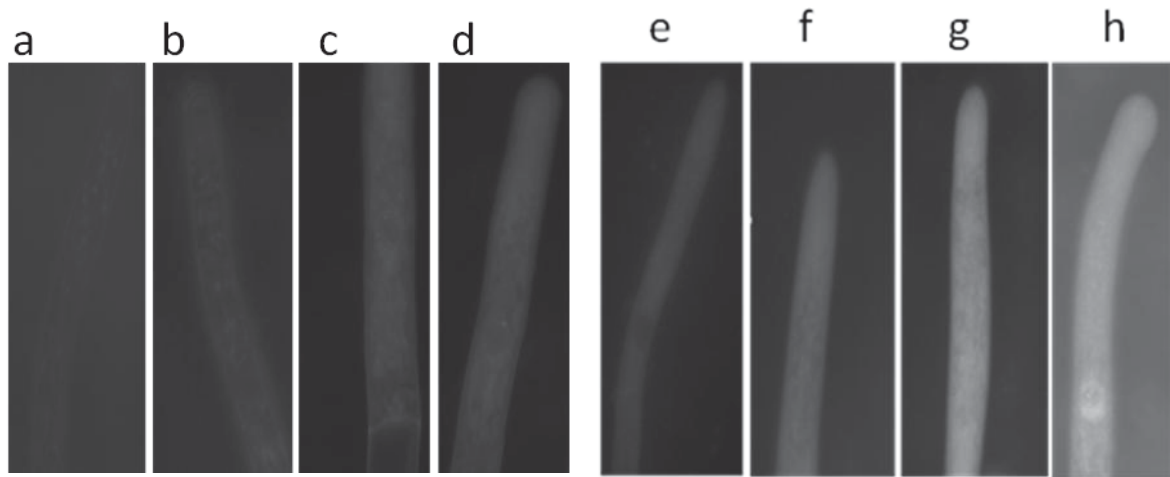
Figure 3.24 Time course of Phytochrome-PEB signal in moss filaments. a-d, K1 filaments incubated with PEB. For continues a, 2 h. b, 4 h. c, 8 h. d, 24 h; e-h, *ptr201* filaments incubated with PEB. For continues e, 2 h. f, 4 h. g, 8 h. 24 h.

3.2.2.4 15*Za*PCB staining shows a weak membrane signal

In chromophore staining experiments using PCB, there were almost no fluorescence signals detected in *ptr201* (Figure 3.25 b). 15*Za*PCB induced a weak fluorescence signal, and most induced signal was detected in cell membrane in *ptr201* (Figure 3.25 c). Figure 3.25 e shows the quantification of the fluorescence signals of different chromophores in both K1 and *ptr201* filaments, compared with control samples without chromophore. Both PEB and 15*Za*PCB can significantly induce the fluorescence signal, student *t* test shows 1 % and 5 % significance, respectively.
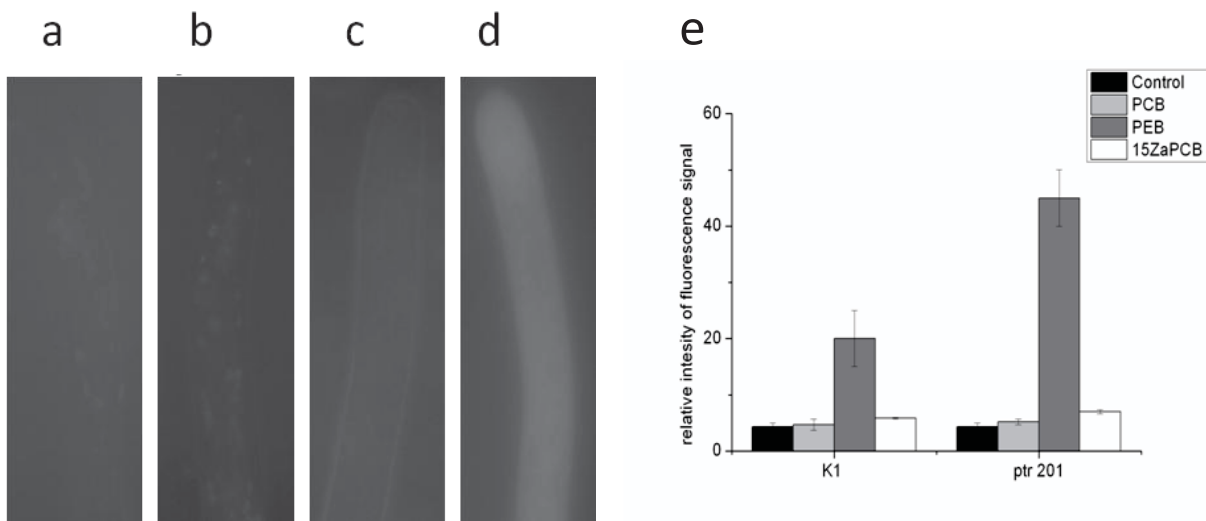
Figure 3.25 Phytochrome fluorescence signals in moss filaments. a-d, *ptr201* filaments after one day incubated with chromophores in darkness. a, control. b, incubated with PCB. c, incubated with 15*Za*PCB. d, incubated with PEB. e, quantification of fluorescence intensity of PCB,PEB and 15*Za*PCB using Image J 1.42.

3.3 Temperature effect of phytochrome

Phytochrome, known as a photoreceptor, has been studied by many groups for almost 60 years, since the 1950s when it was first discovered. Their function at different temperatures is studied; also the signal pathway connection between light and temperature, but whether phytochrome might be itself a thermo sensor was not questioned yet. Recent studies in our group suggest that *A. tumefaciens* phytochrome Agp1 serves as a thermo sensor (Njimona, I. and Lamparter, T. 2011). Temperature effects on spectral properties of Cph1 and its truncated version were performed. *Ceratodon purpureus* and *Arabidopsis thaliana* wild type and phytochrome mutants, were used in order to find out whether plant phytochrome also works as thermo sensor.

Cph1 was chosen as a second model phytochrome. Cph1 is the first real prokaryotic phytochrome to be discovered, but its biological function in the host *Synechocystis PCC 6803* is as yet unclear. In this thesis, the temperature effect on Cph1 was investigated. Before temperature studies, Cph1 was first assembled with its natural chromophore PCB for 2 h and then pass through a NAP 10 column to get rid of the free chromophore.

3.3.1 Cph1 photoconversion with high intensity light at different temperatures

Figure 3.26 A-D shows the absorbance spectral changes of far red and red light irradiation forms of full-length Cph1-PCB adduct before and after 2 h temperature treatment. At room temperature (20 °C), there was almost no spectral change for the far red irradiation form after 2 h temperature treatment (Figure 3.26 B). In contrast the red irradiation form showed a decrease at 710 nm and an increase at 655 nm within 2 h incubation at 20 °C (Figure 3.26 B). At 3 and 30 °C there were also no obviously changes of far red irradiation form, and decrease (710 nm) and increase (655 nm) for red irradiation form (Figure 3.26 A, C). Comparing the far red and red light irradiation forms before and after 2 h 40 °C treatment, it showed both forms had decreased absorbance peaks (Figure 3.26 D). In order to find out if those decrease reversible or not, samples were slowly return to 20 °C in 90 min in the photometer with continuous red light irradiation. Spectra of far red and red light irradiation were taken again, and then compared them with 40 °C temperature treatment spectra measured before. No reversible was detected at all (Figure 3.26 F). That may be indicated the damage or loss of the chromophore at high temperature and high intensity of irradiation light. Figure E, shows the time drive spectra at different temperatures, measured at 710 nm. The red light was switch on at first 180 s, and continues during the whole measurement, 7000 s. It clearly showed that after switch on the red light, the photoconversion immediately happened for all the temperatures treated samples, and then followed by a quick absorbance decrease, within the first 200 s, after that, the photo-equilibrium reached for 3, 20, and 30 °C treated samples. At 40 °C the decrease was continued during the whole measurement, about 7000 s, and do not reach an equilibrium till end of measurements. The high intensity of irradiation light and high temperature together courses those changes.

Figure 3.26 Spectral changes of full-length Cph1-PCB adducts at different temperatures: High intensity of irradiation light (red, 250 µmol m^{-2} s^{-1}, far red, 500 µmol m^{-2} s^{-1}). Panel A to D shows series of spectra that were measured at different temperatures during a defined irradiation schedule. E, Monitor A$_{710\,nm}$ under continuous red light irradiated samples during 7000 s at different temperatures. F, absorbance spectra of 40 °C treated samples compared with 40 °C treated samples returned to 20 °C. Whole schedule: After assembly and NAP 10 column separation, far red light was first given, measure the full-length spectra (blue line, A-D), followed immediately by the red light irradiation, measure the full-length spectra (red line, A-D). Far red light irradiated again, change the measure program from full-length to time drive measurement, only measure the A$_{710\,nm}$, start the measurement, switch the red light after 180 s, the red light irradiation is continuous during the 7000 s time drive measurement

(E). After the time drive change program back to full-length measurement, immediately measure (black line, A-D), followed by far red light irradiation, measure (green line, A-D). Only 40 °C treated samples were used to test the recover ability, when reduce the temperature back to 20 °C in 90 min.

3.3.2 Cph1 photoconversion with low intensity light at different temperatures

The high intensity of light course loss of chromophore at the beginning of light irradiation, which cannot be reversed through reduce temperature (Figure 3.26). To get rid of the strong light effect at the beginning, low irradiation light (10 µmol m^{-2}s^{-1}) was used. In this case the absorbance spectra measured at 710 nm did not have that sharp decrease at the beginning (Figure 3.27 E), all the other temperatures treatment reach the photo equilibrium immediately, except 40 °C sample. Again 40 °C sample did not reach the equilibrium, till the end of measurement. The full wavelength absorbance spectra kept unchanged after 2 h temperature treatments of 3, 20 and 30 °C, no matter whether the far red or red light irradiation form were measured (Figure 3.27 A, B, C). Only at 40 °C, temperature and light treatment induced the decrease of both forms, at absorbance peaks either 710 nm, or 710 nm and 655 nm (Figure 3.27 D). The decrease of both peaks, were again test for reversible. Interestingly at low light intensity the spectra indeed were recovered when cooling down the temperature, both peaks return to the level of untreated samples stay at 20 °C, especially, the Pfr peak at 710 nm (Figure 3.27 F). That makes me concluded that might be because of conformation change of chromophores at high temperature and low light irradiation. When reduce the temperature, the chromophore conformation change back to normal Pr or Pfr. Different from spectra of Agp1 the response of Cph1 to 40 °C and light irradiation were less sensitive, and there is not clearly evidence showing the new forming of Prx, at the first 500 s. The evidence only showed after long time irradiation and temperature treatment, and the new species cannot photoconvert back to Pr at high temperature. Another things need to pay attention to is 3 °C treated samples, the full wavelength spectral shape was not the same as at other temperatures, where the Pfr peak was a little bit higher than the Pr peak after red light irradiation, whereas others lower (Figure 3.27 A-D). This could also maybe a temperature effect. At low temperature the efficiency of photoconversion to Pfr is higher than at room or higher temperature.

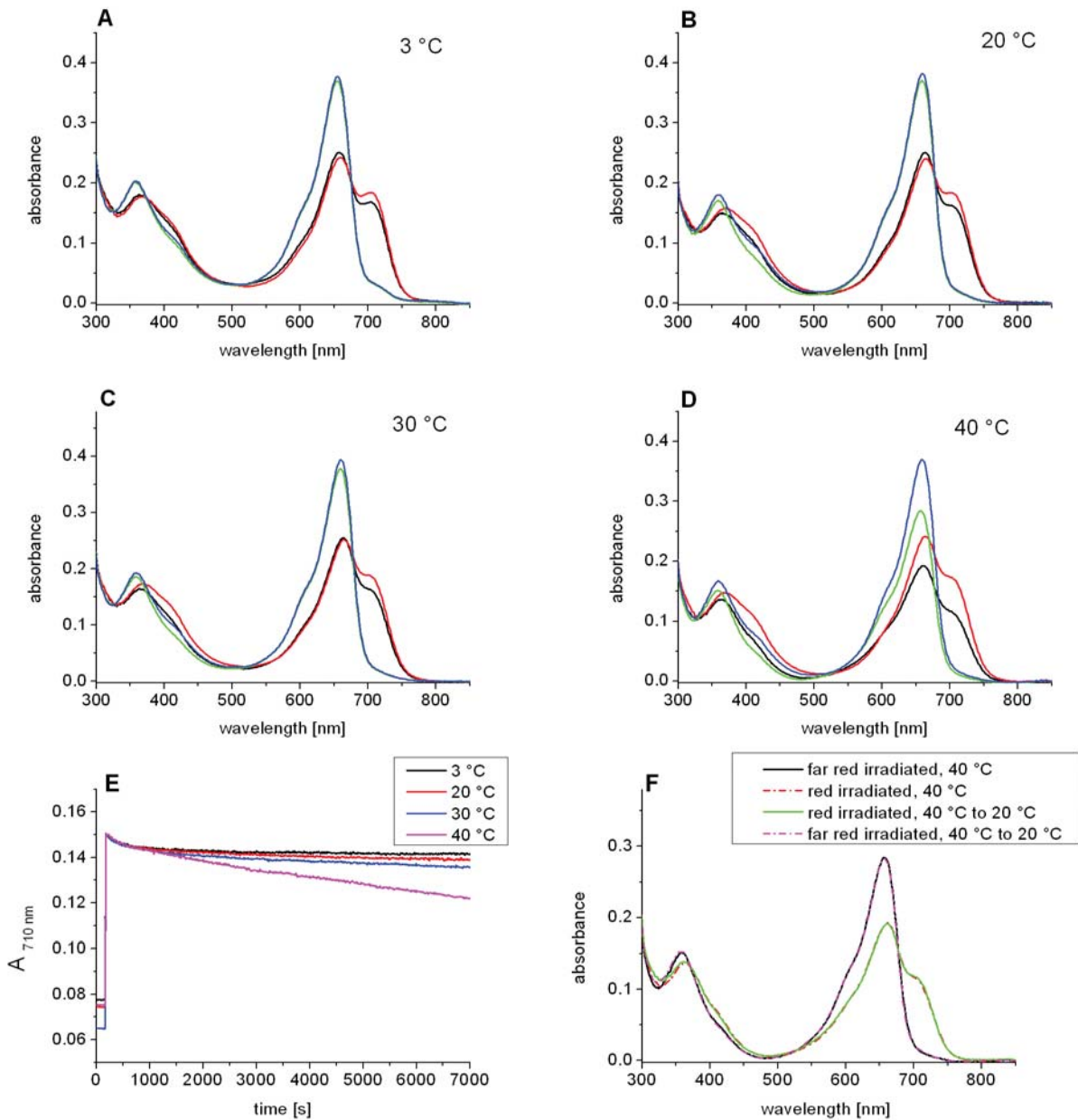**Figure 3.27 Spectral changes of full-length Cph1-PCB adducts at different temperatures: Low intensity of irradiation light (red, 10 µmol m^{-2} s^{-1}, far red, 10 µmol m^{-2} s^{-1}).** Panel A to D shows series of spectra that were measured at different temperatures during a defined irradiation schedule. E, Monitor $A_{710 nm}$ under continuous red light irradiated samples during 7000 s at different temperatures. F, absorbance spectra of 40 °C treated samples compared with 40 °C treated samples returned to 20 °C. Whole schedule: After assembly and NAP 10 column separation, far red light was first given, measure the full-length spectra (blue line, A-D), followed immediately by the red light irradiation, measure the full-length spectra (red line, A-D). Far red light irradiated again, change the

measure program from full-length to time drive measurement, only measure the $A_{710\,nm}$, start the measurement, switch the red light after 180 s, the red light irradiation is continuous during the 7000 s time drive measurement (E). After the time drive change program back to full-length measurement, immediately measure (black line, A-D), followed by far red light irradiation, measure (green line, A-D). Only 40 °C treated samples were used to test the recover ability, when reduce the temperature back to 20 °C in 90 min.

3.3.3 N-terminal of Cph1 photoconversion with high intensity light at different temperatures

NCph1, which comprises only the N-terminal part of Cph1 was also tested at different temperatures under different irradiation intensities. In order to find out whether the spectral change above at 40 °C and light irradiation are depending on C-terminal or not. Figure 3.28 A-D shows, almost no changes happened at Pr form before or after temperature treatment, even at 40 °C, the red irradiation form shows a slightly decreased peak at 710 nm and same time increased at 655 nm. The reason might be a stronger light effect, like the full-length Cph1-PCB adduct at high light irradiated intensity, the time drive spectra measured at 710 nm, only shows a decrease at the beginning (Figure 3.28 E). There is no need to test the recover ability, because of almost no change happened at all the temperature treated samples.
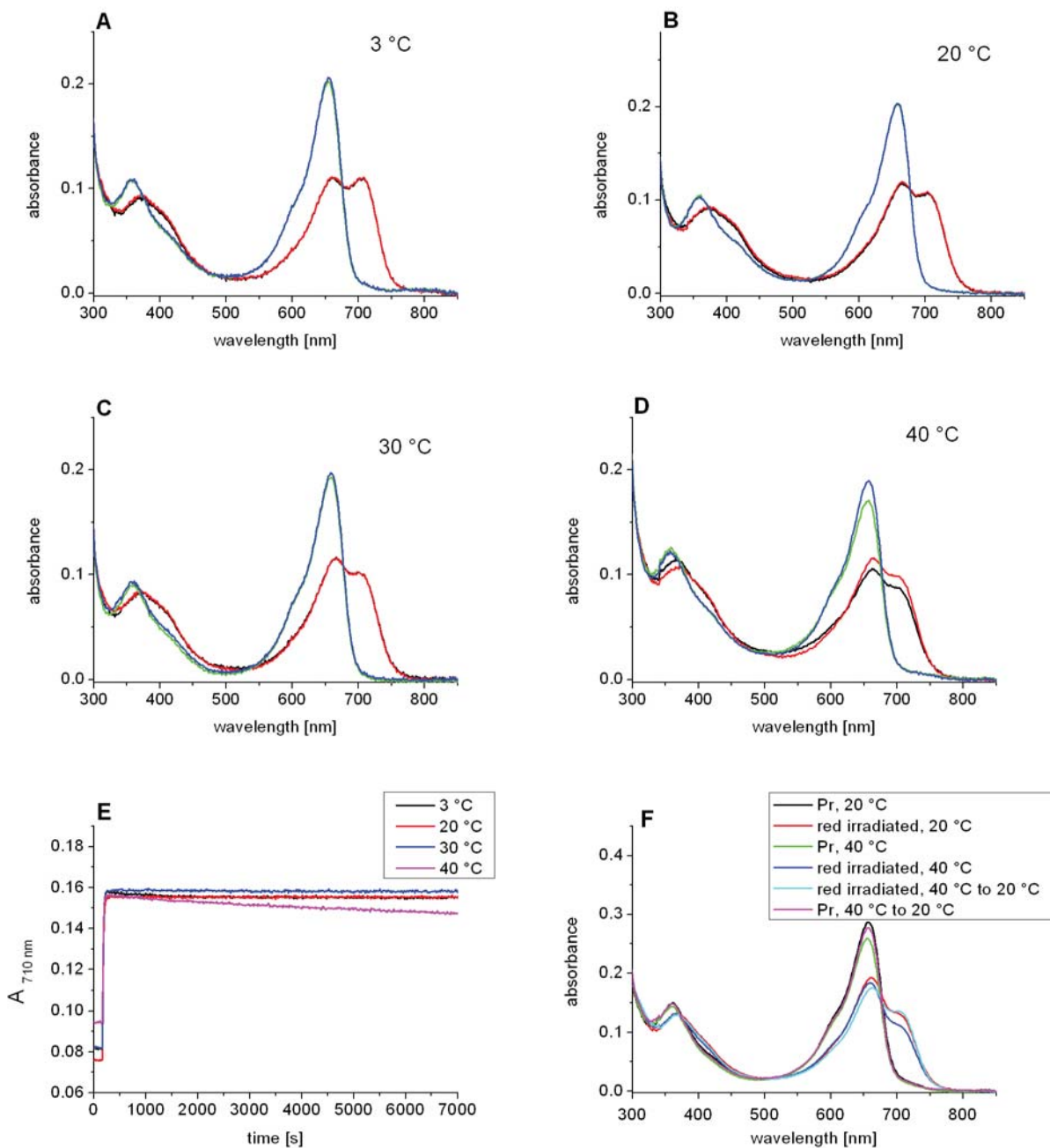
Figure 3.28 Spectral changes of NCph1-PCB adducts at different temperatures: High intensity of irradiation light (red, 250 μmol m^{-2} s^{-1}, far red, 500 μmol m^{-2} s^{-1}). Panel A to D shows series of spectra that were measured at different temperatures during a defined irradiation schedule. E, Monitor A$_{710\,nm}$ under continuous red light irradiated samples during 7000 s at different temperatures. F, absorbance spectra of 40 °C treated samples compared with 40 °C treated samples returned to 20 °C. whole schedule: After assembly and NAP 10 column separation, far red light was first given, measure the full-length spectra (blue line, A-D), followed immediately by the red light irradiation, measure the full-length spectra (red line, A-D). Far red light irradiated again, change the measure program from full-length to time drive measurement, only measure the A$_{710\,nm}$, start the measurement, switch the red light after 180 s, the red light irradiation is continuous during the 7000 s time drive measurement

(E). After the time drive change program back to full-length measurement, immediately measure (black line, A-D), followed by far red light irradiation, measure (green line, A-D).

3.3.4 N-terminal of Cph1 photoconversion with low intensity light at different temperatures

Using the weak irradiation light (10 μmol m^{-2} s^{-1}) NCph1-PCB adducts showed totally no spectral changes of before and after temperature treatment (Figure 3.29). At 3 °C, here again shows an increased Pfr peak then Pr same as full-length Cph1-PCB adducts. This means that the efficiency of photoconversion to Pfr at 3 °C is not C-terminal dependent. But the observed temperature effect at 40 °C is actually C-terminal dependent.

Short conclusion for the spectra studies above: There is an effect of temperature (40 °C) and light for full length protein, this is reversible if low intensity light is chosen and irreversible if high light intensity is chosen. Without the His Kinase, the photoconversion is normal with low intensity light and again unmoral with high intensity light, but there is no temperature effect. The His Kinase may be used for sense the temperature and then pass this signal to chromophore module, at the same time chromophore module also sense the light signal, those two signals light and temperature, together induce the spectral change.
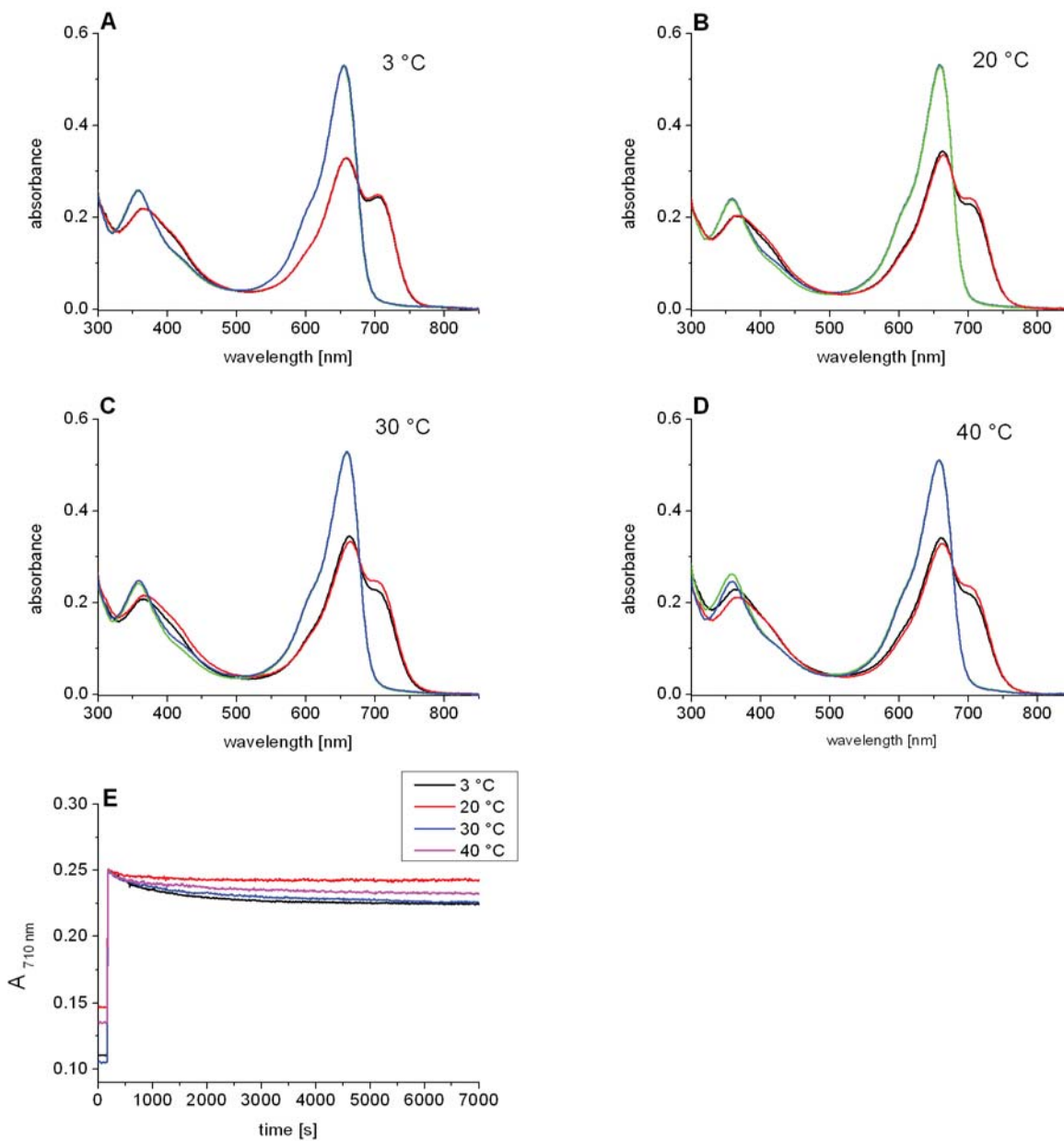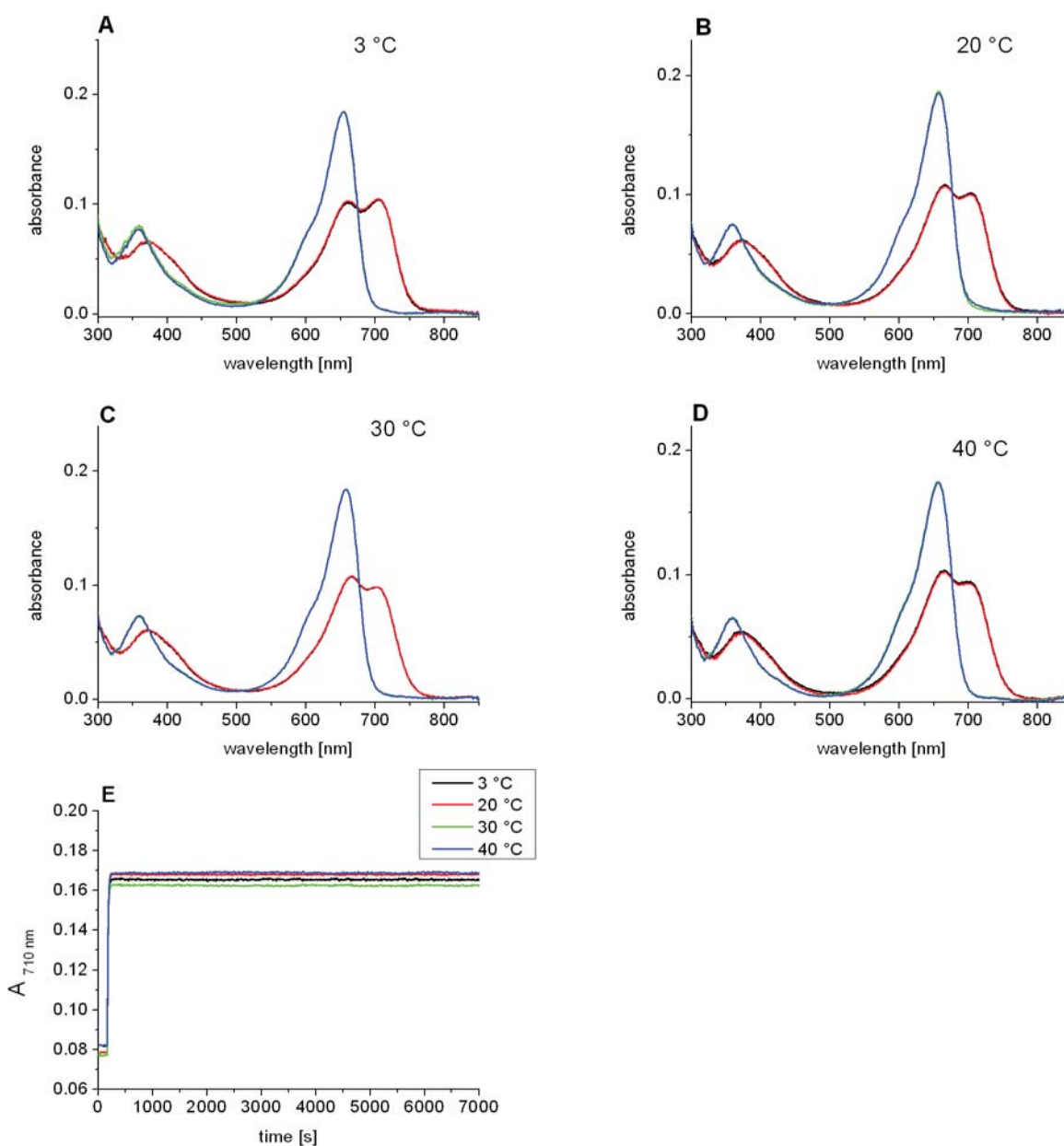
Figure 3.29 Spectral changes of NCph1-PCB adducts at different temperatures: Low intensity of irradiation light (red, 10 μmol m^{-2} s^{-1}, far red, 10 μmol m^{-2} s^{-1}). Panel A to D shows series of spectra that were measured at different temperatures during a defined irradiation schedule. E, Monitor A$_{710 \text{ nm}}$ under continuous red light irradiated samples during 7000 s at different temperatures. F, absorbance spectra of 40 °C treated samples compared with 40 °C treated samples returned to 20 °C. Whole schedule: After assembly and NAP 10 column separation, far red light was first given, measure the full-length spectra (blue line, A-D), followed immediately by the red light irradiation, measure the full-length spectra (red line, A-D). Far red light irradiated again, change the measure program from full-length to time drive measurement, only measure the A$_{710 \text{ nm}}$, start the measurement, switch the red light after 180 s, the red light irradiation is continuous during the 7000 s time drive measurement (E). After the

86

time drive change program back to full-length measurement, immediately measure (black line, A-D), followed by far red light irradiation, measure (green line, A-D).

3.3.5 His Kinase studies of Cph1 at different temperatures

Concluded from the above those temperature induced spectral changes, I think C-terminal part of His-Kinase domain is responsible for sense the temperature. So later the phosphorylation activity of the Cph1-PCB adduct was test, under low light irradiation intensity, in order to check whether the phosphorylation of His Kinase also depending on temperature change. All the phosphorylation experiments were done by Ibrahim Njimona.

In Cph1, at 10 and 20 °C the activities of the red treated sample was about 25 % compared to the far red light treated sample, in accordance with previous reports (Esteban, B. et al. 2005, Yeh, K. C. et al. 1997). Figure 3.30 B shows the quantification of phosphorylation. It can be seen that the phosphorylation dropped in accordance with increased temperature, from 10 to 40 ℃, drop were slowly of Pfr than Pr. The red irradiated sample had a different behavior. Between 30 to 40 °C there was already no phosphorylation difference obvious. And the reduction of phosphorylation activity between 10 to 40 °C was less obvious as for Pr.
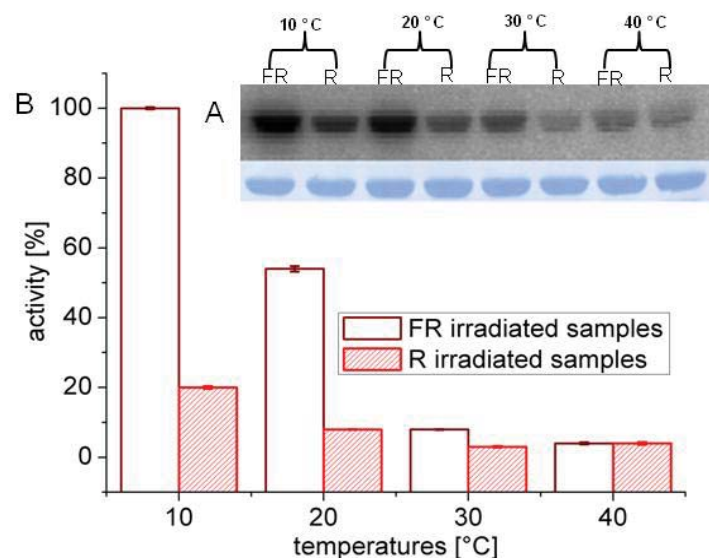
Figure 3.30 Autophosphorylation of Cph1 holo-protein at different temperatures. Cph1 samples were irradiated either with far red or red light before incubating with γ-^{32}P ATP in darkness at various temperatures. A, The upper panel shows the autoradiogram of the Cph1 band, the lower panel shows the same blot after Coomassie staining. B, Calculated phosphorylation intensity. Mean from 3 experiments ± SE.

Next step Only Pr form was used to extend our temperature effect. To test the phosphorylation activity at more detailed temperature. The highest phosphorylation of the Pr form of was at 10 °C, and then decreased till 40 °C (Figure 3.31 A, B). The quantification of phosphorylation shows the decrease of phosphorylation activity was roughly like the relationship between temperature and enzyme activity, Q10 = 2-3, at 10 to 30 °C temperature range. After 30 °C, only slightly decrease was detected.
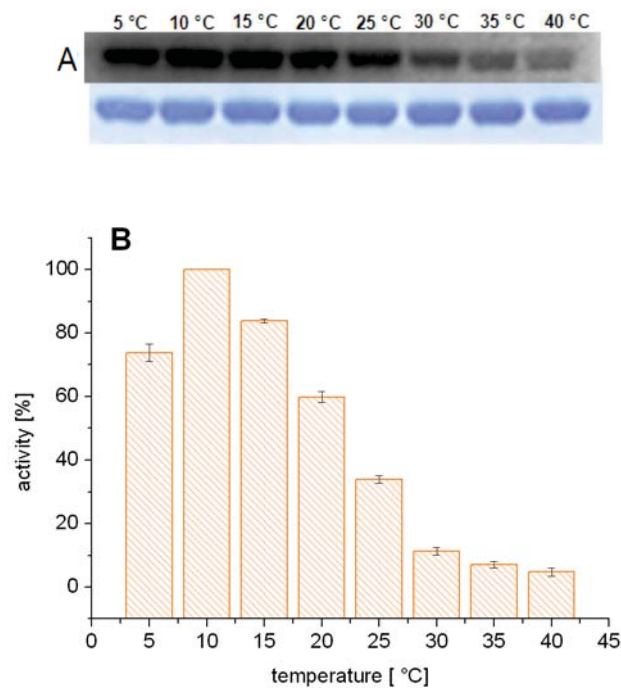
Figure 3.31 Phosphorylation of Cph1. Cph1 samples were incubation with γ-^{32}P ATP in darkness at various temperatures. The upper panel shows the autoradiogram of Cph1 band, the lower panel shows the same blot after Coomassie staining. A, Phosphorylation activity of Pr form of holoprotein, B Quantified phosphorylation activity. Mean values from 3 experiments ± SE.

3.3.6 *In vivo* physiological studies at different temperatures

3.3.6.1 *ptr201* lost gravitropism response at 29 °C

Four different temperatures were test, moss filaments were grown under totally darkness for 4 days at 23 °C, then transport to different temperatures. For gravitropism test, the plates were rotated 90 °, before change to different temperatures. All the plates keep vertically. Figure 3.32, shows the gravitropism response under different temperatures. At 32 °C, the gravitropism response of both wild type and *prt201* mutants were loss; they had the bending angle around 50 ° no difference can be distinguished between wild type and mutant and the BV treatments. At other temperatures, 18, and 29 °C wild type the filaments grown normal and response to gravitropism as room temperature 23 °C, for *ptr201* at 29 °C, the gravitropism response began to loss, the bending angle of tip cell was around 60 °, feeding with BV can rescue this response the bending angle to gravity recovered to 83 °C. Evidence here shows that phytochrome might play a role here, to work at 29 °C. At 32 °C both wild type and mutants loose gravitropism, I thought might because of the high temperature induce another signal pathway, which phytochrome might not participant in.
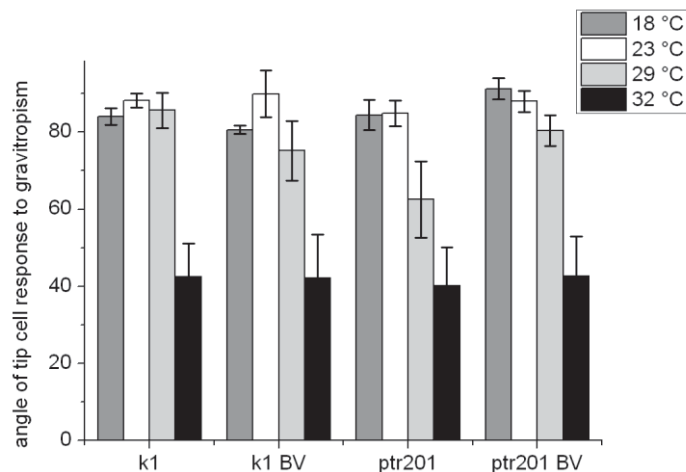
Figure 3.32 Gravitropism response at different temperatures of *Ceratodon purpureus* K1 and ptr201 filaments. Quantification of angle: tip cell to base cell. Mean values of 30 filaments for chlorophyll, 150 filaments for gravitropism from 3 experiments ± SE.

3.3.6.2 *phyA* and *phyB* had shorter hypocotyl at 32 ℃

Arabidopsis seedlings were kept in totally darkness, to get rid of the effect of light. Figure 3.33 shows the quantified hypocotyl elongation, under different temperatures conditions. 23 °C was used as room temperature, at 32°C the elongation of hypocotyl was significantly reduced at *phyA* and *phyB* mutants, but not wild type, Which means in those cases both *phyA* and *phyB* can remain the hypocotyl grow at high temperature, to neutralize the damage of warm temperature. At 29 °C there both have increased hypocotyl, which has no difference between wild type and mutant, indicates *phyA* and *phyB* have a higher working temperature. Elongation of hypocotyl is control by auxin, at 29 °C the level of auxin is much higher (Gray, W. M. et al. 1998). The inhibition of hypocotyl elongation at 32 °C may be because of the inhibition of the auxin transport, which can be controlled by phytochrome. 32 °C normally is not high enough to course the damage of *Arabidopsis*, except seed germination (Alia et al. 1998).

Figure 3.33 Quantified hypocotyl lengths under different temperatures of *Arabidopsis* wild type and *phyA, phyB* mutant. Mean value of 150 seedlings from 3 independent experiments± SE.

4 Discussion

4.1 Phytochrome chromophores configuration/conformation

Locked BV derived chromophores have so far contributed to questions concerning the stereochemistry of the phytochrome in the Pr and Pfr forms. Based on these studies it became clear that bacterial phytochrome can adopt light-stable Pr and Pf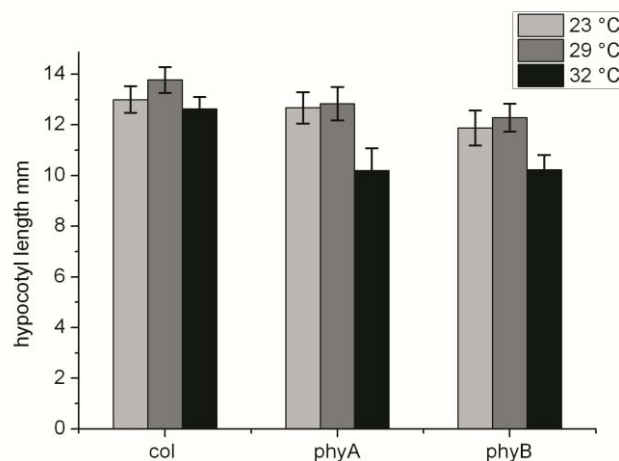r corresponding forms if the appropriate chromophores are incorporated. For experiments with plants, the BV derivatives are inappropriate because plant phytochromes incorporate PΦB as a natural chromophore. Besides PΦB, plant phytochrome accepts also PCB, which also has the same ring A ethylidene side chain. BV with the ring A vinyl side chain may also bind to plant or cyanobacterial phytochrome (Lamparter, T. et al. 2001c, Li, L. et al. 1995a), but does not function well. In the presented *in vitro* studies I used BV as a reference to test the incorporation in recombinant phytochrome. I confirmed that BV is not only incorporated into bacterial but also in a non-covalent manner into plant and cyanobacterial phytochrome (Figure 3.3-4, 3.7-8). In addition, I showed that also cyanobacterial and plant phytochrome BV adducts are photoactive. The absorption spectra are however clearly dissimilar from those of the corresponding PCB or PΦB adducts (Figure 3.3-4).

Hence, the new chromophores 15*Za*PCB and 15*Ea*PCB were synthesized and tested for their incorporation into phytochrome. By *in vitro* studies information about chromophore assembly and spectral properties of locked-chromophore adducts were gained. Both 15*Za*PCB and 15*Ea*PCB assembled with recombinant proteins under investigation, including truncated PhyB from *Arabidopsis thaliana* (Figure 3.1-4). For bacterial and plant phytochrome, the spectral properties of the 15*Za*PCB and 15*Ea*PCB adducts were comparable to those of the Pr and Pfr forms of these phytochrome (Figure 3.1-2, 4). For cyanobacterial Cph1, both the 15*Za*PCB and the 15*Ea*PCB adducts seem to be composed of two spectrally distinct species (Figure 3.3). The reason for this finding is maybe the C2 atom of PCB but not that of BV is a chiral C atom, and synthetic chromophores contain a mixture of both enantiomers. These enantiomers are

interconvertible under mild acidic and/or basic conditions and any preparation of PCB will thus also consist of a racemic mixture (these results will be reported elsewhere). It could be that the combination of locked chromophores and Cph1 stabilizes spectrally different species which otherwise would not accumulate. In recently published NMR work on Cph1, evidence was provided for two chemically different Pr forms which are distinguished by charge distributions around the chromophore (Song, C. et al. 2011). Plant phytochrome here show the covalent bond with locked chromophores the spectra of locked chromophore are according to Pr and Pfr forms (Figure 3.4). Although PhyB-651 has a low affinity to all used chromophores, this does not affect the shape of the absorbance spectrum, which is described in other papers. When plant phytochrome protein were used for *in vitro* assemble with chromophores also a low assembly efficiency was found (Hanzawa, H. et al. 2001). By spectral studies, I can conclude all used locked chromophores can form a covalent bond with the protein and the 15*Za*PCB adduct is Pr like, whereas 15*Ea*PCB adduct is Pfr like.

Phytochromes are biliproteins which exhibit only very weak fluorescence under ambient conditions. This property distinguishes them from the strongly fluorescent phycobiliproteins of cyanobacteria and red algae (Tooley, A. J. and Glazer, A. N. 2002). However, phytochrome fluorescence intensity can be increased by lowering the flexibility of the chromophore (Zienicke, B. et al. 2011a). Due to the free mobility of the pyrrole rings the fluorescence of free bilin molecules is very weak (Li, L. et al. 1995b). Incorporation into the chromophore pocket of a biliprotein such as phycocyanin or phytochrome restricts this mobility and results in an increase of the fluorescence quantum yield. Locked 15*Za*PCB chromophores further restricted in their flexibility of bilins, induce even strong fluorescence assembled to phytochrome (Figure 3.10, Table 3.2). The bacterial phytochrome Agp1-M15 uses BV as a natural chromophore that incorporates locked PCB chromophore through a non-covalent bond. Agp1-M15CV mutants which have a 249 Cys can incorporate locked PCB chromophores as well as PEB in a covalent manner. Cph1 and PhyB-N651 were also used in these experiments; which use PCB and PÖB as natural chromophores respectively, and form covalent bonds with locked chromophores. Compared to PEB, locked 15*Za*PCB has a lower quantum yield (Zienicke, B. et al. 2011a). This can be explained by an energy dissipation pathway through D ring and proton transfer. The

difference between the covalent bond and no covalent bond might also limit the flexibility. The slightly stronger fluorescence of Cph1compared to PhyB-N651 and Agp1-M15CV might because of the molecular weight (Sineshchekov, V.A., 1995).

The moss *Ceratodon purpureus* has been used in this work as a first model plant for the *in vivo* action of locked chromophores. Feeding of 15*Ea*PCB resulted in an increase of chlorophyll content in tip cells of dark grown protonemata of the chromophore deficient mutant *prt116* (Figure 3.11). The increase had the same magnitude as that of BV treated mutant in red light. Conclusions from these observations that (i) locked chromophores are efficiently taken up by the tip cells, as other bilin chromophores, (ii) the phytochrome adduct which according to *in vitro* studies should be photo-stable is fully active and induces the signal transduction cascade, and (iii) in the moss cells, no other input is required for the induction of chlorophyll synthesis. This finding reveals an interesting experimental insight into the evolution of chlorophyll synthesis. One of the latest steps in chlorophyll synthesis is the conversion of protochlorophyllide to chlorophyll, catalyzed by the protochlorophyllide-chlorophyll oxidoreductase (POR). Two versions of POR exist, a light dependent and a light independent enzyme, termed LPOR and DPOR, respectively. Angiosperms have only LPORs and chlorophyll synthesis is strictly light dependent. Other plants and photosynthetic bacteria may have DPOR and LPOR, and it has been shown that gymnosperms, ferns, algae, cyanobacteria and other bacteria can synthesize chlorophyll in darkness (Fujita, Y. 1996, Reinbothe, C. et al. 2010). The situation in moss is less examined. The genome of the moss *Physomitrella patens* is fully sequenced, and BLAST searches revealed two genes that might encode for LPORs and one that might encode for DPOR. Here I show for the first time that a DPOR is indeed active in mosses. This results speak against any action of an LPOR because after 15*Ea*PCB feeding in the dark, cells reached the same chlorophyll synthesis level as BV treated cells in red light. Studies with a new *Ceratodon purpureus* strain showed that 15*Ea*PCB, but not 15*Za*PCB, can induce phytochrome responses also in wild type plants (Figure 3.12-14). Although the response of fern spores to 15*Ea*PCB was only weak (Figure 3.15), it is reasonable to assume that 15*Ea*PCB chromophores will induce phytochrome responses also in other wild type organisms, thus other

phytochrome effects can be found and / or investigated by such feeding experiments even if mutants are not available.

For studies with *Arabidopsis* chromophore deficient mutants: *hy1* and *hy2* were used. These mutants have been investigated by many groups and have led to the identification of heme oxygenase and phytochromobilin-synthase genes. In these studies, both mutants responded in a similar manner to chromophore feeding. It is particularly noteworthy that the light effects on hypocotyl expansion and cotyledon opening were both rescued by BV in the *hy2* mutant (Figure 3.17). These results are striking because PΦB biosynthesis is blocked in a step downstream of BV. Those results are in agreement with earlier work, where BV feeding results in a complete restoration of photo-chemically active phytochrome (Parks, B. M. and Quail, P. H. 1991). Apparently, HY2 is not the only phytochromobilin synthase in *Arabidopsis*, as HY1 is not the only heme oxygenase (Emborg, T. J. et al. 2006). For this reason, the low amount of endogenous PΦB in the *hy2* mutant cell might be overcome by excess BV supplied through the growth medium. HY2 is located in the plastid. A cytosol, yet unknown enzyme might efficiently convert BV which is supplied through the medium into PΦB.

The major outcome of our *Arabidopsis* studies was that all phytochrome responses under investigation can be induced by 15*Ea*PCB in darkness (Figures 3.16-19). Not only chromophore deficient mutants, but also wild type plants showed such an induction. Another finding is equally important: in most *Arabidopsis* phytochrome effects investigated here, the induction by 15*Ea*PCB in the dark is not as strong as the induction by red light given to the wild type plant or to a BV-grown *hy1* or *hy2* mutant (Figures 3.16-19). The magnitude of the response could be related to subtle structural differences between natural Pfr and the 15*Ea*PCB adducts that result in differential coupling to the signal transduction cascade. We consider however that the induction by 15*Ea*PCB is limited because the adducts do not undergo cycling through Pr and Pfr. Studies with the Y276H mutant of phyB (Su, Y. S. and Lagarias, J. C. 2007) and the corresponding Y242H mutant of phyA (Rausenberger, J. et al. 2011) show that these mutants induce a constitutive de-etiolated phenotype when expressed in *Arabidopsis* in darkness, just as the locked 15*Ea*PCB chromophore. The effect of phyA_Y242H was less pronounced than that of

phyB_Y276H, and phyA_Y242H induced a dominant negative effect in the light when over expressed in wild type *Arabidopsis* (Rausenberger, J. et al. 2011). The difference in the action of both phytochrome mutants is explained by a phyA/phyB differential nuclear import mechanism: maximal uptake of phyA into the nucleus requires cycling through Pr and Pfr (Rausenberger, J. et al. 2011), whereas nuclear uptake of phyB does not include cycling (Pfeiffer, A. et al. 2009). According to this model, phyB responses can be maximally induced by 15*Ea*PCB, whereas phyA responses are only partially induced by this chromophore. We presently investigate the effect of 15*Ea*PCB on particular phytochrome mutants. The specific properties of phytochrome A have evolved in the angiosperms (Lamparter, T. 2006, Mathews, S. 2005a, Schneider-Poetsch, H. A. W. et al. 1998), and mosses do not contain a phytochrome A homolog. The finding that chlorophyll synthesis is induced by 15*Ea*PCB in the *ptr116* mutant of *Ceratodon purpureus* to the same extent as by red light after BV treatment (Figure 3.13) is consistent with a phyB-like nuclear uptake mechanism, or a phytochrome action outside the nucleus. It should be noted that microbeam experiments provided evidence that cycling is used by *Ceratodon* phytochrome to measure very strong light intensities (Lamparter, T. et al. 2004).

A more general conclusion also arises from our studies. The 15*Ea* chromophores yield Pfr-like adducts, result in Pfr-like protein conformations *in vitro* (Inomata, K. et al. 2005), and do also actively induce phytochrome responses *in vivo*, as shown here. These results support the idea that an isomerization around the C15=C16 double bond is the driving force for the Pr to Pfr conversion, and argue against the recent hypothesis formulated in the context of NMR data on a cyanobacterial phytochrome like SyCph1 (Ulijasz, A. T. et al. 2010) that ring A motions might be the first step.

4.2 Overlapping functions of *Ceratodon purpureus* phytochromes and cytosol/membrane localization

The moss *Ceratodon purpureus* has been studied for quite a long time, because of its simple life cycle and haploid stage. The single cells easily accessible from filaments and the dark growth characters all makes it a wonderful tool to study the function of light receptors. Four phytochromes have been fully sequenced in *Ceratodon purpureus*. Each of the phytochromes

knockout mutations was made and their functions were studied. It was found that Phy4 was responsible for the phototropism response (Mittmann, F. et al. 2009), whereas for the other phytochromes the function was still unclear, the membrane localization of the phytochrome also need to be invested.

DNA interference is a useful method used by many groups to silence specific genes, because DNA is much simpler to handle compared to RNA. Lots of endogenetic genes were already successfully silenced by this method. The silence efficiency is quite high; in the case of ferns it reached 90 %. Differences in silencing by using different DNA fragments are determined by the length of the coding sequence, but not the source of DNA (gDNA or cDNA). There is also not much difference between using the PCR product or plasmid. So for specific genes silencing, one can either use the full-length or only parts of a gene. One can use genes in a vector or directly use PCR product (Kawai-Toyooka, H. et al. 2004, Palauqui, J. C. and Balzergue, S. 1999, Voinnet, O. et al. 1998). In some case it was reported that PCR product has a better efficiency (Kawai-Toyooka, H. et al. 2004, Palauqui, J. C. and Balzergue, S. 1999, Voinnet, O. et al. 1998). Experiments also showed that several genes can be silenced at the same time (Kawai-Toyooka, H. et al. 2004). In this experiment by using DNA interference specific genes were silenced without disturbing others. Several phytochrome genes were silenced at the same time. According to the results there was a different transformation rate between heme oxygenase and other phytochrome genes, and also differences between different phytochrome genes. But for the same gene (only heme oxygenase investigated here) the difference is not obvious between different gene parts.

Using this method I was able to specifically silence PHY2, PHY3 gene, respectively, and then using the mutant, to check the function of phytochrome. According to the results CerpuPhy2 might responsible for branches formation. The mutant has more branches under red light compared to the wild type (Figure 3.21). CerpuPhy3 might have overlapping functions in controlling phototropism, although in my case I did not find any phenotype of CerpuPhy4 filaments, as reported by Mittamann that also might because the transformation of phy4 gene was not successful. The action mechanism of CerpuPhy3 and CerpuPhy4 might be different.

CerpuPhy3 moss filaments growth randomly under unilateral red light, whereas CerpuPhy4 (Mittmann, F. et al. 2009) shows an aphototropic phenotype. CerpuPhy3 might also responsible for the chlorophyll synthesis, which is indicated by a lighter color compared to the wild type. Mittamann et al. assumed that this might be a function of CerpuPhy1. The similar phenotype of CerpuPhy3 and Class II moss mutants (Lamparter, T. et al. 1997), makes it is possible that some of the Class II mutant might be CerpuPhy3 deficient.

PEB without a double bound at C and D rings shows a very strong fluorescence assembled to phytochrome. This can be used as a marker to monitor phytochrome localization. The CerpuPhy2Phy4heme triple mutant that was produced by DNA interference, stained with PEB showed a fluorescence signal only in the cell membrane (Figure 3.22), which means CerpuPhy3 or CerpuPhy1, might be located at the membrane. As mentioned before, the CerpuPhy2 silenced mutant showed more branches formation, indicating a function of CerpuPhy2 as a negative regulator for branches formation during protoplast regeneration. Some research demonstrates that branches formation is an action dichroism process, which means CerpuPhy2 might also membrane attached. Lamparter could show that around 10 % of extracted CerpuPhy2 appear to be associated with pellet-able membranes (Lamparter T., 2006). PEB staining of protoplast also indicated the membrane attachment of phytochrome (Figure 3.23).

According to time course PEB staining experiments, the chromophore need at least 2 hours to enter the cell. In the case of wild type, where the natural chromophore is already there, PEB need more time. In this case it takes about 8 h to reach maximal fluorescence signal. The signal increases from 2 h to 8 h. The longer development of fluorescence is probably due to the competition of PEB with the natural chromophore. Interestingly phytochrome assembling PEB in wild type might also be heterodimers, because of the weaker signal compared to chromophore deficient mutant. This is same as in the experiments using 15EaPCB to treat wild type samples in darkness. For the first time it was shown that in mosses phytochromes can also work as heterodimers, which in seeds plants normally formed by PhyA.

Taken together I conclude from the localization experiments three hypotheses (1) Like *Arabidopsis thaliana*, moss phytochromes might also have overlapping functions. (2) Each

phytochrome might be attached to the cell membrane by using same or different co-factors. And phytochrome might be translocated from the cell membrane to the cytosol and vice versa under different condition. (3) Phytochrome heterodimers might also occur in mosses like higher plants.

4.3 Phytochrome functions as a thermo sensor

Temperature is a very important factor for organisms to sense their environment. Plants, bacteria and fungi can change their growth character according to temperature changes. As early as in the 1970[ies] people already begun to study temperature effects on phytochrome (Anderson, G. R. et al. 1969). There are two main ways in which temperature can be measured. First, indirect signaled by a sudden temperature shift. Such indirect signals are known to be the accumulation of denatured proteins (heat shock) or stalled ribosome (cold shock). Second, direct through temperature sensor. Now lots of results show that His-Kinase or His-Kinase like domains may serve as a temperature sensors (Klinkert, B. and Narberhaus, F. 2009).

Phytochrome is known by its photoconversion under red/far red light irradiation, as a photoreceptor. Recent studies of Agp1 in our group showed, Agp1 might work as a thermo sensor also (Njimona, I. and Lamparter, T. 2011). *Agrobacterium tumefaciens* has two phytochromes: Agp1 and Agp2. His-Kinase activity of Agp1 is changing according to temperature. Increasing the temperature to 40 °C almost shuts down the His-Kinase activity. The highest phosphorylation occurs at 25 °C. Following a temperature increase the activity of phosphorylation decrease (Njimona, I. and Lamparter, T. 2011). Njimona and Lamparter also found out that at 40 °C a new form of phytochrome is formed called "Prx", formation of which needs the C-terminal of phytochrome and light irradiation. In my experiments, Cph1 Kinase activities showing the same phosphorylation activity model as Agp1 and VirA (Albanesi, D. et al. 2009). Phosphorylation of the His-Kinase is down regulated by temperature, but for Cph1 at 10 °C, highest phosphorylation was detected (Figure 3.30-31). While showing the same negative response to temperature, the sensitivity of Cph1 was not as strong as for Agp1 at all temperature conditions. This is in accordance with earlier studies (Lamparter, T. et al. 2002).

98

Several phytochrome-like proteins are known to exhibit temperature-dependent spectral changes in the physiological range. The cyanobacterial phytochrome Tlr0924 (Rockwell, N. C. et al. 2008), SyB-Cph1 (Ulijasz, A. T. et al. 2008), Agp1 (Njimona, I. and Lamparter, T. 2011), for example. In Cph1, temperature and light dependent spectral changes also happen. At high temperature a long red irradiation time (R, 10 µmol $m^{-2}s^{-1}$), convert Pfr to a new form, which cannot photoconvert back to either Pr or Pfr at the higher temperature, but when returned the temperature to 20°C, accompany with red light irradiation (R, 10 µmol $m^{-2}s^{-1}$), this form totally converts to Pfr, and then can be convert back to Pr (FR, 10 µmol $m^{-2}s^{-1}$) (Figure 3.26). The absorbance change might be induced by a change in the C-terminal Kinase, because N-terminal domain alone does not have this spectral change (Figure 3.28). Irreversible at high intensity irradiate light (R, 250 µmol $m^{-2}s^{-}1$; FR, 500 µmol $m^{-2}s^{-1}$), when returns the 40 °C samples back to 20°C, shows high intensity of light might be induce irreversible chromophore bleach.

High temperature and light irradiation induced protein conformational changes through C-terminal, then pass to N-terminal, which may induce some signal path way. This could indicate a function for Cph1 might also be as a thermo sensor. Because the function of phytochrome in Cph1 is not clear, this hypothesis could not be tested. As showing by other temperature regulated Kinase, the phosphorylation activity change can affect bacterial virulence, like VirA (Albanesi, D. et al. 2009).

Phytochrome functions at different temperature were followed by *in vivo* studies using plants phytochromes; on basis of well studied phenotypes. Chromophore deficient mutant of moss and phytochrome deficient mutants of *Arabidopsis thaliana* were used.

In a chromophore mutant of the moss *Ceratodon purpureus* the tip cell shows a less pronounced gravitropism response at 29°C (Figure 3.32), whereas the wild type shows the normal gravitropism response. Loss of gravitropism can be rescued by BV treatment which means that this response is under phytochrome control. The loss of gravitropism might because of less plastid sediments at the other side, which is under phytochrome control (Kim, K. et al, 2011). At 32°C, moss filaments grow greener and more randomly in both the wild type and the

mutant. This could mean that 32°C is already out of the physiological range of moss phytochrome, and some other signaling pass way should be activated.

In *Arabidopsis thaliana* lots of studies have been done to test the growth ability and signaling path way that cross temperature and light signaling (Franklin, K. A. and Whitelam, G. C. 2004a). Different phytochromes have their own best working temperature under light conditions. PhyA has an important role in promoting germination at warmer temperatures, phyE was important for germination at colder temperatures and phyB was important for germination across a range of temperatures (Donohue, K. et al. 2007; Shinomura et al. 1994; Poppe and Schäfer 1997; Shinomura 1997; Hennig et al. 2002), a recent investigation of temperature effects on hypocotyl elongation in *hfr1-*, *pif4-*, and *phyB* mutant indicated that phyB might also work as a thermo sensor (Foreman, J. et al. 2011). Lots of studies show flowering timing is controlled by both, temperature and light conditions (Franklin, K. A. and Whitelam, G. C. 2004b). Growth at 16 °C abolished the early flowering phenotypes of *phyB* and *phyAphyBphyD*-triple mutants (Halliday, K. J. and Whitelam, G. C. 2003). In most of the cases these studies were done combined with different light conditions, which cannot exclude the function of light. In my work the whole experiments expect seed germination induce, were done under total darkness. The results show that both PhyA and PhyB might work as thermo sensors. The hypocotyl length was shorter compared to the wild type (Figure 3.33). That difference can only be found at 32 °C. Wild type seedlings had the normal length compared to 23 °C, but both mutants had a shorter hypocotyl length.

According to those results, both *in vitro* and *in vivo*, I can conclude: (1) Studies concerning phytochrome as light receptor, which regulate a lot of activities by sensing light, photo-converting and then switch on and off the activity. It is clear that the N-terminal is the initial part undergoing photoconversion, and inducing the conformation changes, conformational changes then may further then initiate signaling pathways. (2) Phytochrome might as also be a temperature sensor that regulates lots of activities by sensing temperature changes. Temperature may be first sensed by the His Kinase (bacteria) or His Kinase Related Domain (plant) and is then subsequently passed to the N-terminal chromophore module, induce the

conformation change. The light sense of N-terminal and temperature sense of C-terminal may together further induce the signal pathway.

5 Acknowledgement

6 Reference list

Ahmad,M., Grancher,N., Heil,M., Black,R.C., Giovani,B., Galland,P., and Lardemer,D. (2002) Action spectrum for cryptochrome-dependent hypocotyl growth inhibition in Arabidopsis. Plant Physiol **129**:774-785.

Akamatsu,T. and Taguchi,H. (2001) Incorporation of the whole chromosomal DNA in protoplast lysates into competent cells of Bacillus subtilis. Biosci.Biotechnol.Biochem. **65**:823-829.

Albanesi,D., Martin,M., Trajtenberg,F., Mansilla,M.C., Haouz,A., Alzari,P.M., de,M.D., and Buschiazzo,A. (2009) Structural plasticity and catalysis regulation of a thermosensor histidine kinase. Proc.Natl.Acad.Sci.U.S.A **106**:16185-16190.

Alia, Hayash,H., Sakamoto,A., and Murata,N. (1998) Enhancement of the tolerance of Arabidopsis to high temperatures by genetic engineering of the synthesis of glycinebetaine. Plant J. **16**:155-161.

Anderson,G.R., Jenner,E.L., and Mumford,F.E. (1969) Temperature and pH studies on phytochrome in vitro. Biochemistry **8**:1182-1187.

Moglich,A., Yang,X.J., Ayers,R.A., Moffat,K. (2010) structural and function of plant photoreceptors. Annual Review of Plant Biology **61**:21-47.

Berkelman,T.R. and Lagarias,J.C. (1986) Visualization of bilin-linked peptides and proteins in polyacrylamide gels. Anal.Biochem. **156**:194-201.

Bonnassie,S., Burini,J.F., Oreglia,J., Trautwetter,A., Patte,J.C., and Sicard,A.M. (1990) Transfer of plasmid DNA to Brevibacterium lactofermentum by electrotransformation. J.Gen.Microbiol. **136**:2107-2112.

Borucki,B., Otto,H., Rottwinkel,G., Hughes,J., Heyn,M.P., and Lamparter,T. (2003) Mechanism of Cph1 phytochrome assembly from stopped-flow kinetics and circular dichroism. Biochemistry **42**:13684-13697.

Borucki,B., von Stetten,D., Seibeck,S., Lamparter,T., Michael,N., Mroginski,M.A., Otto,H., Murgida,D.H., Heyn,M.P., and Hildebrandt,P. (2005) Light-induced proton release of phytochrome is coupled to the transient deprotonation of the tetrapyrrole chromophore. Journal of Biological Chemistry **280**:34358-34364.

Boese,G., Schwille,P., and Lamparter,T. (2004a) The mobility of phytochrome within protonemal tip cells of the moss Ceratodon purpureus, monitored by fluorescence correlation spectroscopy. Biophysical Journal **87**:2013-2021.

Boese,G., Schwille,P., and Lamparter,T. (2004b) The mobility of phytochrome within protonemal tip cells of the moss Ceratodon purpureus, monitored by fluorescence correlation spectroscopy. Biophys.J. **87**:2013-2021.

Braun,Y., Smirnova,A.V., Schenk,A., Weingart,H., Burau,C., Muskhelishvili,G., and Ullrich,M.S. (2008) Component and protein domain exchange analysis of a thermoresponsive, two-component regulatory system of Pseudomonas syringae. Microbiology **154**:2700-2708.

Bruecker,G., Mittmann,F., Hartmann,E., and Lamparter,T. (2005) Targeted site-directed mutagenesis of a heme oxygenase locus by gene replacement in the moss Ceratodon purpureus. Planta **220**:864-874.

Casazza,A.P., Rossini,S., Rosso,M.G., and Soave,C. (2005) Mutational and expression analysis of ELIP1 and ELIP2 in Arabidopsis thaliana. Plant Mol.Biol. **58**:41-51.

Clack,T., Mathews,S., and Sharrock,R.A. (1994) The Phytochrome Apoprotein Family in Arabidopsis Is Encoded by 5 Genes - the Sequences and Expression of Phyd and Phye. Plant Molecular Biology **25**:413-427.

Cove,D.J., Perroud,P.F., Charron,A.J., McDaniel,S.F., Khandelwal,A., and Quatrano,R.S. (2009a) Isolation and regeneration of protoplasts of the moss Physcomitrella patens. Cold Spring Harb.Protoc. **2009**:db.

Cove,D.J., Perroud,P.F., Charron,A.J., McDaniel,S.F., Khandelwal,A., and Quatrano,R.S. (2009b) Transformation of the moss Physcomitrella patens using direct DNA uptake by protoplasts. Cold Spring Harb.Protoc. **2009**:db.

Donohue,K., Heschel,M.S., Chiang,G.C., Butler,C.M., and Barua,D. (2007) Phytochrome mediates germination responses to multiple seasonal cues. Plant Cell Environ. **30**:202-212.

Esch,H., Hartmann,E., Cove,D., Wada,M., and Lamparter,T. (1999) Phytochrome-controlled phototropism of protonemata of the moss Ceratodon purpureus: physiology of the wild type and class 2 ptr-mutants. Planta **209**:290-298.

Esteban,B., Carrascal,M., Abian,J., and Lamparter,T. (2005) Light-induced conformational changes of cyanobacterial phytochrome Cph1 probed by limited proteolysis and autophosphorylation. Biochemistry **44**:450-461.

Etzold,H. (1965) Der Polarotropismus und Phototropismus der Chloronemen Von Dryopteris Filix Mas (L) Schott. Planta **64**:254-&.

Foreman,J., Johansson,H., Hornitschek,P., Josse,E.M., Fankhauser,C., and Halliday,K.J. (2011) Light receptor action is critical for maintaining plant biomass at warm ambient temperatures. Plant J. **65**:441-452.

Forsburg,S.L. (2003) Introduction of DNA into S. pombe cells. Curr.Protoc.Mol.Biol. **Chapter 13**:Unit.

Franklin,K.A. and Quail,P.H. (2010) Phytochrome functions in Arabidopsis development. J.Exp.Bot. **61**:11-24.

Franklin,K.A. and Whitelam,G.C. (2004a) Light signals, phytochromes and cross-talk with other environmental cues. J.Exp.Bot. **55**:271-276.

Franklin,K.A. and Whitelam,G.C. (2004b) Light signals, phytochromes and cross-talk with other environmental cues. J.Exp.Bot. **55**:271-276.

Fujita,Y. (1996) Protochlorophyllide reduction: a key step in the greening of plants. Plant Cell Physiol **37**:411-421.

Furuya,M. (1983) Photomorphogenesis in ferns. H.Mohr and W.Shropshire, eds (Berlin, Heidelberg, New York: Springer Verlag), pp. 569-600.

Furuya,M., Kanno,M., Okamoto,H., Fukuda,S., and Wada,M. (1997) Control of mitosis by phytochrome and a blue-light receptor in fern spores. Plant Physiology **113**:677-683.

Gray,W.M., Ostin,A., Sandberg,G., Romano,C.P., and Estelle,M. (1998) High temperature promotes auxin-mediated hypocotyl elongation in Arabidopsis. Proc.Natl.Acad.Sci.U.S.A **95**:7197-7202.

Halliday,K.J. and Whitelam,G.C. (2003) Changes in photoperiod or temperature alter the functional relationships between phytochromes and reveal roles for phyD and phyE. Plant Physiol **131**:1913-1920.

Hanzawa,H., Inomata,K., Kinoshita,H., Kakiuchi,T., Jayasundera,K.P., Sawamoto,D., Ohta,A., Uchida,K., Wada,K., and Furuya,M. (2001) In vitro assembly of phytochrome B apoprotein with synthetic analogs of the phytochrome chromophore. Proc.Natl.Acad.Sci.U.S.A **98**:3612-3617.

Harari-Steinberg,O., Ohad,I., and Chamovitz,D.A. (2001) Dissection of the light signal transduction pathways regulating the two early light-induced protein genes in Arabidopsis. Plant Physiol **127**:986-997.

Hartmann,E., Klingenberg,B., and Bauer,L. (1983) Phytochrome-Mediated Phototropism in Protonemata of the Moss Ceratodon-Purpureus Brid. Photochemistry and Photobiology **38**:599-603.

Haupt,W. (1970) Dichroism of Phytochrome P600 and P730 in Mougeotia. Zeitschrift fur Pflanzenphysiologie **62**:287-&.

Haupt,W. (1992) Phytochrome-mediated fern spore germination: A temperature-sensitive phase in the transduction chain after the action of Pfr. J.Plant Physiol. **140**:575-581.

Heddad,M., Noren,H., Reiser,V., Dunaeva,M., Andersson,B., and Adamska,I. (2006) Differential expression and localization of early light-induced proteins in Arabidopsis. Plant Physiol **142**:75-87.

Hennig L., Stoddart W.M., Dieterle M., Whitelam G.C. and Schaefer,E. (2002) Phytochrome E controls light-induced germination of Arabidopsis. Plant Physiology **128**, 194–200.

Heyne,K., Herbst,J., Stehlik,D., Esteban,B., Lamparter,T., Hughes,J., and Diller,R. (2002) Ultrafast dynamics of phytochrome from the cyanobacterium Synechocystis, reconstituted with phycocyanobilin and phycoerythrobilin. Biophysical Journal **82**:1004-1016.

Hwang,Y.S. and Quail,P.H. (2008) Phytochrome-regulated PIL1 derepression is developmentally modulated. Plant Cell Physiol **49**:501-511.

Inomata,K., Hammam,M.A., Kinoshita,H., Murata,Y., Khawn,H., Noack,S., Michael,N., and Lamparter,T. (2005a) Sterically locked synthetic bilin derivatives and phytochrome Agp1 from Agrobacterium tumefaciens form photoinsensitive Pr- and Pfr-like adducts. J.Biol.Chem. **280**:24491-24497.

Inomata,K., Hammam,M.A.S., Kinoshita,H., Murata,Y., Khawn,H., Noack,S., Michael,N., and Lamparter,T. (2005b) Sterically locked synthetic bilin derivatives and phytochrome Agp1 from

Agrobacterium tumefaciens form photoinsensitive Pr- and Pfr-like adducts. J.Biol.Chem. **280**:24491-24497.

Inomata,K., Noack,S., Hammam,M.A., Khawn,H., Kinoshita,H., Murata,Y., Michael,N., Scheerer,P., Krauss,N., and Lamparter,T. (2006a) Assembly of synthetic locked chromophores with agrobacterium phytochromes Agp1 and Agp2. J.Biol.Chem. **281**:28162-28173.

Inomata,K., Noack,S., Hammam,M.A.S., Khawn,H., Kinoshita,H., Murata,Y., Michael,N., Scheerer,P., Krauss,N., and Lamparter,T. (2006b) Assembly of synthetic locked chromophores with Agrobacterium phytochromes AGP1 and AGP2. J.Biol.Chem. **281**:28162-28173.

Jiao,Y., Lau,O.S., and Deng,X.W. (2007) Light-regulated transcriptional networks in higher plants. Nat.Rev.Genet. **8**:217-230.

Jorissen,H.J., Quest,B., Lindner,I., Tandeau de,M.N., and Gartner,W. (2002) Phytochromes with noncovalently bound chromophores: the ability of apophytochromes to direct tetrapyrrole photoisomerization. Photochem.Photobiol. **75**:554-559.

Kagawa,T., Lamparter,T., Hartmann,E., and Wada,M. (1997) Phytochrome-mediated branch formation in protonemata of the moss *Ceratodon purpureus*. J.Plant Res. **110**:363-370.

Kasperbauer,M.J. and Hamilton,J.L. (1984) Chloroplast Structure and Starch Grain Accumulation in Leaves That Received Different Red and Far-Red Levels during Development. Plant Physiol **74**:967-970.

Kawai-Toyooka,H., Kuramoto,C., Orui,K., Motoyama,K., Kikuchi,K., Kanegae,T., and Wada,M. (2004) DNA interference: a simple and efficient gene-silencing system for high-throughput functional analysis in the fern Adiantum. Plant and Cell Physiology **45**:1648-1657.

Kendrick,R.E. and Cone,J.W. (1985) Biphasic fluence response curves for induction of seed germination. Plant Physiol **79**:299-300.

Kim, K., Shin, J., Lee, S. H., Kweon, H.S., Maloof, J.N. and Choi. G. (2011) Phytochromes inhibit hypocotyl negative gravitropism by regulating the development of endodermal amyloplasts through phytochrome-interacting factors. Proceedings of the National Academy of Sciences of the United States of America **108**:1729-1734.

Kircher,S., Gil,P., Kozma-Bognar,L., Fejes,E., Speth,V., Husselstein-Muller,T., Bauer,D., Adam,E., Schaefer,E., and Nagy,F. (2002) Nucleocytoplasmic partitioning of the plant photoreceptors phytochrome A, B, C, D, and E is regulated differentially by light and exhibits a diurnal rhythm. Plant Cell **14**:1541-1555.

Kircher,S., Kozma-Bognar,L., Kim,L., Adam,E., Harter,K., Schaefer,E., and Nagy,F. (1999) Light quality-dependent nuclear import of the plant photoreceptors phytochrome A and B. Plant Cell **11**:1445-1456.

Kleiner,O., Kircher,S., Harter,K., and Batschauer,A. (1999) Nuclear localization of the Arabidopsis blue light receptor cryptochrome 2. Plant Journal **19**:289-296.

Klinkert,B. and Narberhaus,F. (2009) Microbial thermosensors. Cell Mol.Life Sci. **66**:2661-2676.

Kohchi,T., Mukougawa,K., Frankenberg,N., Masuda,M., Yokota,A., and Lagarias,J.C. (2001) The Arabidopsis HY2 gene encodes phytochromobilin synthase, a ferredoxin-dependent biliverdin reductase. Plant Cell **13**:425-436.

Koornneef,M., Rolff,E., and Spruit,C.J.P. (1980) Genetic-Control of Light-Inhibited Hypocotyl Elongation in Arabidopsis-Thaliana (L) Heynh. Zeitschrift fur Pflanzenphysiologie **100**:147-160.

Laemmli,U.K. (1970) Cleavage of structural proteins during the assembly of the head of bacteriophage T4. Nature **227**:680-685.

Lakowicz,J.R. (1999) *Principles of Fluorescence Spectroscopy, 2*$^{nd\ Ed.}$ New York, London, Boston, Moscow, Dordrecht.

Lamparter,T. (2004) Evolution of cyanobacterial and plant phytochromes. FEBS Lett. **573**:1-5.

Lamparter,T. (2006) Photomorphogenesis of mosses. In Photomorphogenesis in Plants and Bacteria, E.Schaefer and F.Nagy, ed (Netherlands.: pp. 537-565.

Lamparter,T., Esch,H., Cove,D., and Hartmann,E. (1997a) Phytochrome control of phototropism and chlorophyll accumulation in the apical cells of protonemal filaments of wildtype and an aphototropic mutant of the moss Ceratodon purpureus. Plant and Cell Physiology **38**:51-58.

Lamparter,T., Esch,H., Cove,D., Hughes,J., and Hartmann,E. (1996a) Aphototropic mutants of the moss Ceratodon purpureus with spectrally normal and with spectrally dysfunctional phytochrome. Plant Cell and Environment **19**:560-568.

Lamparter,T., Esch,H., Cove,D., Hughes,J., and Hartmann,E. (1996b) Aphototropic mutants of the moss Ceratodon purpureus with spectrally normal and with spectrally dysfunctional phytochrome. Plant Cell and Environment **19**:560-568.

Lamparter,T., Esteban,B., and Hughes,J. (2001a) Phytochrome Cph1 from the cyanobacterium Synechocystis PCC6803 - Purification, assembly, and quaternary structure. Eur.J.Biochem. **268**:4720-4730.

Lamparter,T., Esteban,B., and Hughes,J. (2001b) Phytochrome Cph1 from the cyanobacterium Synechocystis PCC6803. Purification, assembly, and quaternary structure. Eur.J.Biochem. **268**:4720-4730.

Lamparter,T., Esteban,B., and Hughes,J. (2001c) Phytochrome Cph1 from the cyanobacterium *Synechocystis* PCC6803: purification, assembly, and quaternary structure. Eur.J.Biochem. **268**:4720-4730.

Lamparter,T., Hughes,J., and Hartmann,E. (1998) Blue light- and genetically-reversed gravitropic response in protonemata of the moss *Ceratodon purpureus*. Planta **206**:95-102.

Lamparter,T., Michael,N., Mittmann,F., and Esteban,B. (2002) Phytochrome from Agrobacterium tumefaciens has unusual spectral properties and reveals an N-terminal chromophore attachment site. Proceedings of the National Academy of Sciences of the United States of America **99**:11628-11633.

Lamparter,T., Mittmann,F., Goertner,W., Boerner,T., Hartmann,E., and Hughes,J. (1997b) Characterization of recombinant phytochrome from the cyanobacterium *Synechocystis*. Proc.Natl.Acad.Sci.U.S.A. **94**:11792-11797.

Lamparter,T., Podlowski,S., Mittmann,F., SchneiderPoetsch,H., Hartmann,E., and Hughes,J. (1995) Phytochrome from protonemal tissue of the moss Ceratodon purpureus. Journal of Plant Physiology **147**:426-434.

Li,L., Murphy,J.T., and Lagarias,J.C. (1995a) Continuous fluorescence assay of phytochrome assembly in vitro. Biochemistry **34**:7923-7930.

Li,L., Murphy,J.T., and Lagarias,J.C. (1995b) Continuous fluorescence assay of phytochrome assembly in vitro. Biochemistry **34**:7923-7930.

Li,L.M. and Lagarias,J.C. (1992) Phytochrome Assembly - Defining Chromophore Structural Requirements for Covalent Attachment and Photoreversibility. Journal of Biological Chemistry **267**:19204-19210.

Li,L.M., Murphy,J.T., and Lagarias,J.C. (1995) Continuous Fluorescence Assay of Phytochrome Assembly In-Vitro. Biochemistry **34**:7923-7930.

Mackenzie,J.M., Coleman,R.A., Briggs,W.R., and Pratt,L.H. (1975) Reversible Redistribution of Phytochrome Within Cell Upon Conversion to Its Physiologically Active Form. Proceedings of the National Academy of Sciences of the United States of America **72**:799-803.

Mikami,K., Kanesaki,Y., Suzuki,I., and Murata,N. (2002) The histidine kinase Hik33 perceives osmotic stress and cold stress in Synechocystis sp PCC 6803. Mol.Microbiol. **46**:905-915.

Mittmann,F., Dienstbach,S., Weisert,A., and Forreiter,C. (2009) Analysis of the phytochrome gene family in Ceratodon purpureus by gene targeting reveals the primary phytochrome responsible for photo- and polarotropism. Planta **230**:27-37.

Moon,Y.J., Kim,S.J., Park,Y.M., and Chung,Y.H. (2010) Sensing UV/blue: pterin as a UV-A absorbing chromophore of cryptochrome. Plant Signal.Behav. **5**:1127-1130.

Muramoto,T., Kohchi,T., Yokota,A., Hwang,I., and Goodman,H.M. (1999) The Arabidopsis photomorphogenic mutant hy1 is deficient in phytochrome chromophore biosynthesis as a result of a mutation in a plastid heme oxygenase. Plant Cell **11**:335-348.

Murashige,T. and Skoog,F. (1962) A Revised Medium for Rapid Growth and Bio Assays with Tobacco Tissue Cultures. PHYSIOL PLANT **15**:473-&.

Nagy,F. and Schaefer,E. (2000) Nuclear and cytosolic events of light-induced, phytochrome-regulated signaling in higher plants. EMBO J. **19**:157-163.

Nagy,F. and Schaefer,E. (2002) Phytochromes control photomorphogenesis by differentially regulated, interacting signaling pathways in higher plants. Annu.Rev.Plant Biol. **53**:329-355.

Nishiyama,K., Kamiya,A., Hammam,M.A.S., Kinoshita,H., Fujinami,S., Ukaji,Y., and Inomata,K. (2010) Total Syntheses of Sterically Locked Phycocyanobilin Derivatives Bearing a 15Z-anti or a 15E-anti CD-Ring Component. Bulletin of the Chemical Society of Japan 83:1309-1322.

Njimona,I. and Lamparter,T. (2011) Temperature effects on agrobacterium phytochrome agp1. PLoS One **6**:e25977.

110

Oka,Y., Matsushita,T., Mochizuki,N., Quail,P.H., and Nagatani,A. (2008) Mutant screen distinguishes between residues necessary for light-signal perception and signal transfer by phytochrome B. PLoS Genet. **4**:e1000158.

Palauqui,J.C. and Balzergue,S. (1999) Activation of systemic acquired silencing by localised introduction of DNA. Current Biology **9**:59-66.

Parks,B.M. and Quail,P.H. (1991) Phytochrome-Deficient Hy1 and Hy2 Long Hypocotyl Mutants of Arabidopsis Are Defective in Phytochrome Chromophore Biosynthesis. Plant Cell **3**:1177-1186.

Poppe,C. and Schaefer,E. (1997) Seed germination of Arabidopsis thaliana phyA/phyB double mutants is under phytochrome control. Plant Physiol **114**:1487-1492.

Pratt,L.H. (1994) *Distribution and localization of phytochrome within the plant*. The Netherlands.

Quail,P.H., Marme,D., and Schaefer,E. (1973) Particle-Bound Phytochrome from Maize and Pumpkin. Nature-New Biology **245**:189-191.

Reed,J.W., Nagatani,A., Elich,T.D., Fagan,M., and Chory,J. (1994) Phytochrome A and Phytochrome B Have Overlapping but Distinct Functions in Arabidopsis Development. Plant Physiol **104**:1139-1149.

Reed,J.W., Nagpal,P., Poole,D.S., Furuya,M., and Chory,J. (1993) Mutations in the gene for the red/far-red light receptor phytochrome B alter cell elongation and physiological responses throughout Arabidopsis development. Plant Cell **5**:147-157.

Reinbothe,C., El,B.M., Buhr,F., Muraki,N., Nomata,J., Kurisu,G., Fujita,Y., and Reinbothe,S. (2010) Chlorophyll biosynthesis: spotlight on protochlorophyllide reduction. Trends Plant Sci. **15**:614-624.

Rentsch,S., Hermann,G., Bischoff,M., Strehlow,D., and Rentsch,M. (1997) Femtosecond spectroscopic studies on the red light-absorbing form of oat phytochrome and 2,3-dihydrobiliverdin. Photochemistry and Photobiology **66**:585-590.

Rockwell,N.C., Njuguna,S.L., Roberts,L., Castillo,E., Parson,V.L., Dwojak,S., Lagarias,J.C., and Spiller,S.C. (2008) A second conserved GAF domain cysteine is required for the blue/green photoreversibility of cyanobacteriochrome Tlr0924 from Thermosynechococcus elongatus. Biochemistry **47**:7304-7316.

Rohmer,T., Lang,C., Hughes,J., Essen,L.O., Gartner,W., and Matysik,J. (2008) Light-induced chromophore activity and signal transduction in phytochromes observed by 13C and 15N magic-angle spinning NMR. Proc.Natl.Acad.Sci.U.S.A **105**:15229-15234.

Rossini,S., Casazza,A.P., Engelmann,E.C., Havaux,M., Jennings,R.C., and Soave,C. (2006) Suppression of both ELIP1 and ELIP2 in Arabidopsis does not affect tolerance to photoinhibition and photooxidative stress. Plant Physiol **141**:1264-1273.

Rüdiger,W., Thümmler,F., Cmiel,E., Schneider,S. (1983) Chromophore structure of the physiologically active form (Pfr) of phytochrome. PNAS **80**:6244-6248.

Salter,M.G., Franklin,K.A., and Whitelam,G.C. (2003) Gating of the rapid shade-avoidance response by the circadian clock in plants. Nature **426**:680-683.

Sambrook,J. and Russell,D.W. (2001) *Molecular Cloning. A Laboratory Manual. 3rd edition.* Cold Spring Harbor Laboratory Press.

Schaefer,D.G. and Zryd,J.P. (1997) Efficient gene targeting in the moss Physcomitrella patens. Plant J. **11**:1195-1206.

Schaefer,E. and Nagy,F. (2006) Photomorphogenesis in Plants and Bacteria : Function and Signal Transduction Mechanisms. Photomorphogenesis in Plants and Bacteria : Function and Signal Transduction Mechanisms.

Sharrock,R.A. and Quail,P.H. (1989) Novel Phytochrome Sequences in Arabidopsis-Thaliana - Structure, Evolution, and Differential Expression of A Plant Regulatory Photoreceptor Family. Genes & Development **3**:1745-1757.

Shinomura T., Nagatani A., Chory J. & Furuya M. (1994) The induction of seed germination in Arabidopsis thaliana is regulated principally by phytochrome B and secondarily by phytochrome A. Plant Physiology Rockville **104**, 363–371.

Shinomura T. (1997) Phytochrome regulation of seed germination. Journal of Plant Research **110**, 151–161.

Sineshchekov,V.A. (1995) Photobiophysics and Photobiochemistry of the Heterogeneous Phytochrome System. Biochimica et Biophysica Acta-Bioenergetics **1228**:125-164.

Smirnova,A.V., Braun,Y., and Ullrich,M.S. (2008) Site-directed mutagenesis of the temperature-sensing histidine protein kinase CorS from Pseudomonas syringae. FEMS Microbiol.Lett. **283**:231-238.

Song,C., Psakis,G., Lang,C., Mailliet,J., Gartner,W., Hughes,J., and Matysik,J. (2011) Two ground state isoforms and a chromophore D-ring photoflip triggering extensive intramolecular changes in a canonical phytochrome. Proc.Natl.Acad.Sci.U.S.A **108**:3842-3847.

Speth,V., Otto,V., and Schaefer,E. (1987) Intracellular-Localization of Phytochrome and Ubiquitin in Red-Light-Irradiated Oat Coleoptiles by Electron-Microscopy. Planta **171**:332-338.

Tasler,R., Moises,T., and Frankenberg-Dinkel,N. (2005) Biochemical and spectroscopic characterization of the bacterial phytochrome of Pseudomonas aeruginosa. Febs Journal **272**:1927-1936.

Terry,M.J. and Kendrick,R.E. (1999) Feedback inhibition of chlorophyll synthesis in the phytochrome chromophore-deficient aurea and yellow-green-2 mutants of tomato. Plant Physiol **119**:143-152.

Thummler,F., Dufner,M., Kreisl,P., and Dittrich,P. (1992) Molecular-Cloning of A Novel Phytochrome Gene of the Moss Ceratodon-Purpureus Which Encodes A Putative Light-Regulated Protein-Kinase. Plant Molecular Biology **20**:1003-1017.

Tooley,A.J. and Glazer,A.N. (2002) Biosynthesis of the cyanobacterial light-harvesting polypeptide phycoerythrocyanin holo-alpha subunit in a heterologous host. J.Bacteriol. **184**:4666-4671.

Tsuchiya,Y., Vidaurre,D., Toh,S., Hanada,A., Nambara,E., Kamiya,Y., Yamaguchi,S., and McCourt,P. (2010) A small-molecule screen identifies new functions for the plant hormone strigolactone. Nat.Chem.Biol. **6**:741-749.

112

Uchida,K. and Furuya,M. (1997) Control of the entry into S phase by phytochrome and blue light receptor in the first cell cycle of fern spores. Plant and Cell Physiology **38**:1075-1079.

Ulijasz,A.T., Cornilescu,G., Cornilescu,C.C., Zhang,J., Rivera,M., Markley,J.L., and Vierstra,R.D. (2010) Structural basis for the photoconversion of a phytochrome to the activated Pfr form. Nature **463**:250-254.

Ulijasz,A.T., Cornilescu,G., von,S.D., Kaminski,S., Mroginski,M.A., Zhang,J., Bhaya,D., Hildebrandt,P., and Vierstra,R.D. (2008) Characterization of two thermostable cyanobacterial phytochromes reveals global movements in the chromophore-binding domain during photoconversion. J.Biol.Chem. **283**:21251-21266.

van Thor,J.J., Borucki,B., Crielaard,W., Otto,H., Lamparter,T., Hughes,J., Hellingwerf,K.J., and Heyn,M.P. (2001) Light-induced proton release and proton uptake reactions in the cyanobacterial phytochrome Cph1. Biochemistry **40**:11460-11471.

Voinnet,O., Vain,P., Angell,S., and Baulcombe,D.C. (1998) Systemic spread of sequence-specific transgene RNA degradation in plants is initiated by localized introduction of ectopic promoterless DNA. Cell **95**:177-187.

Wada,M. and Furuya,M. (1978) Effects of Narrow-Beam Irradiations with Blue and Far-Red Light on Timing of Cell-Division in Gametophytes. Planta **138**:85-90.

Yamaguchi,R., Nakamura,M., Mochizuki,N., Kay,S.A., and Nagatani,A. (1999) Light-dependent translocation of a phytochrome B-GFP fusion protein to the nucleus in transgenic Arabidopsis. Journal of Cell Biology **145**:437-445.

Yatsuhashi,H., Kadota,A., and Wada,M. (1985) Blue-Light and Red-Light Action in Photoorientation of Chloroplasts in Adiantum Protonemata. Planta **165**:43-50.

Yeh,K.C., Wu,S.H., Murphy,J.T., and Lagarias,J.C. (1997) A cyanobacterial phytochrome two-component light sensory system. Science **277**:1505-1508.

Zienicke,B., Chen,L.Y., Khawn,H., Hammam,M.A., Kinoshita,H., Reichert,J., Ulrich,A.S., Inomata,K., and Lamparter,T. (2011a) Fluorescence of phytochrome adducts with synthetic locked chromophores. J.Biol.Chem. **286**:1103-1113.

Zienicke,B., Chen,L.Y., Khawn,H., Hammam,M.A.S., Kinoshita,H., Reichert,J., Ulrich,A.S., Inomata,K., and Lamparter,T. (2011b) Fluorescence of Phytochrome Adducts with Synthetic Locked Chromophores. J.Biol.Chem. **286**:1103-1113.

Curriculum Vitae

Fichtenweg 43, 76149 Karlsruhe, Germany

Mobile phone: +49(0)17634118986, Office: +49(0)72160848591

Date of Birth: 22.11.1982   Email: dr.rui_yang@yahoo.de

Education:

High School: 09.1998-07.2001   No2. High School of Taigu, Shanxi, China

Bachelor studies: 09.2001-07.2005   Shanxi Agriculture University, Shanxi, China

           Major: Tobacco (Specially for medical use) seed germination

           Thesis: Temperature and water effect during tobacco seed germination

Master studies: 09.2005-07.2008   Northwest A&F University, Shaanxi, China

            Major: Salt stress on cucumber

         Thesis: The effect of ALA on rescue damage of salt stress on cucumber

Doctoral Processing: 09.2008- *approx*.02.2012   Karlsruhe institute of technology, Germany

           Major: phytochrome studies in bacterial and plant

           Thesis: *In vivo* and *in vitro* studies of Phytochrome studies

Awards:

Bachelor period: Four time national scholarship level 2; advanced graduate student;

Master period: Three years full-scholarship;

Doctoral period: Four years full-scholarship from China Scholarship Council

Wissenschaftliche Veröffentlichungen

Publikationen

1. **Yang, R., Zou, Z.R., Qi, X.L.** (2008). The effects of ALA and CaCl$_2$ on cucumbers during initial bloom and fruit-bearing (Cucumis sativus L.) under salt stress. Agricultural research in the arid areas. **26**(4):136-140

2. **Qi, X.L., Zou, Z.R., Yang, R.** (2008). Mitigative Effect of 5-aminolevulinic Acid on Lettuce under NaCl Stress. Acta Agriculturae Boreali-occidentalis Sinica. **17**(2):202-206

3. **Yang, R., Nishiyama, K., Kamiya, A., Ukaji, Y., Inomata, K., and Lamparter,T.**(2012). Assembly of synthetic locked phycocyanobilin derivatives with phytochrome in vitro and in vivo in *Ceratodon purpureus* and *Arabidopsis*. Plant Cell. **24:**1-16.

Konferenzbeiträge

Presented

Yang, R., Zhang, F., Lamparter, T., *et al*. VAAM, Karlsruhe, 04.2011,

Yang, R., Zhang, F., *et al*. From Molecules to Living Systems COS Heidelberg, 05.2011

Poster

Yang, R., Zhang, F. International Symposium on Plant Photobiology (*ISPP*), Beijing, 07.2011

Speech

Yang, R. Moss 2011, Freiburg, 09.2011